Electrophysiological effects of fractions isolated from the venom of *Parabuthus granulatus* on calcium channels in cardiac myocytes

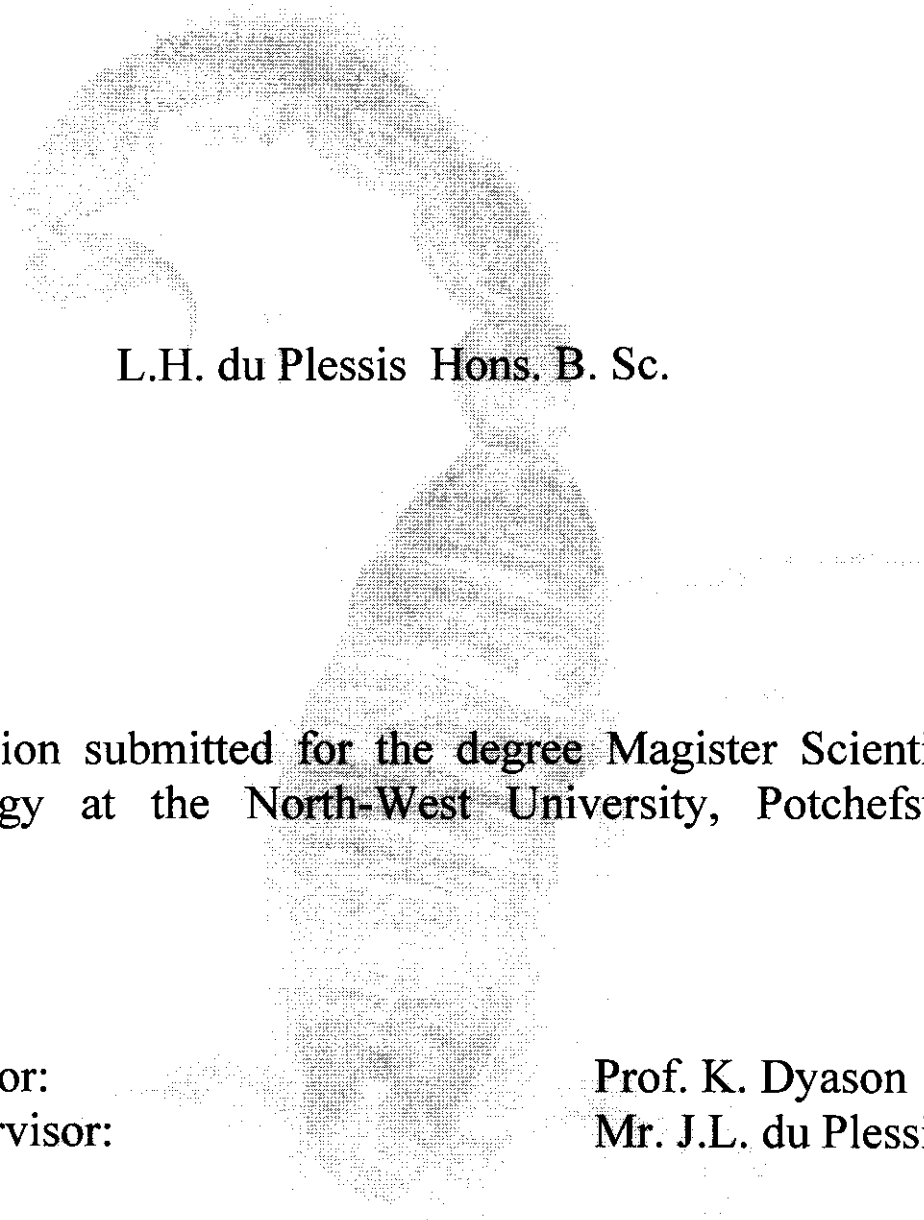

L.H. du Plessis Hons. B. Sc.

Dissertation submitted for the degree Magister Scientiae in Physiology at the North-West University, Potchefstroom Campus.

Supervisor: Prof. K. Dyason
Co-supervisor: Mr. J.L. du Plessis

2004
Potchefstroom

Acknowledgements

I would like to thank The Almighty Father for the blessings, opportunities and talent He provided me to make my studies successful.

I would like to thank my supervisor, Prof. Karin Dyason. Without her sacrifices, expert knowledge, time and guidance, the completion of my dissertation would not have been possible.

To my family, who supported me in many ways. Their guidance and encouragement were the most appreciated.

To my husband, a special word of thanks for supporting me through the difficult times during the study.

A word of thanks to the following persons:

- Mrs. Carla Fourie, not only for the isolation of the ventricular myocytes, but also for the knowledge and support during the two years of this study.
- Dr. Francois van der Westhuizen (subject group Biochemistry), for his assistance in determining the fraction protein concentrations.
- Prof. Lourival Possani for the separation of the fraction and subfractions.
- Prof. J.J. van der Walt, for his continuous interest and valuable input.

Contents

Abbreviations and symbols

α	alpha
A	the amplitude of the maximum Ca^{2+} current that inactivates
AP	action potential
ATP	adenosine triphosphate
AV node	atrioventricular node
B	beta
Ba^{2+}	barium
BHK	baby hamster kidney cells
BmK AS	*Buthus martensi* Karsch peptides AS
C	the time dependent Ca^{2+} current that inactivates slowly or not at all
Ca^{2+}	calcium
cAMP	cyclic adenosine monophosphate
Cd^{2+}	cadmium
cDNA	complementary deoxyribonucleic acid
CHO	chinese hamster ovary cells
CNS	central nervous system
Cl^-	chloride
Co^{2+}	cobalt
C-terminal	carboxy-terminal
δ	delta
DHP/s	dihydropyridine/s
DRG	dorsal root ganglia
E	the membrane potential

E-C	excitation-contraction
E_{Ca}	the equilibrium potential for Ca^{2+}
EGTA	ethylene Glycol-bis (β-aminoethyl Ether) N, N, N', N', - Tetraacetic Acid.
E_h	membrane potential for 50 % activation
ER	endoplasmic reticulum
E-S	excitation-secretion
FTX	funnel web spider toxin
γ	gamma
g	gram
g_{max}	maximum conductance through the Ca^{2+} channel
GΩ	giga ohm
GTP	guanosien triphosphate
HEPES	N- (2-hydroxyethyl) piperazine-N'-(2-ethanesulphonic acid)
HIV	human immunodeficiency virus
Ho^{2+}	holmium
HP	holding potential
HVA	high-voltage activated
I	the maximum current through the Ca^{2+} channel
I_{Ba}	the Ba^{2+} current through the Ca^{2+} channel
IP_3	inositoltriphosphate
$IpTx_a$	Imperatoxin A
$IpTx_i$	Imperatoxin I
K^+	potassium
kD	kilo Dalton

KLI	kurtoxin like peptide I
KLII	kurtoxin like peptide II
La^{3+}	lanthanum
L-type	long-lasting type Ca^{2+} channel
LVA	low-voltage activated
Mg^{2+}	magnesium
MΩ	mega ohm
µg	microgram
µM	micromolar
mM	millimolar
ml	millilitre
mg	milligram
ms	milliseconds
mV	millivolt
Na^{+}	sodium
Ni^{2+}	nickel
NMDA	N-methyl-D-aspartate
NT	neurotransmitter
N-terminal	amino-terminal
N-type	neuronal type Ca^{2+} channel
ω-Aga	ω-Agatoxin
ω-CTx	ω-conotoxin
Pb^{2+}	lead
PBTx1	parabutoxin 1
PBITx3	parabutoxin 3

PEG	polyethelene glycol
PgIII	fraction III isolated from *P. granulatus* venom
PKA	protein-kinase A
PKC	protein-kinase C
PKG	protein-kinase G
P-loop	pore loop
pS	picosiemens
P/Q-type	purkunje type Ca^{2+} channel
RP-HPLC	reverse phase high performance liquid chromatography
R-type	resistant type Ca^{2+} channel
S	slope of voltage dependence
SA node	sinoatrial node
SEM	standard error of the mean
SFI	subfraction I isolated from PgIII
SFII	subfraction II isolated from PgIII
SFIII	subfraction III isolated from PgIII
SR	sarcoplasmic reticulum
τ	the time constant of inactivation
TEA-Cl	tetraethylammonium chloride
TEA-OH	tetraethylammonium hydroxide
TFA	trifluoroacetic acid
T-type	transient type Ca^{2+} channel
TTX	tetrodotoxin
UV	ultra violet
$V_{½}$	membrane potential where 50 % of the Ca^{2+} channels are activated

VDCC/s	voltage dependent calcium channel/s
V_{test}	test potential
Zn	zinc

List of figures and tables

CHAPTER 2

CHAPTER 3

OPSOMMING

Intensiewe navorsing is tot dusver op skerpioentoksiene spesifiek vir Na^+ en K^+ kanale gedoen, maar relatief min navorsing is gedoen op Ca^{2+} kanaal toksiene. Toksiene uit die venoom van slegs twee Suid-Afrikaanse skerpioene, *Parabuthus transvaalicus* en *P. granulatus* het tot dusver effekte getoon op Ca^{2+} kanale. Kurtoksien, geïsoleer uit die venoom van *P. transvaalicus*, inhibeer T- en L-tipe neurale Ca^{2+} kanale, terwyl KLI en KLII (Kurtoksien "Like" peptiede I en II), geïsoleer uit *P. granulatus*, die T-tipe Ca^{2+} kanaal aktiwiteit in muismanlike-kiemselle inhibeer. In die studie is die effek van fraksies geïsoleer uit die venoom van *P. granulatus* op Ca^{2+} kanale in rot ventrikulêre miosiete ondersoek deur gebruik te maak van die heelselspanningsklemmingtegniek. Fraksies van *P. granulatus* heelvenoom is geïsoleer met Sephadex G50 kolomme (Fraksie I-IV). Fraksie III (PgIII) het 'n spanningsafhanklike toename van die inwaartse Ca^{2+} stroom getoon en het die kanaal kinteka beïnvloed deur die spanningsafhanklikheid van aktivering na meer gehiperpolariserende potensiale te verskuif en die tempo van inaktivering en deaktivering te vertraag. Die tyd wat die stroom neem om 'n maksimum te bereik is ook vertraag. PgIII is met behulp van HPLC verder geskei in 'n poging om die subfraksie/s verantwoordelik vir die agonistiese effek te identifiseer. Subfraksie I het 'n agonistiese effek soortgelyk aan PgIII gehad, terwyl subfraksie II en III die Ca^{2+} stroom onderdruk het. Die waargenome agonistiese effek is nog nie in die literatuur beskryf nie. Die identifikasie van nuwe peptiedstrukture met unieke funksies is belangrik in die veld van toksiennavorsing. Peptiede wat Ca^{2+} kanale teiken kan waardevolle hulpmiddels wees om Ca^{2+} kanale te karakteriseer. Ca^{2+} kanale in die hart is betrokke by 'n verskeidenheid patologiese kondisies insluitend angina, iskemie, sommige arrtimië en hipertensie.

Sleutelwoorde: Kardiale Ca^{2+} kanaal, *Parabuthus granulatus,* agonis, skerpioen toksiene.

SUMMARY

Scorpion toxins specific for Na^+ and K^+ channels, have been studied extensively but relatively little has been done on Ca^{2+} channel toxins. Toxins in the venom of only two South African scorpions *P. transvaalicus* and *P. granulatus* have been found to interact with Ca^{2+} channels. Kurtoxin isolated from the venom of *P. transvaalicus* inhibits the T and L-type neuronal Ca^{2+} channels, whereas KLI and KLII (Kurtoxin-like peptide I and II), isolated from *P. granulatus*, inhibits T-type Ca^{2+} channel activity in mouse male germ cells. In this study the effects of fractions isolated from the venom of *P. granulatus* on Ca^{2+} channels in rat ventricular myocytes were investigated by means of the whole-cell patch clamp technique. Fractions of *P. granulatus* crude venom were isolated with Sephadex G50 columns (fraction I-IV). Fraction III (PgIII) showed a voltage dependent increase of the inward Ca^{2+} current and influenced the channel kinetics by shifting the voltage dependence of activation towards more hyperpolarizing membrane potentials and decreased the rate of inactivation and deactivation. The time of the current to reach peak was also delayed. PgIII was further separated by HPLC in an attempt to identify the subfraction/s responsible for the agonistic effect. Subfraction I had an agonistic effect similar to PgIII, whereas subfraction II and III, decreased the Ca^{2+} current. The observed agonistic effect has not been described in the literature. The identification of new peptide structures with unique functions are important in the field of toxin research. Peptides that target Ca^{2+} channels can be valuable tools to characterize Ca^{2+} channels. Ca^{2+} channels in the heart are implicated in a number of pathological disorders like angina, ischemia, some arrythmias and hypertension.

Keywords: Cardiac Ca^{2+} channel, *Parabuthus granulatus*, agonist, scorpion toxins.

CHAPTER 1 – General introduction, problem statement and aims

Ion channels are proteins which are embedded in the plasma membrane of nearly all cells that mediate fast, selective transport of ions through the membrane. VDCCs mediate Ca^{2+} influx into cells in response to depolarization of the plasma membrane. The Ca^{2+} that enters the cells through this pathway is important for the regulation of protein phosphorylation, gene transcription and other intracellular events (Catterall, 1991:1499). VDCCs are also responsible for initiation of E-C coupling in heart muscle and E-S coupling and electrical activities in the nervous system, for example, communication between cells. Membrane VDCCs also play an important role in the influence of hormones and drugs on the cell (Terlau & Stühmer, 1998:437; Chung & Kuyucak, 2002:267). The combination of electrophysiological techniques and molecular cloning has been successful in characterizing different families and subgroups of VDCCs (Nargeot *et al.*, 1997:A15). The heart contains two types of VDCCs, which can be distinguished by their distinct electrophysiological and pharmacological properties. The LVA T-type channels activate at potentials more negative to -50mV, whereas the HVA L-type channels activate at potentials positive to -50 mV (Snutch *et al.*, 2001:11).

It is known that mutations of genes, which encode ion channels, can lead to a variety of neurological and pathological disorders (Terlau & Stühmer, 1998:437). Several pathologies are associated with a rise in resting intracellular Ca^{2+} ion concentration and, therefore, VDCCs represent pharmacological targets of therapeutic interest (Nargeot *et al.*, 1997:A15). Human disorders in which Ca^{2+} channels are implicated includes angina, epilepsy, hypertension, ischemia and some arrythmias (Snutch *et al.*,

2001:11). The investigation of the structure and function of ion channel proteins and how they work can assist in the understanding of the underlying mechanisms of these diseases and ultimately in finding possible cures (Terlau & Stühmer, 1998:437; Lehman-Horn & Jurkat-Rott, 1999:1318; Chung & Kuyucak, 2002:267).

The venom of poisonous animals like bees, wasps, snakes, spiders, marine cone snails and scorpions has been studied extensively (Corzo *et al.*, 2001:256; Kushmerick *et al.*, 2001:991). Scorpions are an ancient and diverse group of animals and their venom presents a rich source of proteins with specialized but related functions (Loret & Hammock, 2001:204). The peptides found in this venom can cause nervous excitation, leading to muscle cramps, vomiting and convulsions or nervous depression, producing symptoms ranging from local numbness to systemic paralysis, respiratory failure and cardiac arrest (Miljanich, 1997:6). The neurotoxic peptides are mainly used for immobilizing prey. Antimicrobial peptides found in the venom of some scorpions are used as defensive mechanisms. Given their broad spectrum of actions within excitable tissues, peptide toxins in scorpion venom have become valuable tools for localization and study of ion channels in nerve, smooth and cardiac muscle (Loret & Hammock, 2001:204).

Over the past few years much research has been done on Na^+ and K^+ toxins, but relatively little on Ca^{2+} toxins in scorpion venom. Toxins isolated from the venom of only two South African scorpions *Parabuthus granulatus* and *P. transvaalicus* have been found to interact with Ca^{2+} channels. Kurtoxin, a 63 amino acid peptide toxin from *P. transvaalicus,* inhibits LVA and HVA-type Ca^{2+} channels (Sidach & Mintz, 2002:2032). Two kurtoxin-like peptides (KL I and KLII) isolated from the venom of

P. granulatus, inhibits T-type Ca^{2+} channel activity in mouse male germ cells and spermatogenic cells. KLII (or kurtoxin from *P. granulatus*, KPg) was found to be identical to kurtoxin, but KLI is a new peptide containing 62 amino acids (Olamendi-Portugal *et al.*, 2002:566; Lopez-Gonzales *et al.*, 2003:410). The characterization of peptide toxins is not only important to elucidate the working mechanisms of ion channels but also to contribute to the knowledge of the composition of South African scorpion venom. This knowledge can contribute valuable information for the development of species' specific scorpion antivenom.

In the study of Botha (2002:58), the crude venom of *P. granulatus* was shown to have an agonistic effect on VDCCs in guinea-pig myocytes. The crude venom was separated in four fractions with Sephadex G50 columns. Three of the four fractions were tested on both rat DRG neurons (Jordaan, 2002:33) and guinea-pig myocytes (Botha, 2002:58). In the DRG neurons fraction II blocked HVA Ca^{2+} channels and fraction I had no distinctive effects. In guinea-pig myocytes fraction I and II increased the LVA and HVA Ca^{2+} current. Fraction III had a prominent effect, increasing the HVA Ca^{2+} currents in both cell types. It also influenced the channel kinetics by increasing the rate of inactivation, but this increase was not statistically significant. The voltage dependence of activation was shited to more negative membrane potentials. This agonistic effect of scorpion venom on VDCC not been described in the literature. However, an agonistic peptide from scorpion venom that acts on ryanodine receptors has been isolated previously. This peptide was named $IpTx_a$ and was isolated from the African scorpion *Pandinus imperator* (Valdivia & Possani, 1998:111).

1.1 Problem statement and aims

Agonistic peptides isolated from scorpion venom specific for VDCCs are rare and the presence of agonistic peptides in the venom of South African scorpions have not been described in the literature. Preliminary studies with fraction III had promising results and further research with fraction III and the subfractions is validated to determine if a novel peptide can be identified.

The aims of the study are:

- To confirm the agonistic effect of Sephadex fraction III, isolated from the venom of *P. granulatus*, on cardiac VDCCs in rat ventricular myocytes by means of the patch clamp technique.
- To characterize the effect of Sephadex fraction III on VDCCs in rat ventricular myocytes.
- To test and characterize the effects of selected subfractions of fraction III on VDCCs in rat ventricular myocytes.
- To confirm that the effect is mediated by Ca^{2+} through the VDCC.

CHAPTER 2 – Literature study

1. Distribution of medically important scorpions

Scorpions are venomous arthropods of the class Arachnida. They are distributed all over the world and dangerous species are found in the South Western United States, Mexico, the East-Central area of South America and the Caribbean Islands, Northern and Southern Africa, the Middle East and Asia (Simard & Watt, 1990:436; Debont *et al.*, 1998:343). In Southern Africa there are more than 130 species, which are widely distributed in a wide variety of habitats including areas where protection and fresh water are available such as tropical forests, rain forests, grasslands, savanna, temperate forests, caves and even snow-covered mountains (Leeming, 2003:6). Medically important scorpion species belong to the family Buthidae, which include the genera *Androctonus, Buthacus, Buthus, Centruroides, Leirus, Mesobuthus, Parabuthus* and *Tityus* (Simard & Watt, 1990:436; Debont *et al.*, 1998:343; Loret & Hammock, 2001:205).

There are four scorpion families in South Africa namely Buthidae (C.L. Koch, 1837), Scorpionidae (Latreille, 1802), Bothriuridae (Simon, 1880) and Ischnuridae (Simon, 1879) (Prendini, 2001:15). The Buthidae family is represented by five genera of which *Parabuthus, Buthotus* and *Uroplectus* are more important. *Parabuthus* (Pocock, 1890) currently comprises 28 species, 20 of which are distributed all over the South Western parts of Southern Africa (Prendini, 2001:14, Dyason *et al.*, 2002:769). Three species - *P. granulatus* (Ehrenberg, 1831), *P. transvaalicus* (Purcell, 1899) and *P. mossambicensis* (Peters, 1861) - are responsible for a number of fatalities annually

(Müller, 1993:407, Leeming, 2003:9). This study will focus primarily on *P. granulatus*, which can be found in arid and semi-arid areas of Southern Africa. This is considered to be the most venomous scorpion in Southern Africa (Prendini, 2001:13; Leeming, 2003:51).

2. Scorpion venom

2.1 Composition of scorpion venom

Many animals including bees, wasps, snakes, spiders, cone snails and scorpions produce venom. The venom is produced in specialized glands and delivered with spines, stingers or fangs (Miljanich, 1997:7). Animal venom is complex mixtures of proteins and peptides with different properties. These components differ from one another in their structure and in the target at which they are aimed (Rees & Bilwes, 1993:385). Scorpion venom is used for both prey capture and defense. The venom can be described as being a complex, aqueous mixture containing mucus, inorganic salts, low-molecular-weight organic molecules and many small basic proteins, namely neurotoxic peptides. Serotonin and enzyme inhibitors are also present in the venom (Simard & Watt, 1990:417; Müller, 1993:407). Unlike most snake and spider venom, scorpion venom generally lacks enzymes or possesses very low levels of enzyme activity (Gwee *et al.*, 2002:796). The neurotoxic peptides in scorpion venom represent some of the most powerful poisons known. The amino acid composition of scorpion toxins has a high content of cysteine and large amounts of glycine, tyrosine, di-carboxylic acids and lysine, but methionine and histidine are absent in most of these toxins (Simard & Watt, 1990:417; Müller, 1993:407).

2.2 Peptide toxins in scorpion venom

Advanced methods of fractionation, chromatography and peptide sequencing have made it possible to characterize the components of scorpion venom (Miljanich, 1997:7). The venom is a rich source of toxic polypeptides affecting molecular targets like receptors and ion channels. By doing this it exerts a wide variety of actions, including blocking of the central and peripheral nervous systems or alteration of smooth or skeletal muscle activity (Ménez *et al.*, 1992:83). Research has shown that some of the most pharmacologically active components of many types of venom, including scorpion venom, are these neurotoxic peptides (Miljanich, 1997:7). Multiple toxins may be present in the venom of a single species of scorpion (Gwee *et al.*, 2002:796). The rich biodiversity of scorpion peptides exists because they have a biological function to accomplish (Tytgat *et al.*, 1999:444).

Peptide toxins in scorpion venom can be divided into four distinct families. Family 1 modulates Na^+ channel activity and contains peptides of 60-70 amino acids linked by four disulphide bridges (Gordon *et al.*, 1998:132). Family 2 comprises of short-chain peptides, with 30-40 amino acids and long-chain peptides, with 60-70 amino acids linked by three or four disulphide bridges that block K^+ channels (Legros *et al.*, 1998:377). Family 3 contains short-chain insectotoxin-like peptides of 36 amino acids with four disulphide bridges that inhibit Cl^- channels (Tytgat *et al.*, 1998:390) and family four includes peptides that modulate ryanodine sensitive Ca^{2+} channels (Valdivia & Possani, 1998:111). Toxins can also be classified according to whether they act on mammals, insects or arthropods (Darbon *et al.*, 1999:41). Most of the individual scorpion toxins investigated to date belong to structurally related families with similarly related mechanisms of action (Kozlov *et al.*, 2000:362). Toxins specific

for VDCCs are scarcely known and have variable amino acid lengths (Possani *et al.*, 2000:862).

2.3 Scorpion envenomation

Scorpion envenomation is a relatively common event in subtropical and tropical countries (Ismail, 1995:825). Several species of scorpions, especially species from the Buthidae family, can cause lethal envenomation in humans, especially in children. Symptoms displayed by victims of scorpion envenomation are usually complex in nature and can be attributed mainly to hyperactivity of the autonomic nervous system (Gwee *et al.*, 2002:796). Severe scorpion envenomation includes objective neurological deficits, various abnormal reflexes, bladder symptoms, dysphagia and hypersalivation. Blood pressure and temperature are often raised and tendon reflexes hyper-reactive. The initial reaction is severe pain accompanied by local paraesthesia and pronounced hyperaesthesia, muscle pain and cramps. This is followed by difficulty to swallow, coarse muscle tremors or myoclonic jerks, fasciculation of the tongue and profuse sweating. The onset of the systemic symptoms can be very rapid, within minutes in children, or delayed, from four to twelve hours in adults (Müller, 1993:406; Bergman, 1997:764). Other symptoms include general weakness, visual disturbances, difficult breathing, tremors, involuntary movements, dysphagia, dysathria and loss of pharyngeal reflexes. There is also a general decrease in motor power, increased perspiration and restlessness (Müller, 1993:409; Bergman, 1997:764).

The clinical manifestations of scorpion envenomation appear to be secondary to activation of both the sympathetic and parasympathetic divisions of the autonomic nervous system. Pulmonary edema is accompanied by sympathetic activation and

variable degrees of myocardial dysfunction (Mazzei de Dàvila *et al.*, 2002:1343). The syndrome primarily reflects a state of generalized neurological hyper-excitability and other excitable tissue, such as skeletal and heart muscle may also be affected. The neurotoxins act on Na^+ channels of excitable cells by delaying inactivation or enhancing activation, thereby leading to spontaneous depolarization of the cells. Noradrenaline is released from adrenergic and cholinergic nerve endings and adrenaline is released from the adrenal medulla. This explains the sympathetic, parasympathetic and skeletal muscle effects of scorpion venom. Symptoms and signs of increased sympathetic activity include hypertension, tachycardia, cardiac dysrhythmias, increased perspiration, fever, hyperglycemia, restlessness and increase in catecholamine levels. Parasympathetic effects include increased salivation, bradycardia, hypotension and gastric distension (Müller, 1993:409; Bergman, 1997:764). *P. granulatus* mainly produce adrenergic effects (Bergman, 1997:765).

3. Ion channels

Ion channels are gated pores of which gating may be intrinsic or regulated by ligand binding or changes in the voltage gradient across the membrane. They are found in all animal, plant and bacterial cell membranes and function in diverse processes such as nerve and muscle excitation, hormonal secretion, learning and memory, cell proliferation, sensory transduction, the control of salt and water balance and regulation of blood pressure (Ashcroft, 2000:1). Ion channels are also responsible for biochemical events including phosphorylation and gene expression. Depolarization of neurons caused by the inward Na^+ current activates voltage dependent Ca^{2+} channels. Ca^{2+} moving into the cell causes a plateau depolarization, prolongs the action potential and

serves as an intracellular second messenger to initiate exocytosis of neurotransmitters and intracellular biochemical events (Catterall, 1993:1).

Three major groups of ion channels can be distinguished by the dominant stimulus that modulates their activity: 1) voltage dependent channels, which are steeply sensitive to changes in the electrical potential across cell membranes; 2) ligand-gated channels, which are directly activated by the binding of specific ligands on the extracellular or intracellular side of the channel and 3) "coupled" channels, in which the transducing element and the channel are found on different proteins but linked by specific second messenger pathways in the cytoplasm (Lawrence *et al.*, 1993:75; Opie, 1998:72).

Voltage dependent channels undergo an extremely rapid conformational change that converts an impermeable structure into a highly permeable but selective hole in the membrane through which specific ions can pass. The most important function of voltage dependent ion channels is to generate electrical activity in cells and they are responsible for many manifestations of life, including movement, the senses and the cognitive functions of the brain (Anderson & Greenberg, 2001:18). The voltage dependent channels selectively conduct specific ions and are named according to the most permeant ion (Lawrence *et al.*, 1993:75) e.g. Na^+, K^+, Cl^- and Ca^{2+} channels. This study will focus on the VDCCs.

3.1 Ca^{2+} channels

Ca^{2+} ions play important roles in regulating a variety of cellular functions. The intracellular Ca^{2+} concentration (10^{-7}M) is lower than the extracellular Ca^{2+} concentration (1-2 mM) and a transient rise in internal Ca^{2+} functions as a second

messenger-coupling-receptor to activate many cellular processes such as cellular excitability, neurotransmitter release, intracellular metabolism and gene expression. The increase in Ca^{2+} concentration is mediated by VDCCs that regulate Ca^{2+} influx across the plasma membrane or by ligand gated Ca^{2+} channels, which control the release of Ca^{2+} from intracellular stores. Advances in research fields such as molecular biology, pharmacology and electrophysiology have led to the identification of diverse VDCCs subtypes (Uchitel & Katz, 1997:37; Ashcroft, 2000:161).

3.1.1 Classification

The two major types of Ca^{2+} channels include the ligand-gated channels and VDCCs. Two distinct classes of ligand-gated Ca^{2+} channels have been identified. They are sensitive either to a plant alkaloid ryanodine or IP_3. The purified ryanodine receptor has a relative molecular mass of 400-450 kD and is a homotetrameric complex. It is morphologically identified by the "foot" structure, which spans the gap between the SR and transverse tubule membranes of muscle (Takeshima, 1993:165). The ryanodine receptor is activated by Ca^{2+} ions entering through the VDCC. It then releases Ca^{2+} from the SR or ER, which is an essential step for contraction of skeletal, heart and smooth muscle (Valvida & Possani, 1998:111; Lehmann-Horn & Jurkat-Rott, 1999:1328). The IP_3 receptor is gated by IP_3, which is an important second messenger and resembles the ryanodine receptor in structure (Mikoshiba *et al.*, 1993:182; Ashcroft, 2000:260). Another ligand-gated channel is the NMDA receptor. These receptors are activated by NMDA and glutamate and although the channel is permeable to Na^+ and K^+, it shows a high permeability for Ca^{2+} (Ashcroft, 2000:305).

VDCCs control a variety of important physiological functions, such as E-C coupling, secretion of hormones and release of neurotransmitters (Nargeot *et al.*, 1997:A15). The different types of VDCCs can be distinguished by their single channel properties, voltage dependence, ionic selectivity and pharmacology. In addition to the activation voltage, different Ca^{2+} channels may also be distinguished by their molecular structure, activation kinetics and inactivation kinetics (Bean, 1989:335; Zhang *et al.*, 1993:1086; Meir *et al.*, 1999:1022; Ashcroft, 2000:161).

Two categories of VDCCs can be distinguished on the basis of their activation threshold. The first category is LVA channels, which includes T-type channels for which the activation is slightly above the resting potential. These channels have similar permeability for Ba^{2+} and Ca^{2+} ions and inactivate rapidly. The second category, or HVA channels are those in which the threshold for activation is substantially above the resting potential (towards 0 mV). At a holding potential that inactivates the LVA channels, a step to -10 mV evokes a large HVA current. Their permeability for Ba^{2+} ions is larger than for Ca^{2+} ions and they inactivate slowly (Nargeot *et al.*, 1997:A16; Meir *et al.*, 1999:1022; Hille, 2001:89; Catterall *et al.*, 2003:579). On the basis of electrophysiological and pharmacological properties, at least five types of HVA channels can be distinguished. They are classified as L, N, P, Q and R-type channels (Bean, 1989:335; Zhang *et al.*, 1993:1086; Ashcroft, 2000:161). The L-type channels are sensitive to DHPs (nisoldipine), phenylalkylamines (verapamil) and benzothiazepines (diltiazem). The N, P, Q and R-type channels are mainly found in the nervous system (Lehmann-Horn & Jurkat-Rott, 1999:1326; Catterall *et al.*, 2003:579). The distinction between the P and Q-type channels is not always obvious and hence they are often grouped together as the P/Q type channels (Meir *et al.*, 1999:1022).

3.1.2 Distribution and properties

The different types of Ca^{2+} currents are defined by different α_1 subunits. Molecular cloning has revealed the existence of multiple genes encoding the subunits of VDCCs. These include 10 genes designated α_1A, α_1B, α_1C, α_1D, α_1E, α_1F, α_1G, α_1H, α_1I and α_1S that encode multiple splice variants of the pore-forming α_1 subunit (Harpold *et al.*, 1998:218; Catterall, 2000:524; Catterall *et al.*, 2003:580). Class C and D genes encode L-type channels α_1C and α_1D for which the sequence is greater than 75 % identical to skeletal muscle L-type α_1S, encoded by Class S genes. α_1C forms the cardiac, smooth muscle VDCC and a DHP-sensitive type of neuronal Ca^{2+} channel; α_1D is responsible primarily for the DHP-sensitive Ca^{2+} channel found in endocrine cells. Class F genes encode the L-type current in the retina. The class A, B and E genes encode P/Q, N and R-type VDCCs respectively, which are expressed primarily in neurons. Class G, H and I genes are responsible for encoding the T-type channel in cardiac, neuronal, endocrine and skeletal tissues (Uchitel & Katz, 1997:38; Birnbaumer *et al.*, 1998:258; Catterall, 2000:526; Catterall *et al.*, 2003:580).

Ca^{2+} channels are widely distributed in the body. Ca^{2+} currents have been described in heart muscle, smooth muscle, skeletal muscle, neurons and endocrine cells. In endocrine cells of anterior pituitary origin there are both HVA and LVA channels with properties that might suggest that the channels are involved with secretion (Armstrong, 1998:11). A study of Seino *et al.* (1992:585) showed that pancreatic islets express two different voltage dependent Ca^{2+} channel α_1 subunits. One corresponding to a α_1 subunit in the heart and one for which partial cDNA clones where described in the brain. Voltage dependent L-type channels in insulin-secreting RINm5F cells are

heterogeneous and a ω-CTx sensitive channel similar to the neuronal type channel is also expressed in endocrine cells (Sher *et al.*, 1992:407). In adrenal glomerulosa cells T and L-type channels have distinct functions during activation of aldosterone production. The L-type channels are exclusively responsible for the cytosolic Ca^{2+} response while the T-type channels control aldosterone secretion (Rossier *et al.*, 1998:176).

LVA Ca^{2+} channels and at least five pharmacologically distinct HVA Ca^{2+} channels exist in most rat CNS neurons, with the exception of cerebellar Purkinje cells, which only contain the L, N and P-type channels. These channels are distributed differentially among the various CNS regions and this distribution may result from the expression of region-specific subunits of HVA channels (Akaike, 1998:57). The N-type channels are blocked by ω-CTx and low Cd^{2+} concentrations, while the P/Q-type channels are blocked by ω-AgaIVA, but are insensitive to DHPs and ω-CTx. The N-type and P/Q-type channels are primarily responsible for triggering neurotransmitter release, but the P-type channels are also involved in Ca^{2+} spike in some neurons and in inducing long-term depression (Mori *et al.*, 1993:88). The most important function of Ca^{2+} channels in neurons is to mediate E-S coupling, thus neurotransmitter release (Catterall, 2000:526). The different properties of all the VDCCs channels are summarized in Table 1, but this study will focus on cardiac VDCCs in heart muscle cells, which will be discussed in more detail.

Table 1 – The properties of the different types of VDCCs.

Ca^{2+} current type	T	L	N	P	Q	R	References
Pore-forming subunit	α_1G	α_1S	α_1B	α_1A	α_1A	α_1E	1, 2, 7
	α_1H	α_1C					
	α_1I	$\alpha_1$1D					
		α_1F					
Ca^{2+} channel	$Ca_V3.1$	$Ca_V1.1$	$Ca_V2.2$	$Ca_V2.1$	$Ca_V2.1$	$Ca_V2.3$	7, 10
	$Ca_V3.2$	$Ca_V1.2$					
	$Ca_V3.3$	$Ca_V1.3$					
		$Ca_V1.4$					
Single channel Conductance (with ~100mM Ba^{2+})	~8 pS Ba^{2+}=Ca^{2+}	~15-2 pS Ba^{2+}>Ca^{2+}	10-20 pS Ba^{2+}>Ca^{2+}	9-19 pS Ba^{2+}>Ca^{2+}	16pS Ba^{2+}>Ca^{2+}	15pS Ba^{2+}>Ca^{2+}	4, 5, 8, 9
Activation threshold	> -70mV LVA	> -30mV HVA	> -30mV HVA	> -40mV HVA	> -40mV HVA	> -40mV HVA	6
Inactivation time course (in ms)	Fast ~50	Slow >500	Moderate 50-500	Very slow >500	Moderate 50-500	Fast ~30	4, 5, 9
Primary tissue location	Skeletal, cardiac, *neuronal, endocrine*	Skeletal, cardiac, *neuronal, endocrine*	Neuronal, nerve *terminals*, dendrites	Neuronal, nerve *terminals*, dendrites, Purkinje cells	Neuronal, nerve *terminals*, dendrites	Neuronal, nerve *terminals*, dendrites, cell bodies	7, 10
Pharmacology	Amiloride, Ni^{2+} Mibefradil	DHP; Agonists/ Antagonists, Cd^{2+}	ωCTx-GVIA, MVIIA, MVIIC, ωAga-IIIA	ωAga-IIA, IVA, ωCTx-MVIIC, FTX	ωAga-IIA, IVA, ωCTx-MVIIC	ωAga-IIA, Ni^{2+}	2, 3, 5,10
Function	Membrane excitability	E-C coupling E-S coupling Ca^{2+} homeostasis Gene regulation Hormone secretion	E-S coupling NT release Dendritic Ca^{2+} transients	E-S coupling NT release Dendritic Ca^{2+} transients	E-S coupling NT release Dendritic Ca^{2+} transients	E-S coupling Ca^{2+} dependent AP NT release	7, 10

Abbreviations: Aga = agatoxin; AP = action potentials; CTx = conotoxin; DHP = dihydropyridine; E-C = excitation-contraction; E-S = excitation-secretion; FTX = Funnel web spider toxin; HVA = high voltage activated; LVA = low voltage activated; NT = Neurotransmitter.

1 = Birnbaumer *et al.*, 1998:258; 2 = Shekter *et al.*, 1998:333; 3 = Uchitel & Katz, 1997:38; 4 = Bean, 1989:335; 5 = Mori *et al.*, 1993:88; 6 = Nargeot *et al.*, 1997:A16; 7 = Catterall, 2000:526; 8 = Meir *et al.*, 1999:1027; 9 = Triggle, 1999:318; 10 = Catterall *et al.*, 2003:579.

3.2 Cardiac Ca^{2+} channels

VDCCs are critical to normal cardiac function and the heart contains at least two types of Ca^{2+} currents (Shorofsky & Balke, 2001:127). The sarcolemmal L and T-type channels in cardiac myocytes move Ca^{2+} into the cell. This inward current tends to make the membrane potential more positive, but it also serves as an important second messenger in the E-C coupling process which leads to activation of contraction (Bers & Perez-Reyes, 1999:339). The L and T-type channels have a unique voltage range of activation and inactivation as well as different sensitivities to drugs (Hess *et al.*, 1986:S19).

3.2.1 Structure

Five subunits of the cardiac VDCC (α_1, α_2, β, γ and δ) have been identified. The five subunits are arranged in a 1:1:1:1:1 stoichiometry as shown in Figure 1 and have molecular masses of 190 (α_1), 160 ($\alpha_2\delta$), 52 (β) and 32 kD (γ) respectively (Hosey *et al.*, 1996:268; Opie, 1998:71; Ashcroft, 2000:165). The α_2 and δ subunits are connected by a disulphide bridge and perceived as a single unit (Meir *et al.*, 1999:1023). The functional ion channel is formed by the α_1 subunit, while the $\alpha_2\delta$, ß and γ subunits modulate the function of the α_1 subunit. The α_1 subunit constitutes the pore through which Ca^{2+} flows into the cell when it opens upon depolarization. The α_1 subunit determines the general profile of VDCCs in terms of electrophysiological and pharmacological properties and gives rise to the different classes of VDCCs described. Auxiliary subunits and other Ca^{2+} channels subtypes may introduce another degree of diversity (Balke & Gold, 1992:401; Nargeot *et al.*, 1997:A22; Uchitel & Katz, 1997:37).

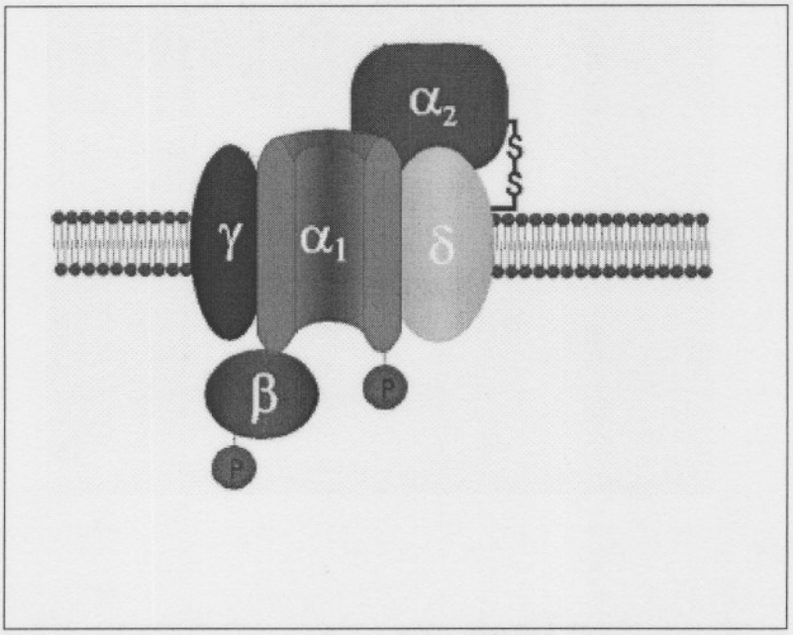

Figure 1 – A diagrammatic representation of the VDCC. The α_1 subunit conveys the functional characteristics of the channel, while the subunits α_2, δ, β and γ modulate channel activity (Modified from Arrikath & Campbell, 2003:300 and Balke & Gold, 1992:402).

The Ca^{2+} α_1 subunit is composed of four transmembrane domains and each domain consists of six transmembrane α helices (S1 - S6), which are connected by membrane-associated cytoplasmic loops. There are also cytoplasmic domains of the N and C-termini. The S4 segment is prominent in activation, while the S5 and S6 segments form the pore lining (P-loop). A large number of phosphorylation sites for various kinases are also found throughout the structure (Nargeot *et al.*, 1997:A19; Uchitel & Katz, 1997:37; Catterall, 2000:529; Shorofsky & Balke, 2001:127).

3.2.1.1 Structure-function relationship of the α_1 subunit

The S4 segment of each domain consists of positively charged lysine residues and serves as the voltage sensor, which detects membrane depolarization. This segment moves outward and rotates under the influence of the electrical field initiating a

conformational change that opens the pore (activation) (Ashcroft, 2000:168). Activation of Ca^{2+} currents approach a steady level within a few milliseconds after a depolarizing step, before much inactivation has occurred (Tsien 1983:341-349).

There is a difference in the inactivation of VDCCs and Na^+ channels. Two types of Ca^{2+} channel inactivation occur, namely inactivation produced by membrane depolarization (voltage dependent inactivation) and inactivation caused by intracellular Ca^{2+} (Tsien 1983:341-349; Hadley & Lederer, 1991:262). The latter is enhanced by the presence of Ca^{2+} at the inner side of the membrane. The importance of Ca^{2+} for inactivation is seen from Ba^{2+} currents through L-type channels. In this case the channel inactivates only slightly during the 500 ms after a voltage step, regardless of holding potential (Mazzanti *et al.*, 1991:332). In contrast to the Ca^{2+}-dependent inactivation exhibited by L-type channels, other types of calcium channels undergo voltage dependent inactivation (Ashcroft, 2000:168) similar to the Na^+ channel. The cytoplasmic linker between S6 of domain III and S1 of domain IV acts as the inactivation gate in Na^+ channels. In VDCCs the structural elements needed for voltage dependent inactivation differ in that residues adjacent to S6 of domain I are important. An additional residue, which lays within the GTP-binding site in the cytoplasmic loop linking, domain I and II are also important. The exact function of these structural elements in voltage dependent inactivation of VDCCs is still unclear, but there is evidence that it closely resembles the C-type inactivation of voltage dependent K^+ channels (Herlitze *et al.*, 1997:1512; Ashcroft, 2000:168). This type of inactivation involves a local conformational change at the external mouth of the pore, which leads to constriction and occlusion of the pore (Ashcroft, 2000:108).

Single channel recordings have led to a detailed description of the mechanisms underlying entry and exit of ions through the channel pore. The open VDCC is a narrow pore in which ions cannot pass each other. As ions move through the pore, they reversibly bind to at least two sites. Relative permeability and selectivity are obtained by the different affinities of the permeant ions for these binding sites (Hess *et al.*, 1989:80). Since cations are abundant in physiological media, HVA and LVA channels must possess an inner pore structure capable of selecting Ca^{2+} against Na^{+} (Carbone *et al.*, 1998:80). Data suggests that T-type and HVA (L and N-type) channels possess one binding site inside the pore that is the common locus for the binding of permeant ions (Ca^{2+}, Na^{+}), permeant blockers (Ca^{2+}, Cd^{2+}, Zn^{2+}, La^{3+}) and impermeant blockers (Mg^{2+}). The site for ion-channel interaction may be able to change the arrangement of its charges depending on the type of ion bound at the time. This could explain the ability of Ca^{2+} to act as a blocker at micromolar Ca^{2+} concentrations, but as permeant ion at millimolar Ca^{2+} concentrations (Carbone *et al.*, 1998:89). The experimental observations are that VDCCs select Ca^{2+} over Na^{+} at a ratio of 1000:1 despite the ions being identical in size (Sather & McClesky, 2003:47). The S5 and S6 segments and the membrane-associated pore loop between them form the pore lining of the VDCC. The P-loop contains a pair of glutamate residues in each domain that are required for Ca^{2+} selectivity. These glutamate residues provide the high affinity binding site for Ca^{2+} (Blumenthal, 1995:400; Nargeot *et al.*, 1997:A16; Opie, 1998:72; Balser, 1999:328; Catterall, 2000:529). The four P-loops of the L-type channel α_1-subunit are asymmetric and are homologous to the Na^{+} channel. The P-loop also forms the receptor site for the pore-blocking Ca^{2+} antagonist drugs specific for the L-type channels (Parent & Gopalakrishnan, 1995:1810; Ashcroft, 2000:167; Corry *et al.*, 2000:1).

3.2.1.2 Auxiliary subunits

The intracellular β subunit (Figure 1) is composed of two conserved domains, while the intracellular N and C-terminus are more variable (Nargeot *et al.*, 1997:A22). Four distinct genes encode the β subunits (β1 – β4) (Arikkath & Campbell, 2003:303). The β subunit regulates the activity of the α_1 subunit in many ways, modifying the current amplitude, current kinetics and voltage dependence. Binding of the β subunit to the α_1 subunit via the I-II cytoplasmic linker may introduce conformation change in the α_1 subunit and therefore, alter some properties (voltage dependence and open probability) of the VDCC. This conformational change or β subunit association may also protect the α_1 subunit from degradation. The β subunit may also be required for the correct transport of the α_1 subunit to the surface membrane (Liu & Campbell, 1998:236). The functional effects of the β subunit include increased peak amplitude, faster rate of activation, modifications in the rate of channel inactivation, hyperpolarizing shift of activation and inactivation, voltage dependent facilitation and ligand binding. The changes introduced by β subunits are all seen in the absence of $\alpha_2\delta$ or γ, which supports a direct interaction between α_1 and β (Walker & De Waard, 1998:148; Birnbaumer *et al.*, 1998:258).

The disulphide linked α_2 and δ subunits are transmembrane glycoproteins as is the γ subunit, which is noncovalently associated with the other subunits (Catterall, 1991:1499). Both subunits interact directly with the α_1 subunit, with no known inter-auxiliary subunit interactions. Four genetically distinct $\alpha_2\delta$ subunits have been described and are named $\alpha_2\delta$1-4, while there are 8 different γ subunit genes (Harpold *et al.*, 1998:218; Arikkath & Campbell, 2003:303). The γ subunit is composed of four transmembrane segments and cytoplasmic domains of the N and C-termini (Walker &

De Waard, 1998:148). The δ subunit consists of one transmembrane segment that acts as a membrane anchor for the α_2 subunit, which is extracellular (Ashcroft, 2000:165). Co-expression of the $\alpha_2\delta$, γ and α_1 subunits change some of the functional characteristics of the α_1 subunit (Catterall, 1991:1499). Co-expression of the $\alpha_2\delta$ and α_1 subunits causes an increase in current amplitude, faster activation and inactivation kinetics and a hyperpolarizing shift in the voltage dependence of activation as well as faster rate of ligand binding. The $\alpha_2\delta$ subunit relies on the co-expression of β subunits in order to have any significant effect (Walker & De Waard, 1998:148). The γ subunit features predominantly in modulating the biophysical properties of the channel and does not have a significant role in transport of the VDCC to the membrane, unlike the $\alpha_2\delta$ and β subunits (Harpold *et al.*, 1998:218; Arikkath & Campbell, 2003:303). The γ subunit causes increased peak currents, acceleration of activation and hyperpolarizing shift in activation (Walker & De Waard, 1998:148).

3.2.2 Distribution

L-type channels appear to be a prominent feature in all types of cardiac myocytes, whereas T-type channels are much more variable (Bers & Perez-Reyes, 1999, 340). T-type current densities are highest in conduction and pacemaker cells, mainly in sinusal or atrial cells and much reduced or nonexistent in ventricular myocytes. The distribution differs among species e.g. T-type currents are prominent throughout the guinea-pig and hamster heart, but are virtually absent in adult ventricular myocytes of rat, cat and dog (Nargeot *et al.*, 1997:A19; Perez-Reyes, 2003:125). L-type channels have a wide distribution in heart muscle being found in most tissues like purkunje fibres, SA-node, AV-node, latent pacemaker cells the ventricle and atrium (Balke & Gold, 1992:398).

3.2.3 Electrophysiological characteristics

VDCCs have only two distinguishable conductance levels, open and closed, and there is no evidence for the intermediate conductance levels sometimes found for other ionic channels. Depolarizing of the membrane causes the opening of the VDCC and Ca^{2+} can cross the hydrophobic lipid membranes by passing through these regulated pores (Katz, 1993:1244).

The LVA T-type channels require less negative potentials to become available, have shorter bursts of opening and are called "fast" because they inactivate rapidly (Opie, 1998:89). They have a single-channel conductance of ~8 pS (Table 1) and conduct Ba^{2+} equally well as Ca^{2+} (Perez-Reyes, 2003:132). L-type channels are HVA, sensitive to DHP's and have a relatively large single channel conductance (~15-27 pS in ~100 mM Ba^{2+}) (Table 1). When Ca^{2+} (10 mM) is used as charge carrier, the single channel conductance is smaller, 4 - 5 pS for T-type channels (Balke *et al.*, 1992:252) and 6.9 pS for L-type channels (Rose *et al.*, 1992:271). From a holding potential of -50 mV, only L-type channels are available to open with depolarization. When the holding potential is kept at -90 mV, T-type channels contribute an additional rapidly inactivating component superimposed upon the L-type current. T-type currents peaked within 10 ms and inactivate completely within 50 - 100 ms. (Balke *et al.*, 1992:252; Rose *et al.*, 1992:271). Experiments with cultured myocytes showed that during depolarization from a holding potential of -100 mV, T-type currents activated at -60mV and peaked between -40 and -30 mV (Balke *et al.*, 1992:252; Richard *et al.*, 1992:97; Nargeot *et al.*, 1997:A17), while L-type currents activated at -30 mV and peaked at more positive potentials, between -5 and 10 mV (Rose *et al.*, 1992:271; Richard *et al.*, 1992:97;

Nargeot *et al.*, 1997:A17; Hille 2001:58). Both currents reversed at around +30 mV (Richard *et al.*, 1992:97; Nargeot *et al.*, 1997:A17).

In electrophysiological studies usually carried out by means of the patch-clamp technique, activity of L-type channels decreases when the cytoplasmic side of the channels is perfused with artificial intracellular solutions. This phenomenon of run-down of VDCCs is well known. Possible mechanisms of run down are 1) dephosphorylation of channel protein due to loss of protein kinases or activation of appropriate protein phosphatases; 2) proteolysis of channel molecule by activation of intrinsic proteases; 3) decoupling of GTP-binding protein from the channel and 4) loss of other cytoplasmic factors required for channel activity. Other hypotheses are that run-down are caused by a rise in intracellular Ca^{2+} concentration and a loss of high energy compounds. The amino acid sequence 1572-1651 in the carboxyl terminal tail of the α_1C subunit was found to be critical for inactivation and independently represents an important structure for L-type channel run-down (Kameyama *et al.*, 1988:329; Belles *et al.*, 1988:358; Kepplinger *et al.*, 2000:128).

3.2.4 Phosphorylation

Many endogenous factors like neurotransmitters, catecholamines and hormones are able to modulate the opening of cardiac VDCCs and then regulate inotropism and chronotropism. The modulation of VDCCs by pacing frequency and protein kinase induced phosphorylation is of major importance. The activity of L-type channels is strongly dependent on the frequency of stimulation or cardiac chronotropism. Several protein kinases (PKA, PKC, cam-kinase II and PKG) may be activated by membrane receptors acting through second messengers to modulate activities of VDCCs. Best

known is the regulation of the L-type current by β-adrenergic stimulation, via PKA dependent phosphorylation (Fozzard, 1992: 6D; Nargeot *et al.*, 1997:A17). β-adrenergic stimulation (catecholamine stimulation) causes the following cascade reaction: activation of adenyl cyclase that increases internal cAMP and then activation of a kinase enzyme that transfers a phosphate group from ATP to the α_1 subunit of the VDCC. The VDCC is phosphorylated in the C-terminal tail increasing the opening probability of the channel. The resulting larger Ca^{2+} current lowers the threshold for action potential initiation and thereby increases the heart rate (increases conduction through the AV node and increases the firing rate of normal and subsidiary pacemakers), whereas the accompanying rise in Ca^{2+} entry enhances Ca^{2+} release from intracellular stores and potentiates contractile force, thus an enhanced inotropic response (Carmeliet, 1986:137; Schneider *et al.*, 1997:9; Opie, 1998:88; Ashcroft, 2000:164).

3.2.5 Pharmacology

Pharmacological modulation by blocking of voltage dependent L-type channels is a major therapeutic principle in the treatment of cardiovascular disorders (Carbone & Lux, 1989:346; Mitterdorfer *et al.*, 1998:351). The Ca^{2+} channel α_1 subunit is the primary target for most Ca^{2+} channel antagonists, which can be subdivided into three general classes: small organic antagonists, inorganic antagonists and peptide toxins. Another type of organic substance that influences VDCCs is the organic agonists (Kamp *et al.*, 1989:338). Each of these classes will be described further.

3.2.5.1 Organic antagonists

The major functional property of the VDCC is to regulate the entry of Ca^{2+}. This process is inhibited when Ca^{2+} antagonist drugs bind to the binding sites on the Ca^{2+} channel protein, causing the closure of the channel and subsequent inhibition of Ca^{2+} flux from the extracellular to the intracellular space (Cummings *et al.*, 1991:251). Ca^{2+} antagonists refer to several structurally different families of synthetic molecules, which specifically inhibit L-type currents. These molecules are potent vasodilators and are widely used in the treatment of hypertension and angina pectoris. L-type channel antagonists depress conduction through the AV node, therefore making them useful drugs for the treatment of many supraventricular arrythmias. Effects of Ca^{2+} channel antagonists at the membrane level causes a negative chronotropic, negative dromotropic and negative inotropic effect in the heart and an intense dilatation in the vasculature in vivo (Carmeliet, 1986:144; Shorofsky & Balke, 2001:137).

The main classes of VDCCs antagonists are DHPs (represented by nifedipine, nicardipine, nisoldipine), phenylalkylamines (represented by verapamil, D600) and benzothiazepines (represented by diltiazem). Various studies have been done to determine the effects of the organic channel antagonists on VDCCs. These molecules bind directly to different sites of the VDCC α_1 subunit. DHPs bind more specifically to the inactivated state of the channel, which is consistent with an enhanced effect on depolarized tissues. Phenylalkylamines are frequency dependent, which means that their affinity is higher for open than for inactivated channels. Benzothiazepines enter the channel from the extracellular side and bind to S6 (Nargeot *et al.*, 1997:A18; Opie, 1998: 72; Noll & Lüscher, 1998:10; Grace & Camm, 2000:44; Kochegarov, 2003:147).

Initial research showed that cardiac L-type channels seemed to be exquisitely sensitive to the DHP, phenylalkylamine and benzothiazepines type antagonists and that T-type channels appeared to be resistant (Hagiwara *et al.*, 1988:240; Tytgat *et al.*, 1988:691; Bean, 1989:335; McDonald *et al.*, 1989:571; Balke & Gold, 1992:401; Mori *et al.*, 1993:88). Recent studies showed that T-type currents are blocked in various tissues by concentrations of L-type antagonists such as DHPs higher than those used for L-type channels (Nargeot *et al.*, 1997:A19). L-type channels are also blocked by pyrimidine derivatives (lamotrignine) and piperazine and piperidine derivatives (flunarizine and cinnarizine). These VDCC antagonists are widely used in the treatment of a variety of diseases, such as arrythmias and hypertension (Kochegarov, 2003:151). More extensive studies have proved that blockers of T-type channels include nimodipine (Randall & Tsien, 1996:38; Perez-Reyes, 2003:148).

In addition to the main classes of VDCCs antagonists, mibefradil (Ro 40-5967), a tetralol derivative, has been found to block VDCCs. The main characteristic of mibefradil is its ability to block both L and T-type channels (Noll & Lüscher, 1998: 10; Jiménez *et al.*, 2000:2; Kochegarov, 2003:156). It was shown that mibefradil blocked L-type channels voltage dependently, while the T-type channel block occurred at hyperpolarized membrane potentials and showed no voltage or use-dependence, suggesting that it bound to the rested state of the T-type channel (Mehrke *et al.*, 1994:1487; Welling *et al.*, 1995:405; Jiménez *et al.*, 2000:9).

3.2.5.2 Inorganic antagonists

VDCCs are also blocked by a number of inorganic antagonists including various cations. Inorganic antagonists interfere with the channel because of their resemblance

to the Ca^{2+} ion itself. The foreign ion is mistaken by the channel for a permeant ion and passes through the membrane (Carmeliet, 1986:137). Cations that block cardiac VDCCs are Ni^{2+}, Cd^{2+} and some other less well-known ions. Ni^{2+} inhibits VDCCs via two distinct mechanisms. Firstly, Ni^{2+} blocks the channel in a 1:1 interaction, which may occur within the permeation pathway and secondly, it increases the threshold for channel activation. The affinities of Ni^{2+} for the various channels subtypes differ, with the L-type channel α_1C being the most sensitive, followed by $\alpha_1E > \alpha_1A > \alpha_1B$. Low concentrations of Ni^{2+} (40-100 μM) block macroscopic T-type currents (Zamponi *et al.*, 1998:93; Lacinová *et al.*, 2000:1257). It was shown by Bean (1985:10) that 2 mM Co^{2+} blocks both the L and T-type channels to a similar degree. Other metal ions that block VDCCs are Cd^{2+} (50 μM) and Ho^{2+} (Hagiwara *et al.*, 1988:238; Le Grand *et al.*, 1990:H1621; Alvarez & Vassort, 1992:529; Snutch *et al.*, 2001:12). Pb^{2+} is a well-known inhibitor of VDCCs in several types of cells. In a study of Peng *et al.* (2002:1420), inward Ba^{2+} currents through L-type channels were decreased by 0.1 μM and 1.0 μM Pb^{2+}. Except for the divalent cations, other substances also block VDCCs. Tetramethrin (0,1 μM) was shown to block T-type channels (Hagiwara *et al.*, 1988:238) and amiloride and octanol are also known antagonists of T-type channels (Randall & Tsien, 1996:38; Uchitel & Katz, 1997:38; Lacinová *et al.*, 2000:1257).

3.2.5.3 Organic agonists

Organic agonists can also be described as channel activators which stabilize the channel in open mode, therfore increasing the time that a channel spends in the open state during depolarization. Some of the DHPs can act as an antagonist and agonist depending on different structural elements of the molecule. Certain enantomers of DHPs show different effects on the VDCC. The most likely role in determining the

agonistic versus antagonistic properties is the orientation of a certain phenyl group (Kochegarov, 2003:146). For example SDZ (+) 202-791 is a channel agonist, while the (-) 202-791 enantomer acts as a blocker (Kamp, *et al.*, 1989). Bay K8644 increases the chances that the channel will show a mode of gating marked by long opening and brief closing events. Bay K8644 has been shown to strongly enhance channel current, peak inward current and whole cell current. Bay K8644 altered the voltage and time-dependence of Ca^{2+} channel currents carried by either Ba^{2+} or Ca^{2+}. The reversal potential remained unchanged. The pronounced changes in kinetics suggest that Bay K8644 modifies Ca^{2+} channel gating (Hess *et al.*, 1984:538; Sanguinetti *et al.*, 1986:370; Kamp *et al.*, 1989:348; Tiaho *et al.*, 1990: 59). T-type channels seem to be unaffected by this agonist (Balke & Gold, 1992:401). Isoproterenol is a β-adrenergic agonist, which increases channel availability and increases the occurrence of a long-opening mode of the L-type channel. The increase in Ca^{2+} current increases conduction through the AV node, increases the firing rate of pacemakers and causes an increased heart rate. Isoproterenol and other agonists like fenoterol are used in the treatment of asthma and bradycardia (Shorofsky & Balke, 2001:131). Another agonist is the benzoylpyrrole FPL 64176 which also prolonged action potential duration and enhanced contractility in guinea-pig papilliary muscle (Rampe, 1993:1128). Ouabain (10^{-6}M) increases both T and L-type currents in guinea-pig myocytes (Le Grand *et al.*, 1990:H1621; Alvarez & Vassort, 1992:529).

3.2.5.4 Interactions of natural toxins with Ca^{2+} channels

Characterization of molecular targets of animal venoms provides information about how they affect cells and as a consequence provides information on how to treat the bites or stings. Moreover, this characterization may reveal which pharmacological

activities are present that could be of interest as tools to investigate ion channel function (Kushmerick *et al*, 2001:991). Natural toxins that interact with Ca^{2+} channels have been isolated from various animals (Miljanich, 1997:7).

Marine cone snail (genus: *Conus*) venom contains peptides known as conopeptides. The conopeptides can be divided into two major groups, the disulphide-rich conotoxins and nondisulphide-rich peptides. The disulphide rich conotoxins can be divided into several superfamilies. The ω-conotoxins, which target the VDCCs, belongs to the O-superfamily. The conotoxins from the other superfamilies target a variety of ion channels including K^+ and Na^+ channels (McIntosh & Jones, 2001:1447, Olivera & Cruz, 2001:12; Terlau & Olivera, 2004:54). Every conotoxin serves as a highly specific ligand, each with a particular molecular target. Binding of the peptide ligand to its target leads to a change in physiological function (Shen *et al.*, 2000:102; Olivera & Cruz, 2001:11). The ω-conotoxins are small, constrained peptides of 24-31 amino acids in length and contain six cysteine residues that form three disulphide bridges (Shen *et al.*, 2000:102). They include the pore blockers ω-CTx GVIA (*C. geographus*), ω-CTx MVIIA and ω-CTx MVIIC (both isolated from *C. magus*). These conotoxins block the N and P/Q-type channels respectively (Shen *et al.*, 2000:102; McIntosh & Jones, 2001:1447, Olivera & Cruz, 2001:12).

Peptide toxins isolated from hunting spiders include the gating inhibitors ω-Aga IVA and ω-Aga-IIIA isolated from *Agelenopsis aperta* and SNX-482 - a peptide isolated from tarantula venom. The Agatoxin, ω-Aga IIIA, blocks L-type channels in atrial myocytes as well as N and P/Q-type channels in neuronal cells, while ω-Aga IVA targets only the P/Q-type channels (Adams, 2004:521). A novel 74 amino acid peptide

toxin (DW 13.3) extracted from the venom of the spider *Filistata hibernalis* blocks L, N, R and P/Q-type currents in a variety of cultured mammalian cells and exogenous expression systems (Sutton *et al.*, 1998:414). The venom of the spider, *Segestria florentina* contains 25 polypeptide components of which a selective Ca^{2+} channel antagonist, SNX325, was recently isolated (Lipkin *et al.*, 2002:125). Venom of another spider, *Lasiodora,* inhibits Ba^{2+} currents through the L-type channels (Kushmerick *et al.*, 2001:1000).

Toxin peptides was also found in the venom of predatory insects. Ptu1 isolated from the venom of the assassin bug *Peirates turpis* blocks Ba^{2+} currents through L, N, and P/Q-type VDCCs expressed in BHK cell lines. This peptide shows considerable homology with ω-CTx GVIA and MVIIA (Corzo *et al.*, 2001:256-261).

Scorpion toxins include toxins that interact with ligand gated Ca^{2+} channels and VDCCs. $IpTx_a$ from the scorpion *Pandinus imperator* is an agonist of the ryanodine receptor, while $IpTx_i$ shows phospholipase A_2 activity and inhibits the ryanodine receptor (Valdivia & Possani, 1998:111). A peptide from the Chinese scorpion *Buthus martensi* Karsch, named BmK AS is also an activator of the ryanodine receptor (Lan *et al.*, 1999:816). Scorpion toxins that block VDCCs include kurtoxin isolated from the venom of the scorpion *P. transvaalicus.* This peptide contains 63 amino acid residues and has as predicted molecular mass of 7386.5 Da. Kurtoxin blocks the T-type channel in oocytes by modifying channel gating (Chuang *et al.*, 1998:668). Kurtoxin also interacted with high affinity with the T, L, N, and P-type channels in neurons and produced very different sets of gating modifications in the different channel types (Sidach & Mintz, 2002:2032). Two kurtoxin-like peptides were isolated from the

venom of *P. granulatus* and named KLI and KLII. KLII was determined to be identical to kurtoxin and KLI was shorter and had 62 amino acids. Kurtoxin from *P. granulatus* (KLII or KPg) blocked native voltage dependent T-type channels in mouse male germ cells. KLI was studied on recombinant $Ca_v3.3$ channels heterologously expressed in *Xenopus* oocytes and shown to shift the voltage for activation toward positive potentials (Olamendi-Portugal *et al.*, 2002:567). These two peptides were also investigated on VDCCs in spermatogenic cells where it inhibited the T-type channel as well as the sperm acrosome reaction (López-González *et al.*, 2003:413).

3.2.6 Physiological role of cardiac Ca^{2+} channels

Ca^{2+} entry into the cell triggers a variety of functional responses including muscle contraction (Tuana & Murphy, 1990:1482). The opening of VDCCs is involved in pacemaker depolarization, supports conduction through the AV node and generates and maintains the distinctive plateau of the cardiac action potential. In addition they serve as the primary gatekeepers for Ca^{2+} entry into cells, therefore transducing the electrical signals at the surface of the myocytes into the biochemical and mechanical events that result in a contraction. Alterations in channel function often lead to abnormal electrical activity and arrythmias (Katz, 1997; 171; Shorofsky & Balke, 2001:127).

The action potential is generated by a sequence of changes in electrical potential between the interior of the cell and the surrounding extracellular space. Depolarization occurs when positively charged Ca^{2+} and Na^{+} ions enter the cytosol of a resting cell to generate inward currents. The VDCCs are responsible for the platue phase of the action potential. Inward Ca^{2+} current underlies the upstroke of the action potential of the SA and AV nodes (Balke & Gold, 1992:398). In pacemaker cells of the SA node variations

in the rate of VDCC opening contribute to the control of heart rate (Fozzard, 1992:5D; Katz, 1993:1244-1248). The slower opening of smaller VDCCs causes slower nodal conduction than in cardiac tissues that use Na^+ as depolarizing cation. In addition to the influx of positive charge, Ca^{2+} ions function as second messengers that regulate a variety of cellular functions. Several intracellular enzyme systems are sensitive to changes in the concentration of intracellular Ca^{2+} (Balke & Gold, 1992:398).

T and L-type channels are ubiquitous and located in most excitable cells, where they are often co-expressed (Nargeot *et al.*, 1997:A16). The L-type channel is important in normal and abnormal cardiac excitation in the SA and the AV node and conduction through the AV node (Katz, 1997;171; Shorofsky & Balke, 2001:127). In cardiac ventricular cells, L-type channels play the predominant role as a source of Ca^{2+} in E-C coupling (Hess *et al.*, 1986:S20). In heart muscle, but also specialized conduction tissue, the main excitatory inward current underlying the action potential plateau flows through the L-type channels where they trigger E-C coupling (Shorofsky & Balke, 2001:128).

It appears that T-type channels do not have a large role in the generation of action potential or in excitation-contraction coupling in normal myocardial cells. T-type channels may be important in cells that normally display automaticity, such as the pacemaking cells of the SA node or the specialized conduction fibres of the Purkinje system (Balke & Gold, 1992:402). Because of their activation at more negative potentials, T-type channels might contribute to the diastolic depolarization found in cardiac pacemaker cells (Hess *et al.*, 1986:S20). T-type channels are also able to maintain current during relatively mild depolarization from rest and this sustained Ca^{2+}

entry has important implications for pacemaker potentials in SA node cells and hence initiation of heart beat (Randall & Tsien, 1996:38).

4. Pathology of Ca^{2+} channels

VDCCs play an important role in regulating Ca^{2+} homeostasis and these channels have been implicated in the pathology of an increasing number of diseases (Triggle, 1999:311). The underlying defects in VDCCs in disease states are wide-ranging and include absence/improper synthesis of channel proteins, aberrant regulation of channel function and autoimmune responses involving aberrant targeting of channel proteins (Richard *et al.*, 1998:300). Consequences of defective VDCC structure, function or regulation are also wide ranging. They include cellular dysfunction as a result of alterations in Ca^{2+}-dependent signaling processes such as E-C coupling or E-S coupling or cell injury and death, resulting from cytotoxic effects of intracellular Ca^{2+} overload (Hosey *et al.*, 1996:266; Richard *et al.*, 1998:300; Triggle, 1999:311).

VDCCs are implicated in a number of pathological disorders, including skeletal muscle, neuronal and cardiac disorders. Neuronal disorders include congenital migraine, cerebellar ataxia, angina and epilepsy (Snutch *et al.*, 2001:11). Skeletal muscle disorders include malignant hyperthermia, an inherited disorder of the ryanodine receptor. Disorders of the VDCC cause sporadic Lambert Eaton myasthenic syndrome in humans and in animals, Dystrophic mouse (Brown, 1993:312).

VDCCs play an important role in the pathology of cardiac disorders. L-type channels play potentially important roles in arrhythmia generation under pathological conditions and their treatment. In addition to various structural and biochemical abnormalities,

regulation of intracellular Ca^{2+} is also defective during heart failure. VDCCs can also support slow conduction in re-entrant circuits, especially in depolarized tissue (Balke & Gold, 1992:402; Shorofsky & Balke, 2001:12). Ca^{2+} antagonists are used in treatment of Angina, atrial fibrillation and flutter, hypertension, peripheral vascular disorders (Raynaud's) and cerebral vasospasms (Triggle, 1999:316).

5. Scientific and therapeutic value of natural peptides

Advances in molecular genetics have been important in identifying ion channel subunits and several inherited disorders termed channelopathies, which result from mutations in ion channels (Lehman-Horn & Jurkat-Rott, 1999:1318). These mutant ion channels represent targets for the study of new drugs and therapies in the treatment of channelopathies. Natural products like morphine derived from opium poppy have been used as therapeutics for a long time (Shen *et al.*, 2000:98). Natural peptides isolated from the venom of poisonous animals have become important in the research of ion channels, for example TTX isolated from the puffer fish (*Tetrodontidae*) has been used extensively in the study of Na^{+} channel pharmacology (Shen *et al.*, 2000:99).

The discovery of specific *Conus* and spider toxins has also been important in identifying the existence of several subtypes of neuronal HVA Ca^{2+} currents. The N-type channels are selectively blocked by ω-CTx GVIA, while the P-type channel is blocked by ω-CTx MVIIC. These conotoxins have been important in the characterization of these channels (Terlau & Olivera, 2004:52). Aside from their functions in identifying and blocking ion channels, the ω-conotoxins may have potential therapeutic functions in stroke and pain (Shen *et al.*, 2000:102). Much of the

resent research in the area of novel Ca^{2+} channel therapeutics to treat neuropathic pain has centered on Ziconotide (SNX-111), a synthetic derivative of ω-CTx MVIIA. Ziconotide has been evaluated in a number of clinical trials for the treatment of various conditions including HIV-related neuropathic pain and certain pain associated with cancer (Snutch *et al.*, 2001:12).

Agatoxins modify insect and mammalian receptors and ion channels. The principle uses for agatoxins have been as pharmacological tools to characterize ion channels. The ω-agatoxins have been especially important in the characterization of the P/Q-type channels (ω-Aga-IVA), while ω-Aga-IIIA has been used in the study of T-type channels in cardiac myocytes because of its specific block of L-type channels (Nargeot *et al.*, 1997:A16; Tottene *et al.*, 1998:77). The μ-agatoxins have been formulated as candidate engineered biopesticides and are being investigated for commercial use (Adams, 2004:521).

Polypeptide scorpion toxins are potent and selective compounds that act on various ion channels. Because of their specificity and high affinity, they have also been used as tools to characterize various receptor proteins involved in ion channel functioning (Lecomte, 1998:151). Long chain scorpion toxins, which include α and β-toxins, have been important in the functional and structural mapping of Na^+ channel proteins and include toxins from Asian (*Buthus martensi* Karsch) and American (*Centroides*) scorpions (Gordon *et al.*, 1998:136). Peptides isolated from South African scorpions like PBTx3 (*P. transvaalicus*) have been important in characterizing K^+ channels (Huys *et al.*, 2002:1854), while Kurtoxin (*P. granulatus*) has been important in blocking of VDCCs (Sidach & Mintz, 2002:2032). PBITx1 (*P. schlechteri*) has also been

important in studies of Cl^- channels of insects (Tytgat *et al.*, 1998:387). An understanding of the structure-function relationship of scorpion toxins is important in the potential use of these toxins for insect control. While scorpion toxins continue being valuable tools in the study of ion channels, they are also contributing to the study of ligand-receptor interactions and drug design (Loret & Hammock, 2001:221). Anti-microbial peptides isolated from scorpion venom are important in the discovery of novel antibiotic molecules (Corzo *et al.*, 2001:44), for example Scorpine (*Pandinus imperator*) has anti-bacterial and anti-malaria effects (Conde *et al.*, 2000:166).

Guidelines for the Author

Toxicon

An interdisciplinary Journal on the Toxins from Animals, Plants and microorganisms. Official Journal of The International Society on Toxinology.

1. Description

To publish articles containing the results of original research on problems related to poisons derived from animals, plants and microorganisms. To provide a medium for the publication of papers on the chemical, pharmacological, zootoxicological, and immunological properties of natural poisons. To publish clinical observations on poisoning where a new therapeutic principle has been proposed or a decidedly superior clinical result has been obtained. To publish material on the use of toxins as tools in studying biological processes and material on subjects related to venom-antivenom problems. To publish occasional review articles on problems related to toxinology. To abstract the current literature on venoms, antivenoms and other poisons and antipoisons. To encourage the exchange of ideas, sections of the journal may be devoted to Short Communications, Letters to the Editor and activities of the International Society on Toxinology.

2. Guide for Authors

2.1 Submission of Papers

Authors are requested to submit three copies of their manuscript and figures (regular papers, short communications, letters to the editor and announcements) to: Prof. Alan L. Harvey, Department of Physiology and Pharmacology, University of Strathclyde, 27 Taylor Street, Glasgow G4 0NR, Scotland, UK.

Review manuscripts on topics of interest to toxinologists and abstracts of articles of interest to toxinologists published in journals other than *Toxicon* should be sent to Prof. P.N. Strong, Sheffield Hallam University, Division of Biomedical Sciences, Sheffield S1 1WB, UK.Mini-reviews and proposals for mini-reviews should be sent to Prof. André Ménez, D.I.E.P., CEA/SACLAY, Bâtiment 152, 91191 Gif-sur-Yvette Cedex, France.
Submission of a paper implies that it has not been published previously, that it is not under consideration for publication elsewhere, and that if accepted it will not be published elsewhere in the same form, in English or in any other language, without the written consent of the publisher. The Editor welcomes submission by the authors of the names and addresses of up to four or five individuals who could expertly review the submitted manuscripts, and who are not from the same institutions as the authors. The Editor, of course, reserves the right to use these or other reviewers of his choice.

Language: English is the preferred language, but where submission of a manuscript in English is not possible, French, German or Spanish can be used as long as the paper is accompanied by a 200-300 word English abstract.

2.2 Manuscript Preparation

General: Manuscripts must be typewritten, double-spaced with wide margins on one side of white paper. Good quality printouts with a font size of 12 or 10 pt are required. The corresponding author should be identified (include a Fax number and E-mail address). Full postal addresses must be given for all co-authors. All numbers should be numbered consecutively. Authors should consult a recent issue of the journal for style if possible. An electronic copy of the paper should accompany the final version. The Editors reserve the right to adjust style to certain standards of uniformity. Authors should retain a copy of their manuscript since we cannot accept responsibility for damage or loss of papers. Original manuscripts are discarded one month after publication unless the Publisher is asked to return original material after use.

Paper length: Toxicon has set no standard length for papers, but the Editors insist upon a clear presentation of data in as concise a form as is consistent with good reporting. The fragmentation of a report into several short papers is discouraged.

Abstracts: There should be an abstract of no more than 200 words.

Text: Follow this order when typing manuscripts: Title, Authors, Affiliations, Abstract, Keywords, Main text (introduction, materials and methods, results and discussions), Acknowledgements, Appendix, References, Vitae, Figure Captions and then Tables. Do not import the Figures or Tables into your text. The corresponding author should be identified with an asterisk and footnote. All other footnotes (except for table footnotes) should be identified with superscript Arabic numbers.

Units: Units of measure must be clearly indicated.

Symbols: The Latin name must be given for all animal and plant species. Trade names or abbreviations of chemicals may be used only when preceded by the chemical or scientific name. Thereafter, trade names, common names or abbreviations should be used.

Mathematical equations: Compound numbers should be in bold face Arabic numerals or underscored.

Acknowledgements: All sources of funding supporting the work are to be declared. Authors are to disclose all financial relationships with any persons or organisations that could be perceived to bias the work described in the manuscript. These acknowledgements should be placed after the text and before the references, under the heading "Acknowledgements". In submitting the article for consideration for publication, the author(s) attest that all potential conflicts of interest have been disclosed and addressed in the manuscript.

References: All publications cited in the text should be presented in a list of references following the text of the manuscript. In the text refer to the author's name (without initials) and year of publication (e.g. "Since Peterson (1993) has shown that?" or "This is in the agreement with results obtained later (Kramer, 1994)"). For three or more authors use the first author followed by "et al.", in the text. The list of references should be arranged alphabetically by authors' names. The manuscript should be carefully checked to ensure that the spelling of authors' names and dates are exactly the same in the text as in the reference list.

References should be given in the following form:

Mihelich, E.D., Carlson, D.G., Fox, N., Song, M., Schevitz, R.W., Snyder, D.W., 1997. Structure based design and therapeutic potential of phospholipase A_2 inhibitors. In: Uhl, W., Nevalainen, T.J., Buchler, M.W. (Eds.), Phospholipase A_2 Basic and Clinical Aspects in Inflammatory Disease, Karger, Basel, pp. 140-145.

Possani, L.D., 1984. Structure of scorpion toxins. In: Tu, A.T.T. (Ed.), Handbook of natural toxins, vol. 2. Marcel Dekker, New York, pp. 513-550.

Smith, L.A., 1998. Development of recombinant vaccines for botulinum neurotoxin. *Toxicon* 36 (11), 1539-1548.

Illustrations: All illustrations should be provided in camera-ready form, suitable for reproduction (which may include reduction) without retouching. Photographs, charts and diagrams are all to be referred to as "Figure(s)" and should be numbered consecutively in the order to which they are referred. They should accompany the manuscript, but should

not be included within the text. All illustrations should be clearly marked on the back with the figure number and the author's name. All figures are to have a caption. Captions should be supplied on a separate sheet.
Line drawings: Good quality printouts on white paper produced in black ink are required. All lettering, graph lines and points on graphs should be sufficiently large and bold to permit reproduction when the diagram has been reduced to a size suitable for inclusion in the journal. Dye-line prints or photocopies are not suitable for reproduction. Do not use any type of shading on computer-generated illustrations.
Photographs: Original photographs must be supplied as they are to be reproduced (e.g. black and white or colour). If necessary, a scale should be marked on the photograph. Please note that photocopies of photographs are not acceptable. Photographs must be kept to a minimum.

Colour: Where colour printing is required the author will be charged for colour printing at the current colour printing costs.

Tables: Tables should be numbered consecutively and given a suitable caption and each table typed on a separate sheet. Footnotes to tables should be typed below the table and should be referred to by superscript lowercase letters. No vertical rules should be used. Tables should not duplicate results presented elsewhere in the manuscript, (e.g. in graphs).

3. Electronic Submission

Authors should submit an electronic copy of their paper with the final version of the manuscript. The electronic copy should match the hardcopy exactly. Always keep a backup copy of the electronic file for reference and safety. Full details of electronic submission and formats can be obtained from http://authors.elsevier.com.

4. Submission on Disk after Acceptance for Publication

Elsevier Science now publishes all manuscripts using electronic production methods and strongly encourages submission on disk. Please send the electronic files of your article along with the hardcopy of the accepted version. To ensure fast and easy processing of your submission, please adhere to the following guidelines:

1. Save text and graphics on separate disks.
2. Label all disks with your name, a short version of the article title, the journal to be published in, and the filenames. Please also include details of the software and platform (PC, Mac, UNIX, etc) used to create your files.
3. Ensure that the files on the disk match the hardcopy exactly. In cases of a discrepancy, the hardcopy version will be used as the definitive version.

5. Proofs

Proofs will be sent to the author (first named author if no corresponding author is identified of multi-authored papers) and should be returned within 48 hours of receipt. Corrections should be restricted to typesetting errors; any others may be charged to the

author. Any queries should be answered in full. Please note that authors are urged to check their proofs carefully before return, since the inclusion of late corrections cannot be guaranteed. Proofs are to be returned to the Log-in Department, Elsevier Science, Stover Court, Bampfylde Street, Exeter, Devon EX1 2AH, UK.

6. Offprints

Where the research is supported by a fund which can be used for pages charges, the author is invited to make a voluntary contribution towards publication costs, in which case 100 offprints will be supplied free of charge. Additional offprints and copies of the issue can be ordered at a specially reduced rate using the order form sent to the corresponding author after the manuscript has been accepted. Orders for reprints (produced after publication of an article) will incur a 50% surcharge.

7. Copyright

All authors must sign the "Transfer of Copyright" agreement before the article can be published. This transfer agreement enables Elsevier Science Ltd to protect the copyrighted material for the authors, without the author relinquishing his/her proprietary rights. The copyright transfer covers the exclusive rights to reproduce and distribute the article, including reprints, photographic reproductions, microfilm or any other reproductions of a similar nature, and translations. It also includes the right to adapt the article for use in conjunction with computer systems and programs, including reproduction or publication in machine-readable form and incorporation in retrieval

systems. Authors are responsible for obtaining from the copyright holder permission to reproduce any material for which copyright already exists.

8. Author Services

For queries relating to the general submission of manuscripts (including electronic text and artwork) and the status of accepted manuscripts, please contact Author Services, Log-in Department, Elsevier Science, The Boulevard, Langford Lane, Kidlington, Oxford OX5 1GB, UK. E-mail: authors@elsevier.co.uk, Fax: +44 (0) 1865 843905, Tel: +44 (0) 1865 843900. Authors can keep a track of the progress of their accepted article on the Internet on our Author Gateway (go to http://authors.elsevier.com/) and key in the corresponding author's name and the Elsevier reference number.

CHAPTER 3 – Article

(Note: Toxicon's Guidelines to Authors state that figure numbering must be done on the reverse side of the figure and captions supplied on a separate page. To enable easier reading of the following article and for the purpose of the dissertation, the numbering and captions are given with each of the respective figures.)

Title

The electrophysiological effects of fractions isolated from the venom of *Parabuthus granulatus* on cardiac Ca^{2+} channels

Authors

L.H. du Plessis[a*], J.L. du Plessis[a], L.D. Possani[b], K. Dyason[a]

Affiliations

[a]*North-West University, Potchefstroom Campus, School for Physiology, Nutrition and Consumer Sciences, Potchefstroom, South Africa.*

[b]*Department of Molecular Medicine and Bioprocesses, Institute of Biotechnology, National Autonomous University of Mexico, Cuernavaca, Mexico.*

Abstract

The effect of fractions isolated from the venom of *Parabuthus granulatus* was investigated on Ca^{2+} channels in rat ventricular myocytes using the whole cell

* Corresponding author. Tel.: +27-18-299-2433.E-mail address: flglhdp@puk.ac.za (L. H. du Plessis) Abbreviations: EGTA, Ethylene Glycol-bis (β-aminoethyl Ether) N,N,N', N', - Tetraacetic Acid; HEPES, N- (2-hydroxyethyl) piperazine-N'-(2-ethanesulphonic acid); PEG polyethelene glycol; RP-HPLC, Reverse Phase High Performance Liquid Chromatography; TEA-Cl, tetraethylammonium chloride; TEA-OH, tetraethylammonium hydroxide.

configuration of the patch clamp technique. Fraction III (PgIII) isolated with a sephadex G50 column showed an agonistic effect on Ba^{2+} currents. PgIII increased the current by 50 % and modified the gating of the channel by delaying inactivation and shifting the voltage dependence of activation to more positive potentials. PgIII also delayed the time to peak significantly. PgIII was separated by RP-HPLC and three subfractions (SF I-III) were tested for Ca^{2+} channel activity. SFI showed agonism comparable to that observed with PgIII, whereas SFII and III decreased the Ba^{2+} current. SFI increased the rate of inactivation and time to peak significantly and shifted the voltage dependence of activation towards more negative potentials. SFII and III both delayed the rate of inactivation significantly, but had opposite effects on the time to peak and voltage dependence of activation. The agonistic effect of scorpion venom on cardiac Ca^{2+} channels has not been described in literature and are of special interest for further research. These fractions represent opportunities to isolate and purify novel peptides active on Ca^{2+} channel.

Keywords

Scorpion venom, agonistic, cardiac Ca^{2+} channels, *Parabuthus granulatus*

1. Introduction

Voltage dependent Ca^{2+} channels control a variety of physiological functions such as excitation contraction coupling in cardiac and smooth muscle, secretion of hormones and release of neurotransmitters (Catterall *et al.*, 2003). Overall, two categories of Ca^{2+} channels can be distinguished on the basis of their activation threshold. The first is LVA (Low voltage activated) channels, which includes T-type channels and the second category is HVA (high voltage activated) channels and includes the L, N,

P, Q, and R-type channels (Nargeot *et al.*, 1997; Catterall *et al.*, 2003). These channels differ in structure, electrophysiological and pharmacological characteristics, functions and distribution. Ca^{2+} channels in the heart only include the T- (LVA) and L- (HVA) type channels, where they play an important role in the generation and control of the action potential (Clozel *et al.*, 1999).

The Southern African scorpion *Parabuthus granulatus* (Ehrenberg, 1831) is part of the Buthidae family and is thought to be the most dangerous scorpion in the region (Prendini, 2001). The venom of scorpions from the Buthidae family is neurotoxic and *P. granulatus* produce mainly adrenergic effects (Müller, 1993). Scorpion venom can be described as complex mixtures that contain proteins and peptides with different but specific properties and functions. Peptide toxins derived from scorpion venom have become valuable tools for studies of voltage dependent ion channels (Sidach & Mintz, 2002). The characterization of compounds and toxins in the venom of scorpions that modulates physiological processes at the cellular level is of great importance. The discovery of new toxins can be of immense value in gaining insight into the mechanism of scorpionism. Furthermore, selective Ca^{2+} channel toxins can be used to purify channels from native tissue, determine subunit composition and the pharmacological and physiological roles of voltage dependent Ca^{2+} channels in certain target tissues (Tytgat *et al*, 1998; Huys *et al.*, 2002).

Numerous peptides isolated from scorpion venom have been found to interact with Na^{+} and K^{+} channels, but relatively little research has been done on Ca^{2+} toxins in scorpion venom (Possani *et al.*, 2000). The first Ca^{2+} channel selective peptides were isolated from the central African scorpion *Pandinus imperator*. These peptides were

proven to interact with the ligand gated Ca^{2+} channel, the ryanodine receptor (Valdivia & Possani, 1998). Toxins isolated from the venom of two South African scorpions *Parabuthus transvaalicus* and *P. granulatus* have been found to interact with voltage dependent Ca^{2+} channels in neuronal tissue and recombinant channels expressed in oocytes (Chuang *et al.*, 1998; Sidach & Mintz, 2002; Olamendi-Portugal *et al.*, 2002 & Lopez–Gonzales *et al.*, 2003). Chuang *et al.* (1998) initially showed that kurtoxin isolated from *P. transvaalicus*, inhibited LVA T-type channels. Later it was found that kurtoxin also interacts with HVA L, N and P-type channels in central and peripheral neurons (Sidach & Mintz, 2002). More recently, KLI and KLII (Kurtoxin-like peptides, KLII were later named KPg) were isolated from the venom from *P. granulatus*. These peptides inhibit T-type Ca^{2+} channel activity in mouse male germ cells and spermatogenic cells (Olamendi-Portugal *et al.*, 2002; Lopez-Gonzales *et al.*, 2003).

In studies using the crude venom of *P. granulatus* agonism of the cardiac L and T- type Ca^{2+} channels was observed in guinea-pig ventricular myocytes. The crude venom was isolated into four fractions using sephadex G50 columns. Although three of the four fractions had an agonistic effect, the effect observed with fraction III referred to as PgIII was more pronounced (Botha, 2002). In this report the electrophysiological effects of PgIII isolated from the venom of *P. granulatus* on cardiac Ca^{2+} channels in rat ventricular myocytes is described. This agonistic effect of scorpion venom on Ca^{2+} channels has not been described yet. PgIII was applied to an analytical RP-HPLC system for further fractionation in an attempt to identify the subfraction(s) containing the agonistic peptide(s). Three of these subfractions, named SFI, SFII and SFIII were selected for use in this study. The

electrophysiological effects of PgIII and the subfractions on Ba^{2+} currents through the Ca^{2+} channel were examined, using the whole cell configuration of the patch clamp technique.

2. Materials and methods

2.1 Venom collection and fractionation

P. granulatus scorpions were collected in the Northern Cape Province of South Africa. The scorpions were gathered by using UV lights during summer months in new moon. Venom was extracted by electrical stimulation of the telson and solubilized in deionized water. It was then freeze dried and kept at -20°C until fractionation was performed. Fractionation consisted of the venom being solubilized in 20mM ammonium acetate buffer (pH 4.7) applied to a Sephadex G-50 column (0.9 x 200cm) equilibrated and run with the same buffer. Four fractions of 2.5 ml were collected and pooled according to the absorbance at 280nm. Fraction III (1.8 mg in 1.5 ml) was used for further fractionation by C_{18} RP-HPLC, which separated over 22 subfractions. The column was calibrated in 0.1 % trifluoroacetic acid (TFA) in water and eluted with a 60 min linear gradient of 0-60% acetonitrile containing 0.1% TFA. Fractions were collected manually by monitoring the absorbance at 230 nm. Three of the subfractions with the highest peaks in the HPLC profile thought to indicate the highest contribution to the total fraction composition were tested for cardiac Ca^{2+} channel activity.

2.2 Cell isolation

Either male or female, six to eight week old Sprague-Dawley rats weighing approximately 150-200 g were used for the isolation of cardiac myocytes. Single ventricular myocytes were enzymatically isolated with the Langendorff-perfusion technique, as described by Mitra and Morad (1985) and later revised by Tytgat (1994). Anesthesia was induced in the animals by intraperitoneal injection with pentobarbitone (30mg/kg). The heart was excised and placed at room temperature in dissection-Tyrode solution containing (in mM) 137 NaCl, 0.5 $MgCl_2$, 11.6 HEPES, 1.8 $CaCl_2$, 60 glucose, 27 KCl, pH 7.4 with NaOH. The aorta was cannulated and mounted on the Langendorff-perfusion system. The heart was perfused for five minutes with heparinised Tyrode (in mM: 137 NaCl, 5.4 KCl, 0.5 $MgCl_2$, 11.6 HEPES, 1.8 $CaCl_2$, 10 glucose, pH 7.4 with NaOH) solution at 37°C and saturated with 100% O_2. The heart was then perfused for five minutes with Ca^{2+}-free Tyrode (in mM: 130 NaCl, 5.4 KCl, 1.2 KH_2PO_4, 1.2 $MgSO_4$, 6.0 HEPES, 10 glucose) solution. This was followed by perfusion for 24 minutes with Ca^{2+} -free Tyrode solution supplemented with Collagenase A and Protease type XXIV (both from Sigma, ST. Louis, MO, USA) and after that, five minutes perfusion with low Ca^{2+} (Tyrode with 0.18 $CaCl_2$) solution. The heart was placed in a petri dish containing low Ca^{2+} solution and single cells dispersed by agitation. The cells were resuspended in the low Ca^{2+} solution and after five minutes the solution was replaced by Tyrode. All experimental procedures were approved by the ethics committee of the North-West University (ethics number FLG-02D01).

2.3 Electrophysiological recordings

Experiments were performed at room temperature (25°C) using the patch clamp technique in the whole cell configuration (Hamill *et al.* 1981). Patch clamp recordings were made by using a DAGAN 8800 total clamp-amplifier. Micro-electrodes were made from borosilicate glass, with a Flaming/Brown micro-electrode puller (model P-97, Sutter Instrument Company, Novato CA. USA) and fire polished to achieve a resistance of two to five MΩ. A GΩ seal was made in Tyrode solution and three to five minutes were allowed for internal dialyses. This was followed by perfusion with the extracellular solution to allow the current to stabilize before control currents were recorded. Currents were recorded by using Clampex software, version 5.5 (Axon Instruments Inc., Foster City, CA, USA). To investigate the effects of the fractions on L-type channels, 120 ms pulses applied from a holding potential (HP) of -80 mV to a test potential of -10 mV was used. Deactivation current was investigated using the same protocol as above, but returning to -45 mV for 30 ms after the initial test potential. Current voltage relationships were measured by a series of 150 ms depolarizing pulses applied from a HP of either -90 or -50 mV to test potentials between -50 and 5 mV in 5 mV increments. Current amplitudes were stable under described conditions with virtually no run-down.

2.4 Solutions and drugs

The intracellular solution contained (in mM): 135 CsCl, 1.2 $MgCl_2$, 5 EGTA, 10 HEPES, 4 Mg-ATP, pH 7.2 with CsOH. The extracellular solution contained (in mM) 3 BaCl, 2 $MgCl_2$, 10 HEPES, 10 glucose, 140 TEA-Cl, pH 7.4 with TEA-OH. Ba^{2+} was used as charge carrier due to the larger currents observed with Ba^{2+} and it

has the additional advantage of suppressing the residual K^+ current (N'Gouemo & Morad, 2003). The fraction and subfractions were diluted in the extracellular solution and volumes of 5-10 µl were added to a static bath (120 µl) with a micropipette to obtain a final concentration as stated in the results. The protein concentrations of the subfractions were determined by resuspending the subfractions in a 100 µl Tyrode and reading the absorbance at 280 nm (assuming 1 unit A280 nm = 1mg/ml concentration). The protein concentrations measured at absorbance of 280 nm were 3.35 $mg.ml^{-1}$, 1.00 $mg.ml^{-1}$ and 0.60 $mg.ml^{-1}$ for SFI, II and III respectively. Stock solutions of BayK 8644 and nisoldipine were prepared in PEG 400 at concentrations of 5 mM. BayK 8644 and nisoldipine were diluted in the extracellular solution to obtain a concentration of 500 µM. A volume of 12 µl was added to a static bath with a volume of 120 µl to obtain a final concentration of 50 µM in the bath.

2.5 Data analysis

Inactivation

Exponential curve fitting of the inactivation phase of the current was done with Clampfit (Axon Instruments, Inc., Foster City, CA, USA) by using the following equation:

$$ICa = A^* \exp - \{-(t/\tau) + C\} \qquad \text{(equation 1)}$$

Where:

A = the amplitude of the maximum current through the Ca^{2+} channel that inactivates

τ = the time constant for inactivation

C = the time dependent current through the Ca^{2+} channel that inactivates slowly or not at all.

Activation

Microcal Origin, version 6 (Microcal Software, Inc., Northampton, MA, USA) was used to determine the maximum conductance. The following equation was used:

$g_{max} = I/ (E - E_{Ca})$ (equation 2)

Where:

I = the maximum current through the Ca^{2+} channel

E = the membrane potential

E_{Ca} = the equilibrium potential for Ca^{2+}.

To determine the shift in voltage dependence of activation, curve fitting was done using a Boltzman equation:

$ICa = g_{max} (E-E_{Ca}) / (1 + \exp(-(E-E_h) /s)$ (equation 3)

Where:

g_{max} = maximum conductance through the Ca^{2+} channel

E = the membrane potential

E_{Ca} = the equilibrium potential for Ca^{2+}

E_h = membrane potential for 50% activation

s = slope of the voltage dependence.

The significance of observed differences was determined by paired or unpaired students t-tests. A probability of 5 % or less was considered to be statistically significant and indicated with an asterisk (*). All experimental values are given as mean±SEM.

3. Results

3.1 Chromatographic separation of *P. granulatus* venom

Solubulized venom of *P. granulatus* was loaded into a Sephadex G-50 column and four main fractions were separated. These fractions were tested on guinea-pig ventricular myocytes as well as dorsal root ganglia neurons (Botha, 2002; Jordaan, 2002) and fraction III (PgIII) showed agonism in both cell types. In this study PgIII was further separated with RP-HPLC to determine whether the agonistic effect could be identified in one or more subfractions. Separation of PgIII resulted in over 22 subfractions and Figure 1 shows the main components. The subfractions at elution times 2.98 22.97, 23.81 and 24.89 minutes showed the highest peaks, probably indicating that these fractions contained larger amounts of protein. Three of the subfractions named SFI (22.97), SFII (23.81) and SFIII (24.89) were tested for Ca^{2+} channel activity.

3.2 Effect of PgIII on cardiac Ca^{2+} channels

Considering the agonistic effect that crude venom of *P. granulatus* as well as PgIII had on Ca^{2+} channels in guinea-pig myocytes and DRG neurons (Botha, 2002; Jordaan, 2002), it was also tested for activity on whole cell Ba^{2+} currents in rat ventricular myocytes. Figure 2A shows the current-voltage (I-V) relationship, where the peak current amplitude (I_{Ba}) is plotted as a function of the test potential (V_{test}). Depolarizing from a HP of -50 mV produced currents that had an apparent activation threshold of between -35 mV and -30 mV and reached the peak at -5 mV, which is representative of L-type currents (Hille, 2001). PgIII produced a large increase in the current as seen with crude venom and PgIII in guinea-pig myocytes (Botha, 2002). For the cell represented in Figure 2A (lower inset), the peak inward current at -5 mV

was increased by 56 % (HP = -50 mV). At a HP of -90 mV the mean peak current was increased by 40.11±5.52 % (n=3). Removal of PgIII, by washout, mostly produced only a partial recovery of the current at HP -50 mV and -90 mV (not shown). At both HP's the agonistic effect appears to be voltage dependent as the % agonism varied in the range of test potentials from -50 mV to 5 mV. PgIII did not significantly influence the reversal potential (E_{Ca}) of the current (20.10 mV in control vs. 17.30 mV with PgIII).

It is well known that *P. granulatus* crude venom is responsible for an α-effect on the Na^+ channel in cardiac myocytes (Debont *et al.*, 1998). Because the voltage dependence of Na^+ and Ca^{2+} channels overlap the observed agonistic effect may be mediated by Na^+ ions due to the α-effect. To eliminate this possibility, experiments were performed with a L-type specific Ca^{2+} channel blocker, nisoldipine. Half blocking concentrations of nisoldipine vary from cell to cell and are usually in the range of 20 nM to 50 μM (Hille, 2001; Kochegarov, 2003). Figure 2B shows traces recorded from a HP of -80 mV with depolarization to a test potential of -10 mV for 120 ms. PgIII increased the current by 54 % after 5 minutes exposure. Adding nisoldipine (50 μM) to the bath resulted in a substantial decrease (66 % with respect to the control) of the current after 8 minutes.

The effect of PgIII on the voltage dependence of activation was determined by fitting the I-V relationship (recorded from a HP of -50 mV) with equation (2) and (3) and the result is depicted in Figure 2C. PgIII increased maximum conductance (g_{max}) by 100 % (0.01 nA in control to 0.02 nA with PgIII). There was a positive shift in the midpoint of activation ($V_{½}$) to depolarizing potentials, from -16.21 mV in control to

-12.39 mV after PgIII. A minimal shift in the $V_{½}$ could be observed at HP = -90 mV (-29.57 mV in control to -27.10 mV with PgIII). The slope of the activation curve was not significantly influenced. An interesting observation with PgIII was the effect on the deactivation current (Figure 2D). Fitting the time course of deactivation with equation (1) showed a significant increase in the time constant for deactivation from 3.51±1.08 ms in control to 4.14±1.00 ms after PgIII (paired t-test, $p \leq 0.05$; n=3).

Analysis of the time to peak duration indicated that activation of the Ba^{2+} currents required times of 10.92±0.52 ms in control and 13.18±0.95 ms in the presence of PgIII at a test potential of -5 mV (n=3). This increase occurred at all test potentials but was only statistically significant at -20 and -10 mV. Exponential fittings for the time course of inactivation were done with equation (1) to determine if PgIII has an influence on the decay phase of the current. In control conditions and after addition of PgIII, the time course of inactivation could best be described with a single exponential (τ). The inactivation time constant increased from 21.48±7.13 ms in control (n=3) conditions to 29.37±.9.21 ms after PgIII at -5mV (n=5). Inactivation was delayed at all the test potentials but it was only statistically significant at -5 mV and 0 mV (unpaired t-test, $p \leq 0.05$).

3.2 Effect of subfractions I, II and III on cardiac Ca^{2+} channels

Figure 3A represents Ba^{2+} currents elicited from a HP of -50 mV in control conditions and in the presence of the subfractions. SFI (140 $\mu g.ml^{-1}$) increases the mean inward peak current by 36.95±9.46 % at -15 mV (n=4). The peak current in control conditions was observed at -10 mV but was shifted to -15 mV after addition of SFI. As with PgIII, the effect of SFI could only be partially washed out (not shown).

When depolarizing from a HP of -90 mV the current is increased by 71.98±24.29 % (n=3) at a test potential of -10 mV (results not shown). SFII (42 $\mu g.ml^{-1}$) and SFIII (25 $\mu g.ml^{-1}$) decreased the peak current by 73.67 % and 81.84 % respectively at a test potential of -10 mV (Figure 3A). The mean decrease in current was 51.51±13.24 % (n=3) in the presence of SFII and 40.83±14.58 % (n=4) with SFIII at a test potential of -10 mV. All three of the subfractions shifted the reversal potential of the current. SFI shifted the reversal potential significantly from 47.60±7.23 mV in control to 39.09±5.72 (n=3), SFII from 15.31 mV in control to 17.91 mV and SFIII significantly from 38.25±13.96 mV in control to 27.95±9.34 mV with SFIII (n=3) (paired t-test, $p \leq 0.05$). The antagonistic effect of SFII and SFIII could only be reversed partially (not shown). Figure 3B summarizes the mean % agonism or antagonism plotted as a function of the test potential. In the presence of SFI the mean % agonism is largest at more negative membrane potentials and decreases at more positive membrane potentials. The % increase in the current at -30 mV is 165.02±65.77 % and at 5 mV only 20.65±8.67 %, which differs statistically from the % at -30 mV (n=3). This indicates that the effect is voltage dependent. The effect of PgIII was only weakly voltage dependent where the % increase was between 21 % and 48% at test potentials -30 mV and 5 mV. The % antagonism in the presence of SFII is largest at a test potential of -15 mV with 61.05±15.20 % (n=3), while for SFIII it is largest at a test potential of 5 mV decreasing by 44.84±15.69 % (n=4). The antagonistic effect of SFII and SFIII appears to be weakly voltage dependent or voltage independent because the degree of antagonism was not much different in the range of test potentials. Similar results were found for all the subfractions when depolarizing from a HP of -90 mV (not shown), indicating that their effect is not dependent on the HP.

Figure 4 shows the influence of the subfractions on the voltage dependence of activation. For the cell shown in Figure 4A, the $V_{½}$ for activation is shifted to more negative membrane potentials from –20.76 mV to –23.23 mV with SFI. The same shift was observed in other cells with the mean shift being -22.04±0.70 mV in control to -25.05±1.06 mV with SFI (n=3), which was statistically significant (paired t-test, $p \leq 0.05$). SFI also influenced the g_{max} (0.02±0.01 nA in control vs. 0.04±0.01 nA with SFI; n=3) and the slope value (3.44±0.21 nA in control to 1.97±0.46 nA after SFI was added; n=3). The decrease in the slope was statistically significant (paired t-test, $p \leq 0.05$), whereas the conductance was not influenced significantly. The $V_{½}$ for activation in the presence of SFII was shifted to more positive membrane potentials from -28.03 mV in control to -25.87 mV after SFII was added (Figure 4B) and the conductance decreased by 50 % from 0.03 nA to 0.02 nA in the presence of SFII. SFIII shifted the $V_{½}$ values to more negative membrane potential (-17.51 mV in control vs. -20.84 mV with SFIII, Figure 4C) and the mean value of the conductance was decreased from 0.02±0.007 nA to 0.007±0.001 nA by 65 % (n=3). SFII and III had no significant effect on the slope.

As with PgIII, it was determined whether the effects of the subfractions are mediated by Ba^{2+} ions through the Ca^{2+} channel by using a selective Ca^{2+} channel blocker (nisoldipine) and agonist (BayK 8644). With SFI (Figure 5A), the current increased by 106 % in respect of the control and addition of nisoldipine resulted in a 64 % decrease, with respect to the control. Fig 5B shows the effect of SFII on the Ca^{2+} channel. The current is decreased by 66 % in the presence of SFII and when BayK 8644 was added, the current increased by 107 % in respect of the control. A similar

effect was observed with SFIII (not shown). This indicates that the effect of the subfractions is mediated by Ba^{2+} ions flowing through the L-type Ca^{2+} channel.

The effect of the subfractions on the time to peak at different test potential is summarized in Table 1. In the presence of SFI, the mean time to peak increased at test potentials between -20 and 5 mV and the increase at -20 and -10 mV was statistically significant from control (paired t-test, $p \leq 0.05$). SFII had no significant effect on the time to peak, with the times increasing at some potentials and decreasing at others. The time to peak increased at all test potentials with SFIII and the increases were statistically significant at test potentials 0 mV and 5 mV (paired t-test, $p \leq 0.05$).

The result of the effects of the subfractions on the time constants of inactivation is summarized in Table 2. The control currents inactivated with time constants between 26 ms and 44 ms, while the currents inactivated much slower in the presence of SFI with time constant of 33 ms to 62 ms. The time constant for inactivation in the presence of SF1 increased a test potentials from -25 mV to 5 mV and this increase was statistically significant for control at test potential -15 mV to 5 mV. The inactivation time constants in the presence of SFII was lower than the control at test potentials between -0 mV and 5 mV, with the increases being statistically significant only at test potentials -25, -10, 0 and 5 mV (paired t-test, $p \leq 0.05$). Inactivation in the presence of SFIII also occurred slower, but the time constants was only significantly different from the control at -20 mV (paired t-test, $p \leq 0.05$).

Discussion

Toxins isolated from scorpion venom have been used extensively as pharmacological tools to characterize ion channels (Possani *et al.*, 2000). To promote knowledge of the structure-function relationship, further necessitates the isolation and characterization of peptides. The number of peptides isolated from scorpion venom has increased considerably in the last decade (Possani *et al.*, 2000). Toxins isolated from the venom of scorpions targeted specifically at voltage dependent Ca^{2+} channels are not well known and agonistic peptides active on cardiac T- and L-type Ca^{2+} channels have not been described. This study focused on the electrophysiological effects of fractions isolated from the venom of *P. granulatus* on Ca^{2+} channels and more specifically L-type Ca^{2+} channels in rat ventricular myocytes. In the results, where only 3 mM Ba^{2+} was used as charge carrier, there was no evidence of T-type channels. The current voltage relationships did in most instances not show the initial hump usually seen with the T-type channels.

PgIII showed an increase in the Ba^{2+} current through L-type Ca^{2+} channels in rat ventricular myocytes. This correlates with previous studies showing that PgIII increased the Ca^{2+} current in both guinea-pig myocytes and dorsal root ganglia neurons (Botha, 2002; Jordaan, 2002). It seems as if PgIII is not tissue specific. In rat ventricular myocytes, the increase is also not dependent on the HP (agonism observed at HP = -90 and -50 mV). The increase was observed at all test potentials and the % increase was different in the range of test potentials, indicating that the effect is voltage dependent. Using a selective L-type Ca^{2+} channel blocker, nisoldipine (50 μM), confirmed that the effect is indeed mediated by Ba^{2+} ions through the Ca^{2+} channels and not by the Na^{+} α-effect. The agonistic effect observed

at a HP of -50 mV further confirms this result seeing that most, if not all Na^+ channels will be unavailable at a HP of -50 mV (Sontheimer, 1995; Anderson, 2001). PgIII had a statistical significant effect on the time to peak duration at test potenitals -20 and -10 mV. The mean time constants for deactivation were increased slightly which indicated a slower deactivation rate in the presence of PgIII. Due to the availability of PgIII, this effect could not be studied further using a protocol measuring the deactivation current before the onset of inactivation. The rate of inactivation was also decreased with a statistically significant difference only at -5 mV and 0 mV (unpaired t-test, $p \leq 0.05$) and the voltage dependence of activation was shifted by approximately 4 mV to depolarizing potentials. The conductance through the channel increased, which indicates that there is an increase in the number of open channels at the peak current. It is expected that the $V_{½}$ values would be shifted to more negative membrane potentials as the peak current increases, but this was not observed in the experimental conditions of this study. Further research with PgIII is needed to increase the number of experiments so that it can be determined whether this effect is repeatable. PgIII did not influence the reversal potential significantly indicating that PgIII does not influence the selectivity of the channel and seems to be selective for the L-type Ca^{2+} channel. The results found with SFI contradicts this where SFI had a significant effect on the reversal potential. This indicates that PgIII is not selective for the channel. The results found with PgIII may also indicate that the binding site of the toxin is not located in the selectivity filter of the channel. The selectivity for the L-type Ca^{2+} can only be determined once the active peptide has been isolated.

RP-HPLC separation of PgIII led to the identification of three prominent peaks at 22.97, 23.81 and 24.89 minutes in the HPLC profile. These fractions were named

SFI, SFII and SFIII. The increase in current observed with SFI is in most instances comparable to that observed with PgIII. The increase in peak current in the presence of SFI was voltage dependent because the % increase was significantly larger at more negative membrane potentials. The increase in current is not dependent on HP for both PgIII and SFI because it was observed when holding at -50 and -90 mV. Where PgIII shifted the $V_{½}$ with ±4 mV. SFI shifted the voltage dependence of activation with a average of 3 mV to hyperpolarized potentials, which was significantly different from the control (paired t-test, $p \leq 0.05$). SFI influenced the slope of the voltage dependence of activation significantly, whereas PgIII did not (paired t-test, $p \leq 0.05$). The conductance was increased by 50 % and the rate of inactivation delayed, which indicates that SFI prolonged the open time of the channel. SFI influenced the reversal potential significantly (paired t-test, $p \leq 0.05$), whereas PgIII had no significant effect. As with PgIII, SFI had a significant effect on the time to peak only at -20 and -10 mV. A L-type Ca^{2+} channel agonist could have important physiological implications, which include a rise in intracellular Ca^{2+} concentration which can result in heart muscle contraction and therefore, a positive inotrope effect. In neurons it can lead to an increase in neurotransmitter secretion. If an agonistic peptide can be isolated for *P. granulatus* venom, it could have important implications in ion channel research. The agonist could be used in studies where multiple types of Ca^{2+} channels exist in neuronal and cardiac preparations to enhance L-type Ca^{2+} channels. There is also great academic value in the identification and isolation of new peptide structures and in this case it is especially important because this effect has not been described yet.

Toxins generally fall into two categories based on their mode of action. The first category is where the channel is physically blocked by the toxin, which binds to the

pore opening of the channel. The second category is where the toxins modulate the channel gating by binding to the voltage sensor and altering the voltage dependence of gating (Loret & Hammock, 2001). Peptides isolated from scorpion venom that block Ca^{2+} channels, include kurtoxin from *P. transvaalicus* and KLI and II from *P. granulatus*. Kurtoxin was found to bind with high affinity to LVA and HVA-type channels and more specifically interacted with the α_1 subunit of the $Ca_V3.1$ and 3.2 T-type Ca^{2+} channels with high affinity and inhibited channel activity by modifying voltage-dependent gating (Chuang *et al.*, 1998). The inhibition of whole cell Ca^{2+} currents in spermatogenic cells caused by KLI and KLII in the ±40 mV range was weakly voltage dependent and only partially reversible, suggesting that these toxins might act by a pore-blocking mechanism in addition to their capacity to modify the gating mechanism of the channel (Lopez-Gonzalez *et al.*, 2003). SFII and SFIII were found to be antagonists of the L-type Ca^{2+} channel by decreasing the peak current. At a HP of -50 mV SFII (42 $\mu g.ml^{-1}$) decreased the peak current on average by 51 %, while SFIII (25 $\mu g.ml^{-1}$) decreased the current on average by 41 %. Both subfractions had no significant effects on the reversal potential. SFII shifted the voltage dependence of activation to more positive membrane potentials with an average shift of 2 mV which did not differ significantly from the control, while SFIII shifted it in the opposite direction on average 3 mV, which was significantly different (paired t-test, $p \leq 0.05$). The maximum conductance was decreased by 50 % in the presence of both subfractions. The slope was not influenced by SFII and III. The rate on inactivation was delayed by SFIII and the time to peak increased significantly (paired t-test, $p \leq 0.05$). SFII had a opposite effect on the rate of inactivation by increasing it and did not influence the time to peak significantly. This indicates that SFII and III block the channel by modifying the gating of the channel. It seems that

the effect SFII and SFIII was also weakly voltage dependent and could only be partially washed out. The preliminary results indicates that the Ca^{2+} channel seems to be more sensitive for SFIII.

Conclusion

The data in this article suggest that the fractions isolated from the venom of the Southern African scorpion *P. granulatus* are a source of pharmacological interesting toxins active on L-type Ca^{2+} channels. The next step will be to isolate and purify the peptides responsible for the agonistic and antagonistic effects. This will, furthermore, enable the sequencing and cloning of these peptides for further characterization. The information thus obtained will provide insight into the mechanism of agonism of scorpion toxins on Ca^{2+} channels as well as contributing to the growing knowledge of peptide toxin structure-function relationships.

Acknowledgements

Dr. F. van der Westhuizen (subject group Biochemistry, North-West University, Potchefstroom Campus), for assistance in the determination of the subfractions concentrations. Mrs. C. Fourie (subject group Physiology, North-West University, Potchefstroom Campus), for the isolation of the cardiac ventricular myocytes.

References

ANDERSON, M.E. 2001. Ca^{2+}-dependent regulation of cardiac L-type Ca^{2+} channels: is a unifying mechanism at hand?. *Journal of molecular cell cardiology*, 33; 639-650.

BOTHA, E.M. 2002. Die effek van *Parabuthus granulatus* venoom op kalsiumkanale in ventrikulêre miosiete geïsoleer uit marmothart. Potchefstroom : PU vir CHO. (Verhandeling – M. Sc.) 75p.

CATTERALL, W.A., STRIESSING, J., SNUTCH, T.P. & PEREZ-REYES, E. 2003. International union of pharmacology. XL. Compendium of voltage-gated ion channels: Calcium channels. *Pharmacological Reviews,* 55(4):579-581.

CHUANG, R.S-I., JAFFE, H., CRIBBS, L., PEREZ-REYES, E. & SWARTZ, K.J. 1998. Inhibition of T-type voltage-gated calcium channels by a new scorpion toxin. *Nature neuroscience,* 1(8): 668-674.

CLOZEL, J-P., ERTEL, E.A. & ERTEL S.I. 1999. Voltage-gated T-type Ca^{2+} channels and heart failure. *Proceedings of the Association of American Physicians,* 111(5):429-437.

DEBONT, T., SWERTS, A., VAN DER WALT, J.J., MÜLLER, G.J., VERDONCK, F., DAENENS, P. & TYTGAT, J. 1998. Comparison and characterization of three *Parabuthus* scorpion species occurring in southern Africa. *Toxicon,* 36(2): 341-352.

HAMILL, O.P., MARTY, A., NEHER, E., SAKMAN, B. & SIGWORTH. 1981. Improved patch-clamp techniques for high resolution current recording from cells and cell free membrane patches. *Pflügers archives. European Journal of Physiology,* 319(2):85-100.

HILLE, B. 2001. Ion channels of excitable membranes. 3rd ed. Sunderland Mass: Sinauer. 607p.

HUYS, I., DYASON, K., WAELKENS, E., VERDONCK, F., VAN ZYL, J., DU PLESSIS, J., MÜLLER, G.J., VAN DER WALT, J., CLYNEN, E., SSCHOOFS, L. & TYTGAT, J. 2002. Purification, characterization and biosynthesis of parabutoxin 3, a component of *Parabuthus transvaalicus* venom. *European Journal of Biochemistry*, 269:1854-1865.

JORDAAN, E.E. 2002. Die elektrofisiologiese effekte van KLII en Sephadex Fraksies I-IV, geïsoleer uit die venom van *Parabuthus granulatus*, op Ca^{2+} -kanale in dorsale wortel ganglia van die rot. Potchefstroom : PU vir CHO. (Skripsie – Honns.) 42p.

KOCHEGAROV, A.A. 2003. Pharmacological modulators of voltage-gated calcium channels and their therapeutical application. *Cell calcium*, 33:145-162.

LORET, E. & HAMMOCK, B. 2001. Structure and Neurotoxicity of venoms (*In* Brownell, P. & Polis, G. Scorpion biology and research, Oxford University Press, New York, 204p.)

LOPEZ-GONZALEZ, I., OLAMENDI-PORTUGAL, T., DE LA VEGA-BELTRAN, J.L., VAN DER WALT, J., DYASON, K., POSSANI, L.D., FELIX, R. & DARZON, A. 2002. Scorpion toxins that block T-type Ca^{2+} channels in spermatogenic cells

inhibit the sperm acrosome reaction. *Biochemical and Biophysical research communications*, 300:408-414.

MITRA, R. & MORAD, M. 1985. A uniform enzymatic method for dissociation of myocytes from hearts and stomachs of vertebrates. *American Journal of Physiology*, 249:H1056-H1060.

MüLLER, G.J. 1993. Scorpionism in South Africa – A report of 42 serious scorpion envenomations. *South African Medical Journal*, 83:405-411.

NARGEOT, P., LORY, P. & RICHARD, S. 1997. Molecular basis of the diversity of calcium channels in cardiovascular tissues. *European Heart Journal*, 18:A15-A26.

N'GOUEMO, P. & MORAD, M. 2003. Voltage-gated calcium channels in adult rat inferior colliculus neurons. *Neuroscience*, 120:181-826.

OLAMENDI-PORTUGAL, T., INEZ GARCIA, B., LOPEZ-GARCIA, I., VAN DER WALT, J., DYASON, K., ULENS, C., TYTGAT, J., FELIX, R., DARZON, A. & POSSANI, L.D. 2002. Two new scorpion toxins that target voltage-gated Ca^{2+} and Na^{+} channels. *Biochemical and Biophysical research Communications*, 299:562-568.

POSSANI, L.D., MERINO, E., CORONA, M., BOLIVAR, F. & BECERRIL, B. 2000. Peptides and genes coding for scorpion toxins that affect ion-channels. *Biochimie*, 82:861-868.

PRENDINI, L. 2001. Phylogeny of *Parabuthus* (Scorpiones, Buthidae). *Zoologica Scripta,* 30:13-35, Jan.

SIDACH, S.S. & MINTZ, I.M. 2002. Kurtoxin, a gating modifier of neuronal high- and low- threshold Ca channels. *The journal of Neuroscience,* 22(6):2023-2034, Mar.15.

SONTHEIMER , H. 1995. Whole cell patch clamp recordings. (*In* Boulton, A., Baker, G. & Walz, W. *ed.* Neuromethods, Vol. 26: Patch clamp applications and protocols. Humana Press Inc. p.

TYTGAT, J. 1994. How to isolate cardiac myocytes. *Cardiovascular Research,* 28:280-283.

TYTGAT, J., DEBONT, T., ROSTOLL, K., MÜLLER, G.J., VERDONCK, F., DAENENS, P., VAN DER WALT, J. & POSSANI, L.D. 1998. Purification and partial characterization of a 'short' insectotoxin-like peptide from the venom of the scorpion *Parabuthus schlechteri. FEBS letters,* 441:387-391.

VALDIVIA, H.H. & POSSANI, L.D. 1998. Peptide toxins as probes of ryanodine receptor structure and function. *Trends in cardiovascular medicine,* 8(3): 111-118.

Vitae

Mrs. L.H. du Plessis

M. Sc. Student

School for Physiology, Nutrition and Consumer Sciences

North-West University, Potchefstroom Campus

Private Bag X6001

Potchefstroom

2520

South Africa.

Email address: flglhdp@puk.ac.za

Mr. J.L. du Plessis

Lecturer

School for Physiology, Nutrition and Consumer Sciences

North-West University, Potchefstroom Campus

Private Bag X6001

Potchefstroom

2520,

South Africa.

Email address: flgjldp@puk.ac.za

Prof. L.D. Possani

Department of Molecular Medicine and Bioprocesses

Institute of Biotechnology

National Autonomous University of Mexico

Apartado Postal 510-3

Cuernavaca

Mexico.

Email address: Possani@ibt.unam.mx

Prof. K. Dyason

Extraordinary Associate Professor

School for Physiology, Nutrition and Consumer Sciences

North-west University, Potchefstroom campus

Private Bag X6001

Potchefstroom

2520,

South Africa.

Email address: flgkd@puk.ac.za

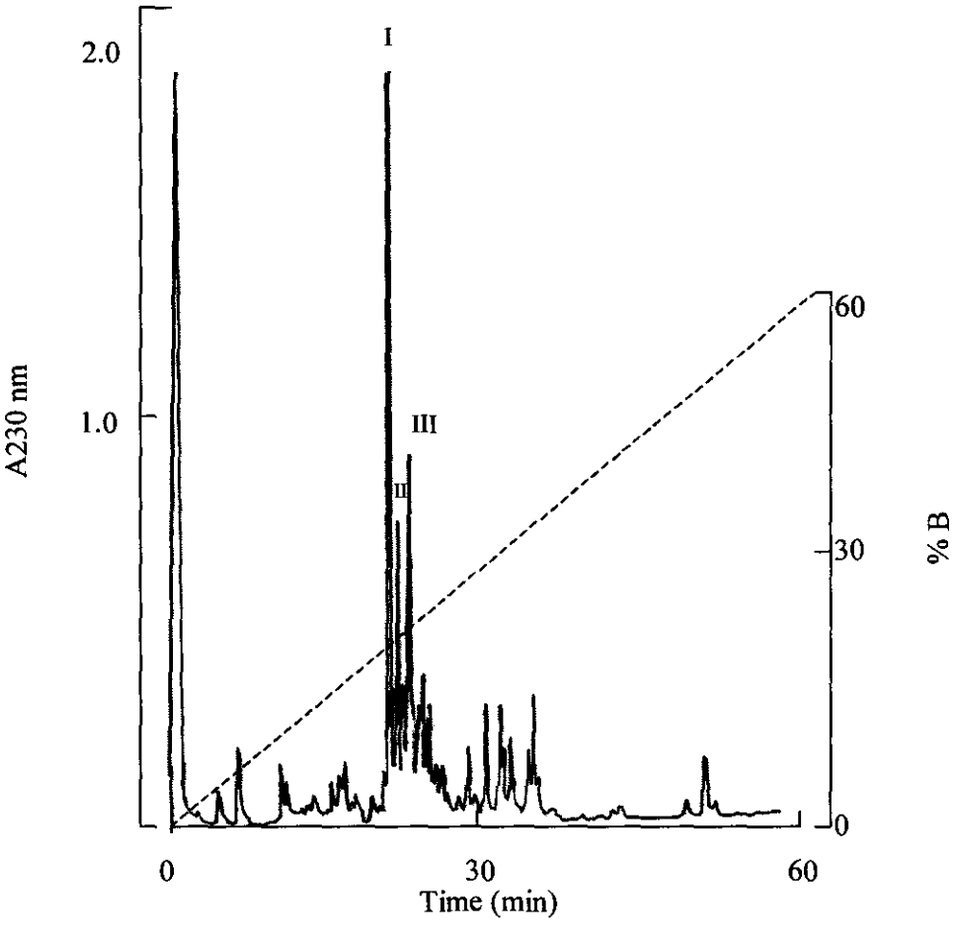

Figure 1. Chromatographic profile of subfractions from PgIII separated by RP-HPLC. PgIII (1.8 mg) was loaded into a C_{18} reverse phase analytical column for 60 min with a flow rate of 2 $ml.min^{-1}$ as described in materials and methods. The three components (named SFI, SFII and SFIII) labelled were used in the experiments.

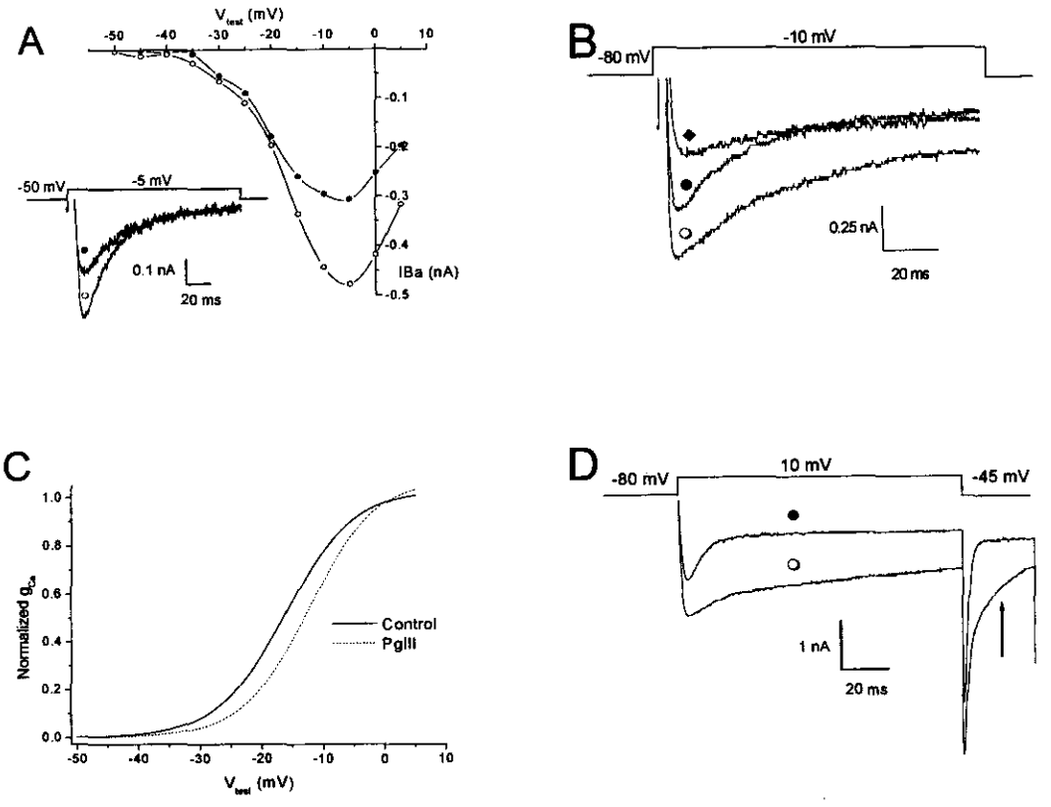

Figure 2. Effect of PgIII on Ba^{2+} currents in ventricular myocytes. (A) The I-V relationship in control conditions (•) and in the presence of PgIII (o). Inset showing representative recordings of currents in response to depolarizing from a holding potential of -50 mV to a test potential of -5 mV. (B) Current recordings from a holding potential of -80 mV to a test potential of -10 mV in control (•), in the presence of PgIII (o) and with 50 μM nisoldipine (♦). (C) Effect of PgFIII on the voltage dependence of activation in control (solid line) and after the addition of PgIII (dotted line). $V_{1/2}$ = -16.21 mV (control) and -12.39 mV (PgIII); slope = 5.52 (control) and 5.34 (PgIII); g_{max} = 0.01 nA (control) and 0.02 nA (PgIII); E_{Ca} = 20.10 mV (control) and 17.30 mV (PgIII). (D) Currents recorded from a HP of -80 mV to a test potential of 10 mV and then returning to -45 mV to observe the deactivation currents. The arrow indicates the increase in the deactivation current after addition of PgIII (o). The deactivation time constants were 4.56 ms in control and 5.26 ms with PgIII.

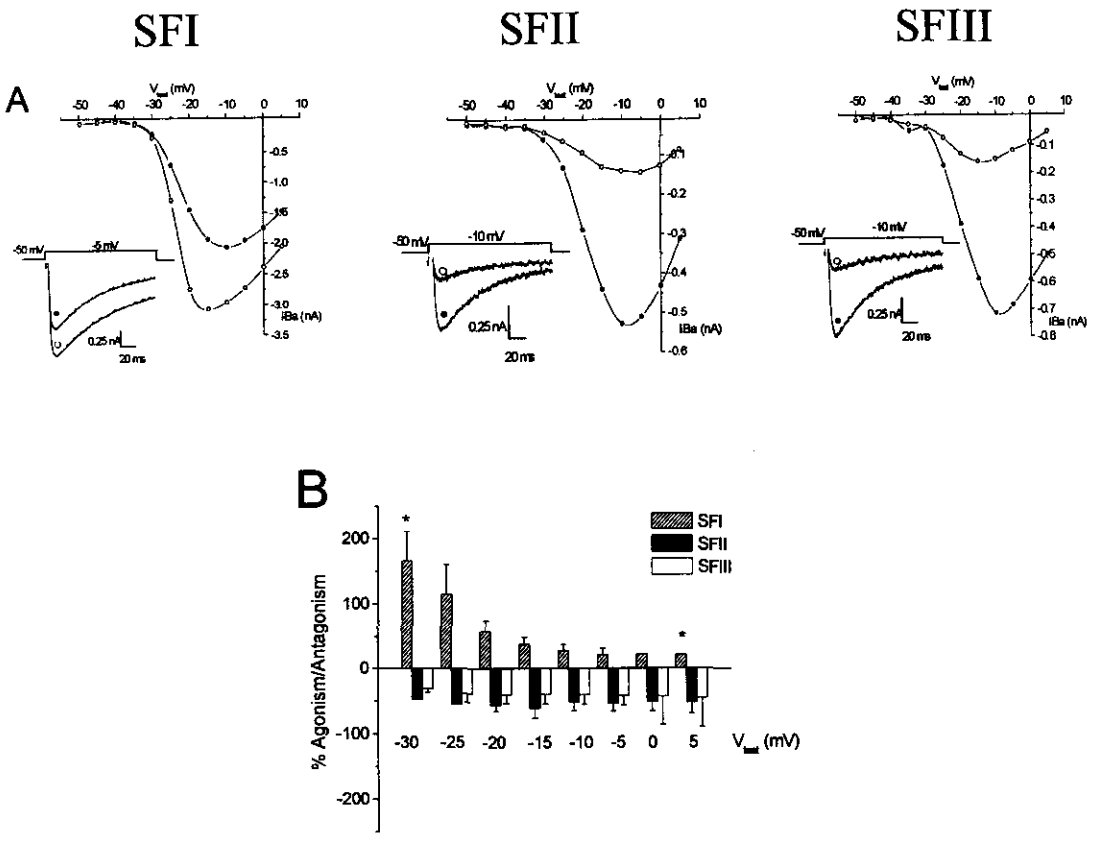

Figure 3. Effects of subfractions on Ca^{2+} channels in ventricular myocytes. (A) Current-voltage relationship in control conditions (•) and after exposure to the subfractions (o) SF1 (140 $\mu g.ml^{-1}$), SF2 (42 $\mu g.ml^{-1}$) and SF3 (25 $\mu g.ml^{-1}$). Lower insets shows peak currents elicited using the same protocol as Figure 1. (B) % Agonism or antagonism as a function of the test potential (V_{test}) at potentials -30 mV to 5 mV for SFI (n=3), SFII (n=3) and SFIII (n = 4). The asterisk indicates a statistical significant difference between the % agonism at test potentials -30 mV and 5 mV ($p \leq 0.05$).

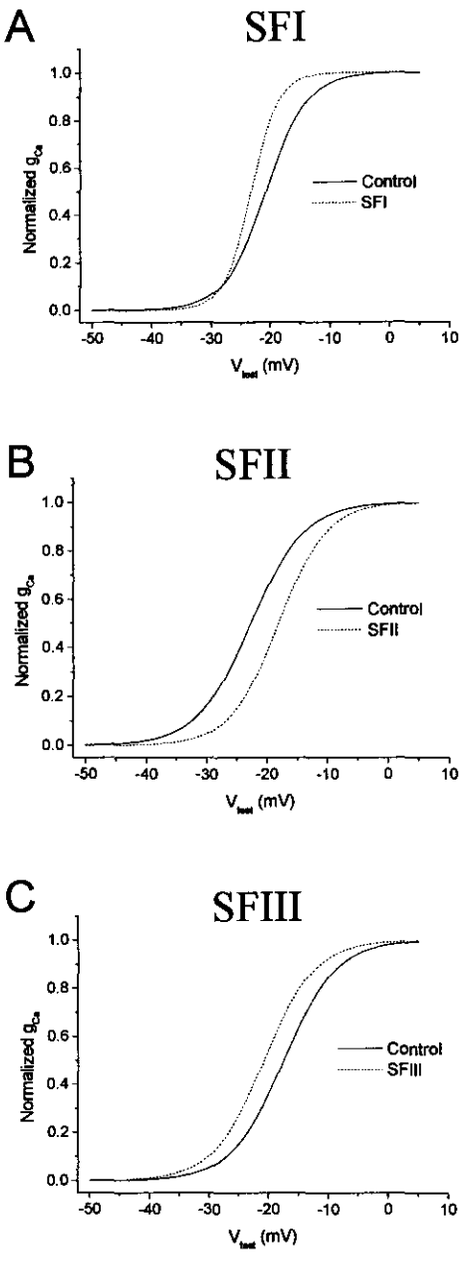

Figure 4. Comparison of the voltage dependence of activation in the presence of the subfractions (A) SFI, (B) SFII, (C) SFIII. Solid lines represent fits of the control data by equation (3) and the dotted lines represent fits of data in the presence of the subfractions. The current voltage relationships of Figure 3 were used. V½ values are -20.76 mV (control) and -23.23 mV (SFI); -28.03 mV (control) and -25.87 mV (SFII); -17.51 mV (control) and -20.84 mV (SFIII).

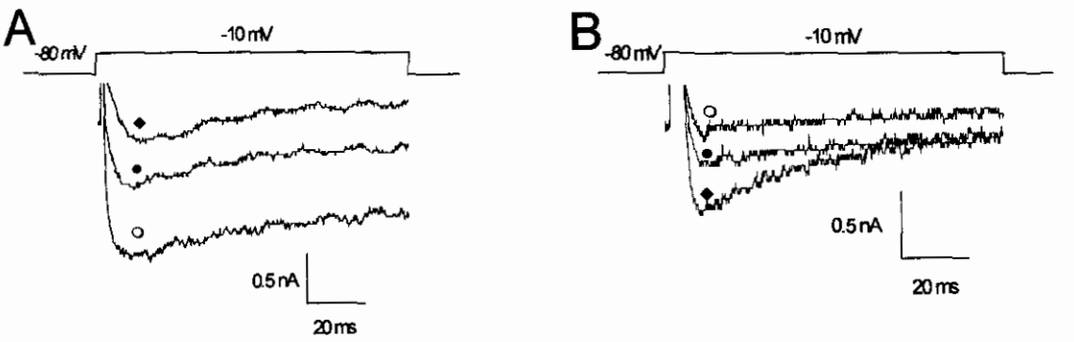

Figure 5. Representative superimposed current traces recorded from a HP of -80mV with depolarization to -10 mV. (A) Recordings in control (•), after application of SFI (o) and with 50 μM nisoldipine (♦). (B) Recordings of current using the same protocol as in A, in control (•), after application of SFII (o) and with 50 μM Bay K 8644 (♦).

Table 1. Effects of subfractions on the time to peak (HP = -50 mV). All values are expressed as mean±SEM in ms. (V_{test} = test potential).

V_{test} (mV)	Control (ms) (n=4)	SFI (ms) (n=4)	Control (ms) (n=3)	SFII (ms) (n=3)	Control (ms) (n=4)	SFIII (ms) (n=4)
-30	27.41±5.27	23.78±7.54	24.70±1.15	31.40±9.18	22.42±1.46	24.11±3.11
-20	16.35±1.48	20.24±0.79*	16.10±1.81	13.50±2.22	16.84±1.54	17.29±1.84
-10	10.80±0.58	14.58±1.00*	12.70±0.95	12.08±1.35	13.16±1.27	13.28±1.84
-5	9.68±0.75	13.11±1.45	13.90±0.21	12.10±0.91	11.36±1.55	13.28±1.90
0	9.30±0.74	12.48±1.41	11.35±1.76	12.35±2.09	10.35±1.71	12.52±1.67*
5	9.22±0.17	11.76±1.79	11.00±0.91	12.70±2.24	11.51±2.28	14.48±2.62*

* Statistically significant from control at $p \leq 0.05$, paired t-tests.

Table 2. Effects of the subfractions on the time constants of inactivation (τ) when holding at -50 mV. All values are expressed as mean±SEM in ms. (V_{test} = test potential)

V_{test} (mV)	Control (ms) (n=4)	SFI (ms) (n=4)	Control (ms) (n=3)	SFII (ms) (n=3)	Control (ms) (n=4)	SFIII (ms) (n=4)
-25	28.77±14.59	33.14±14.07	76.70±35.33	81.37±35.61*	32.05±9.82	46.46±17.12
-20	26.85±10.91	38.13±10.62	60.10±17.07	46.28±0.85	35.22±8.21	48.18±13.30*
-15	31.57±10.81	51.70±13.62*	51.90±4.88	42.91±7.08	40.36±8.61	48.95±9.09
-10	35.67±10.05	59.31±13.70*	48.28±2.14	38.91±3.60*	44.87±7.74	48.75±5.00
-5	39.29±9.92	62.62±12.67*	47.17±0.73	39.01±4.80	48.39±6.64	49.18±3.97
0	42.12±9.63	62.53±10.45*	47.38±2.51	39.34±3.90*	49.71±5.07	51.53±2.60
5	44.58±8.71	60.78±8.44*	48.25±2.82	39.86±2.82*	51.40±3.96	51.90±2.09

* Statistically significant from control at p≤0.05, paired t-tests.

CHAPTER 4 – Conclusion and recommendations

The venom of various scorpion species has been a great source of novel peptides. The identification of these peptides has played an important role in the identification and characterizing of the molecular structure and functions of ion channels in excitable cells. These peptides have also been an invaluable tool in identifying possible pharmaceutical and therapeutical compounds. The availability of scorpion toxin peptides as antagonists of Na^+ and K^+ channels has facilitated detailed physiological and pharmaceutical characterization of these peptides. Scorpion peptides specific for Ca^{2+} channels are much less common and not extensively studied.

The South African scorpion *P. granulatus* is considered to be the most dangerous scorpion in Southern Africa and a large number of serious envenomations have been reported. The toxicity of the venom is comparable to *Centruroides noxius*, the most venomous scorpion specie in Mexico. Research on the venom scorpions is important not only in the development of specie specific antivenom, but also in identifying novel toxin peptides. Up to now research done on Ca^{2+} channel toxins from scorpion venom has focused on the effects of the toxins on neuronal preparations, spermatogenic cells, germ cells or cloned channels. The cloning of channels makes it possible to compare structure, function and pharmacology in different tissues and the results found in animals can be compared to that of humans. With cloned channels specific currents can be studied in isolation. Many factors influence the function of channels *in vivo* and this can be studied

using native channels. Research on native channels are therefore important and it was validated in this study because the isolation of rat ventricular myocytes are standardized in the laboratory.

The purpose of the present study was to identify and characterize the effect of fractions and subfractions isolated from the venom of *P. granulatus* on cardiac Ca^{2+} channels in rat ventricular myocytes. The primary aim of the study was to first of all confirm the agonistic effect of PgIII on cardiac Ca^{2+} channels and then to characterize the interaction with the Ca^{2+} channel. Another important aim was to determine whether the agonistic effect could be limited to one or more subfractions. During the project, a number of limiting factors were identified:

- The experimental data was collected by using the whole cell configuration of the patch-clamp technique. This technique is commonly used in ion channel research. The electrophysiology laboratory of the NWU, Potchefstroom Campus is well equipped and cardiac myocytes were readily available, but the technique is difficult to master and the quality of viable myocytes varied from day to day. Both these factors limited the number of successful experiments and made testing of the fractions very time consuming. In addition it limited the variation in experimental protocols and the number of experiments that had to be done for statistical analysis.
- During some of the experiments a degree of run-down was observed, where the activity of the Ca^{2+} channel decreased when the cytoplasmic side of the channel

was perufused with the intracellular solution. This phenomenon is well known in the literature and this was also a limiting factor in the study.

- The fractionation of venom components as well as the purification and sequencing of peptides are done by collaborators in Mexico and Belgium. This is a time consuming process and limited the availability of fractions. The ideal would be to extend the study to include experiments with the purified peptides, but it was not possible in the duration of the study. Because scorpion venom is composed of various components, initial research with fractions is important in the screening of the venom to determine possible effects of the components.
- PgIII and the subfractions contained various components, which made it impossible to determine concentration used but the protein concentration of the subfractions was determined. The subfraction at elution time 2.98 minutes on Figure 1 (Chapter 3) was destroyed by bacterial growth and could not be used for experiments. This subfraction is one of the main components of PgIII and it would be interesting to study the effect of this subfraction.
- The degree of the effects varied between the cells, which made statistical analysis and the determination of statistical significant differences difficult. This can also explain the large standard errors observed in some experiments.

In the study, the agonistic effect of PgIII isolated from the venom of *P. granulatus* was confirmed and the interaction with the Ca^{2+} channel characterized. PgIII increased the peak current amplitude by 40 - 56 % and this increase could be observed at all the test potentials. The effect was larger at more negative membrane potentials, which indicates

that the effect is voltage dependent. This effect was not dependent on the HP. PgIII did not influence the reversal potential of the current. Using the selective L-type channel antagonist, nisoldipine, it was found that the effect of PgIII is mediated by Ba^{2+} ions through the L-type channel. PgIII shifted the voltage dependence of activation with 4 mV towards more positive membrane potentials and increased the conductance, while the slope was not influenced significantly. An interesting effect was observed on the deactivation current, where the deactivation time course was prolonged. This effect on the deactivation current should be investigated with a protocol specifically designed to measure the deactivation current. This could not be done in this study because of the limited amount of PgIII. Statistically significant effects could be observed on the time to peak duration at -20 and -10 mV, whereas the inactivation time constants were influenced significantly at test potentials -5 and 0 mV.

SFI (140 $\mu g.ml^{-1}$) also increased the peak current and the effect was found to be voltage dependent, with the degree of agonism being larger at more negative membrane potentials. The peak current was increased on average between 37 % and 72 % (HP of -50 and -90 mV respectively). SFI shifted the voltage dependence of activation with 3 mV towards more negative membrane potentials and statistically significant increases in the time constants of inactivation were found at test potentials between -15 and 5 mV. SFI influenced the time to peak significantly only at test potentials -20 and -10 mV. SFI increased the maximum conductance through the channel, but this increase was not statistically significant. The slope of the voltage dependence of activation as well as the reversal potential were influence significantly in the presence of SFI. It was confirmed

with nisoldipine that the effect of SFI is mediated by Ba^{2+} ions through the Ca^{2+} channel. SFII (42 $\mu g.ml^{-1}$) and SFIII (25 $\mu g.ml^{-1}$) showed antagonism of the L-type channel by decreasing the peak current respectively with 25 % and 41 % at a HP of -50 mV. The effects with SFII and SFIII seemed to be voltage independent with no significant differences in the degree of antagonism at various test potentials. Both of the subfractions caused a shift in the reversal potential. The shift in the presence of SFII was not significant, whereas SFIII shifted the reversal potential significantly. The voltage dependence of activation in the presence of SFII was shifted with 2 mV towards more positive membrane potentials and in the presence of SFIII with 3 mV towards more negative membrane potentials. SFII and III both had no significant influences on the slope. The maximum conductance was decreased by 50 % and 65 % respectively by SFII and III. SFII had no significant effect on the time of the current to reach a peak, but statistically significant decreases were observed in the rate of inactivation at test potentials -10, 0 and 5 mV. Inactivation in the presence of SFIII occurred slower, but the time course was not statistically different from the control, while SFIII increased the time of the current to reach peak. The antagonistic effect with SFII and III was observed at both -50 and -90 mV.

In the study all of the aims were obtained. The agonistic effect found with PgIII could be limited to one subfraction. Further research is needed to identify the agonistic peptide(s) present in SFI and to characterize not only the effect on cardiac VDCCs but also on channels in other tissues to determine its specifity. It would be important to determine whether the peptide is specific for the L-type channel by testing it on various

HVA channel subtypes in various tissues. The agonistic effect found with PgIII and SFI has not been described for scorpion venom. The results found in this study are important in the knowledge of the composition of scorpion venom and especially South African scorpion venom. It would also be of great academic importance to identify a novel venom peptide with a unique structure and function.

ADDENDUM A

1. The agonistic effect of PgIII on Ca^{2+} channels at different test potentials

Table 1.1 - The agonistic effect of PgIII on Ca^{2+} channels at different test potentials (HP = -90 mV)

Exp.	-30 mV			-25 mV			-20 mV			-15 mV		
	Contr. (nA)	PgIII (nA)	% Agon.	Contr. (nA)	PgIII (nA)	% Agon.	Contr. (nA)	PgIII (nA)	% Agon.	Contr. (nA)	PgIII (nA)	% Agon.
1	-0.27	-0.33	22.06	-0.51	-0.86	68.30	-0.60	-0.88	46.77	-0.58	-0.84	44.21
2	-0.09	-0.07	-18.60	-0.11	-0.14	19.30	-0.13	-0.17	30.71	-0.11	-0.16	43.64
3	-0.54	-0.87	59.67	-0.59	-0.93	57.72	-0.55	-0.75	36.93	-0.48	-0.66	37.74
χ	-0.30	-0.42	21.04	-0.31	-0.50	48.44	-0.55	-0.75	38.14	-0.39	-0.55*	41.86
SE	0.28	0.41	39.15	0.02	0.51	25.78	0.25	0.02	8.10	0.14	0.20	3.58
Σ	-0.90	-1.27	63.12	-0.31	-0.50	145.32	-0.55	-0.75	114.40	-1.17	-1.65	125.59
n	3	3	3	3	3	3	3	3	3	3	3	3

Table 1.1 - continue

Exp.	-10 mV			-5 mV			0 mV			5 mV		
	Contr. (nA)	PgIII (nA)	% Agon.	Contr. (nA)	PgIII (nA)	% Agon.	Contr. (nA)	PgIII nA)	% Agon.	Contr. (nA)	PgIII (nA)	% Agon.
1	-0.53	-0.72	34.08	-0.43	-0.60	37.64	-0.36	-0.48	30.77	-0.29	-0.38	30.21
2	-0.10	-0.14	43.30	-0.08	-0.12	50.65	-0.05	-0.09	77.36	-0.04	-0.07	75.42
3	-0.38	-0.50	33.33	-0.28	-0.37	32.03	-0.21	-0.28	29.91	-0.12	-0.15	24.58
χ	-0.34	-0.45*	36.90	-0.26	-0.36*	40.11	-0.21	-0.28*	46.01	-0.15	-0.20	43.40
SE	0.12	0.21	3.20	0.12	0.24	5.52	0.16	0.11	15.68	0.07	0.09	16.09
Σ	-1.01	-1.36	110.71	-0.79	-1.08	120.32	-0.36	-0.85	138.03	-0.45	-0.59	130.21
n	3	3	3	3	3	3	3	3	3	3	3	3

Exp.	= Experiment number	mV	= test potential measured in millivolts
Contr.	= Control	χ	= The statistical average
% Agon.	= Percentage agonism	SE	= The standard error of mean
nA	= current in nano Ampere measured at the specific test potential	Σ	= The sum total of the column
		n	= The total number of experiments

* significantly different from control ($p \leq 0.05$)

2. The effect of PgIII on the time constants of inactivation

Table 2.1 – The effect of PgIII on the time constants of inactivation at HP = -90 mV

Exp.	-30mV						-25mV					
	Control			PgIII			Control			PgIII		
	τ_1	A1	C	τ_1	A1	C	τ_1	A1	C	τ_1	A1	C
1	23.10	-0.25	-0.02	46.81	-1.63	0.16	22.51	-0.54	-0.02	45.12	-1.51	0.15
2	9.40	-0.08	0.01	12.54	-0.14	-0.01	10.93	-0.12	-0.03	12.14	-0.16	-0.04
3	32.14	-0.57	0.01	33.10	-1.08	-0.03	32.14	-0.57	0.01	34.91	-0.98	-0.04
4	-	-	-	6.65	-0.67	0.01	-	-	-	7.66	-0.78	0.01
5	-	-	-	-	-	-	-	-	-	25.41	-0.16	0.03
χ	21.55	-0.30	0.01	24.78	-0.88	0.03	21.86	-0.41	0.02	25.05	-0.72	0.02
SE	6.61	0.14	0.03	9.28	0.32	0.04	6.13	0.15	0.04	9.31	0.26	0.03
Σ	64.64	-0.90	0.01	99.10	-3.53	0.12	65.58	-1.23	-0.04	125.24	-3.58	-0.04
n	3	3	3	4	4	4	3	3	3	5	5	5

Table 2.1 - continue

Exp.	-20mV						-15mV					
	Control			PgIII			Control			PgIII		
	τ_1	A1	C	τ_1	A1	C	τ_1	A1	C	τ_1	A1	C
1	23.45	-0.63	-0.01	45.25	-1.32	0.10	28.83	-0.59	-0.04	47.32	-1.17	0.05
2	11.90	-0.13	-0.04	13.92	-0.16	-0.04	10.72	-0.11	-0.03	12.03	-0.14	-0.04
3	31.71	-0.60	0.04	33.86	-0.82	-0.03	31.34	-0.53	0.05	33.86	-0.67	-0.04
4	-	-	-	8.01	-0.86	0.02	-	-	-	7.27	-0.80	-0.05
5	-	-	-	29.37	-0.10	0.01	-	-	-	33.72	-0.19	0.01
χ	22.35	-0.45	0.01	26.08	-0.65	0.01	23.63	-0.41	0.01	26.84	-0.59	-0.01
SE	4.25	0.16	0.000	10.22	0.23	0.02	5.64	0.15	0.02	11.01	0.19	0.02
Σ	67.06	-1.36	-0.01	130.41	-3.25	-0.03	70.90	-1.24	-0.02	134.20	-2.97	-0.07
n	3	3	3	5	5	5	3	3	3	5	5	5

Table 2.1 - continue

Exp.	-10mV						-5mV					
	Control			PgIII			Control			PgIII		
	τ_1	A1	C	τ_1	A1	C	τ_1	A1	C	τ_1	A1	C
1	28.68	-0.54	0.01	48.32	-0.94	-0.01	29.30	-0.45	0.02	49.11	-0.77	-0.01
2	9.46	-0.11	-0.02	10.93	-0.12	0.01	7.86	-0.09	-0.01	9.13	-0.10	-0.04
3	29.82	-0.44	0.07	32.14	-0.54	-0.02	27.28	-0.36	0.08	30.08	-0.41	0.01
4	-	-	-	-	-	-	-	-	-	-	-	-
5	-	-	-	32.25	-0.16	0.01	-	-	-	29.17	-0.14	0.03
χ	22.65	-0.36	0.02	30.91	-0.44	-0.01	21.48	-0.30	0.03	29.37*	-0.35	-0.01
SE	7.46	0.13	0.03	11.54	0.19	0.01	7.13	0.10	0.03	9.21	0.16	0.01
Σ	67.96	-1.08	0.06	123.64	-1.76	-0.01	64.44	-0.90	0.09	117.49	-1.42	-0.03
n	3	3	3	4	4	4	3	3	3	4	4	4

Table 2.1 - continue

Exp.	0mV						5mV					
	Control			PgIII			Control			PgIII		
	τ_1	A1	C	τ_1	A1	C	τ_1	A1	C	τ_1	A1	C
1	30.42	-0.36	0.02	49.32	-0.63	-0.00	30.01	-0.29	0.04	49.51	-0.48	-0.09
2	6.42	-0.07	-0.01	7.17	-0.07	-0.03	4.60	-0.05	-0.01	-	-	-
3	28.49	-0.29	0.09	-	-	-	28.57	-0.22	0.11	29.51	-0.21	0.05
4	-	-	-	-	-	-	-	-	-	-	-	-
5	-	-	-	31.4	-0.12	0.01	-	-	-	29.86	-0.10	0.01
χ	21.78	-0.24	0.03	29.30*	-0.2743	-0.01	21.06	-0.19	0.05	36.29	-0.26	-0.01
SE	7.35	0.08	0.03	15.08	0.18	0.01	7.58	0.07	0.04	6.19	0.11	0.04
Σ	65.33	-0.72	0.10	87.89	-0.82	-0.02	63.18	-0.57	0.14	108.88	-0.78	-0.03
n	3	3	3	3	3	3	3	3	3	3	3	3

τ_1 = time constant for inactivation
A_1 = maximum current through the channel (nA)
C = maximum current through channel that inactivates slowly or not at all
Exp. = Experiment number

χ = The statistical average
SE = The standard error of mean
Σ = The sum total of the column
n = The total number of experiments

*significantly different from control ($p \leq 0.05$)

3. Effect of PgIII on the time of the current to reach a peak at HP = -90 mV

Table 3.1 – Effect of PgIII on the time of the current to reach a peak at HP = -90 mV

Exp.	-30 mV		-20 mV		-10 mV		-5 mV		0 mV		5 mV	
	Contr. (ms)	PgIII (ms)	Contr. (ms)	PgIII (ms)	Contr. (ms)	PgIII (ms)	Contr. (ms)	PgIII (ms)	Contr. (ms)	PgIII (ms)	Contr. (ms)	PgIII (ms)
1	20.25	22.80	15.75	18.75	12.45	15.45	11.25	12.15	10.05	11.25	12.45	10.35
2	18.30	18.80	16.80	18.70	14.00	18.20	11.60	15.70	11.00	14.00	11.50	12.50
3	16.35	16.35	13.95	16.20	11.55	13.80	9.90	11.70	13.20	11.55	13.00	13.65
χ	18.30	19.32	15.50	17.88*	12.67	15.82*	10.92	13.18	11.42	12.27	12.32	12.17
SE	0.01	0.01	0.01	0.60	0.72	1.09	0.52	0.95	0.93	0.64	0.44	0.69
Σ	54.90	57.95	46.50	53.65	38.00	47.45	32.75	39.55	34.25	36.80	36.95	36.50
n	3	3	3	3	3	3	3	3	3	3	3	3

χ = The statistical average
SE = The standard error of mean
Σ = The sum total of the column
n = The total number of experiments
ms = Time of the current to reach peak (in ms)

*significantly different from control ($p \leq 0.05$)

4. Effect of PgIII on the time constants of deactivation

Table 4.1 - Effect of PgIII on the time constants of deactivation

	Control			PgIII		
Exp.	τ_1	A1	C	τ_1	A1	C
1	4.56	-0.06	0.18	5.26	-0.45	-0.57
2	1.34	-0.05	0.08	2.14	-0.07	-0.09
3	4.63	-0.02	-0.02	5.02	-0.82	-0.08
χ	3.51	-0.04	0.08	4.14*	-0.44	-0.25
SE	1.08	0.01	0.06	1.00	0.22	0.16
Σ	10.54	-0.14	0.24	12.43	-1.33	-0.74
n	3	3	3	3	3	3

τ_1 = time constant for deactivation
A_1 = maximum current through the channel (nA)
C = maximum current through channel that inactivates slowly or not at all
Exp. = Experiment number

χ = The statistical average
SE = The standard error of mean
Σ = The sum total of the column
n = The total number of experiments

*significantly different from control ($p \leq 0.05$)

ADDENDUM B

1. The agonistic effect of SFI on Ca^{2+} channels at different test potentials

Table 1.1 - The agonistic effect of SFI on Ca^{2+} channels at different test potentials (HP = -50 mV)

Exp.	-30 mV			-25 mV			-20 mV			-15 mV		
	Contr. (nA)	SFI (nA)	%Agon.	Contr. (nA)	SFI (nA)	%Agon.	Contr. (nA)	SFI (nA)	%Agon.	Contr. (nA)	SFI (nA)	%Agon.
1	-0.20	-0.26	34.69	-0.72	-1.29	80.17	-1.44	-2.75	90.38	-1.93	-3.07	58.95
2	-0.02	-0.19	96.91	-0.36	-1.35	274.03	-0.86	-1.41	65.15	-1.03	-1.34	29.96
3	-0.03	-0.12	337.04	-0.25	-0.28	14.23	-0.30	-0.33	11.45	-0.29	-0.31	7.60
4	-0.04	-0.10	191.43	-0.11	-0.20	86.92	-0.18	-0.28	60.57	-0.19	-0.29	51.28
χ	-0.09	-0.17*	165.02	-0.36	-0.78	113.84	-0.69	-1.19	56.89	-0.86	-1.25	36.95
SE	0.08	0.07	65.77	0.26	0.63	111.71	0.29	0.58	33.00	0.40	0.65	9.46
Σ	-0.12	-0.27	356.44	-0.46	-0.98	200.75	-0.87	-1.48	117.46	-3.44	-5.01	147.80
n	4	4	4	4	4	4	4	4	4	4	4	4

Table 1.1 - continue

Exp.	-10 mV			-5 mV			0 mV			5 mV		
	Contr. (nA)	SFI (nA)	%Agon.	Contr. (nA)	SFI (nA)	%Agon.	Contr. (nA)	SFI (nA)	%Agon.	Contr. (nA)	SFI (nA)	%Agon.
1	-2.05	-2.95	44.04	-1.95	-2.71	38.78	-1.74	-2.39	34.27	-1.48	-2.05	38.97
2	-1.06	-1.19	12.96	-1.01	-1.05	3.76	-0.79	-0.89	11.67	-0.71	-0.75	5.50
3	-0.26	-0.28	7.55	-0.24	-0.25	4.54	-0.21	-0.23	9.71	-0.18	-0.19	6.18
4	-0.19	-0.28	43.59	-0.19	-0.25	35.48	-0.17	-0.22	30.95	-0.14	-0.90	31.94
χ	-0.89	-1.18	27.03	-0.85	-1.07	20.64	-0.73	-0.93	21.65	-0.63	-0.97	20.65
SE	0.43	0.63	9.75	0.41	0.58	9.54	0.37	0.51	6.38	0.31	0.39	8.67
Σ	-3.56	-4.71	108.14	-3.39	-4.26	82.57	-0.89	-1.15	52.60	-0.77	-1.88	52.58
n	4	4	4	4	4	4	4	4	4	4	4	4

Exp. = Experiment number
Contr. = Control
% Agon. = Percentage agonism
nA = current in nano Ampere measured at the specific test potential

mV = test potential measured in millivolts
χ = The statistical average
SE = The standard error of mean
Σ = The sum total of the column
n = The total number of experiments

*significantly different from control ($p \leq 0.05$)

Table 1.2- The agonistic effect of SFI on Ca^{2+} channels at different test potentials (HP = -90 mV)

Exp.	-25 mV			-20 mV			-15 mV			-10 mV		
	Contr. (nA)	SFI (nA)	%Agon.	Contr. (nA)	SFI (nA)	%Agon.	Contr. (nA)	SFI (nA)	%Agon.	Contr. nA)	SFI (nA)	%Agon.
1	-0.51	-1.36	167.45	-1.08	-2.84	162.78	-1.48	-3.12	111.65	-1.56	-2.91	86.74
2	-0.94	-1.65	75.91	-1.08	-1.61	48.61	-1.10	-1.50	36.02	-1.07	-1.33	24.51
3	-0.08	-0.28	258.97	-0.10	-0.29	183.65	-0.12	-0.28	126.61	-0.13	-0.26	104.69
χ	-0.51	-1.10*	167.44	-0.76	-1.58	131.68	-0.90	-1.63	91.43	-0.92	-1.50	71.98
SE	0.43	0.72	91.53	0.56	1.27	72.69	0.69	1.43	48.56	0.42	0.77	24.29
Σ	-1.53	-3.29	502.33	-2.27	-4.74	395.05	-2.70	-4.90	274.29	-2.76	-4.51	215.94
n	3	3	3	3	3	3	3	3	3	3	3	3

Table 1.2 - continue

Exp.	-5 mV			0 mV			5 mV		
	Contr. (nA)	SFI (nA)	%Agon.	Contr. (nA)	SFI (nA)	%Agon.	Contr. (nA)	SFI (nA)	%Agon.
1	-1.45	-2.62	80.71	-1.22	-2.30	88.40	-0.95	-1.89	98.11
2	-0.99	-1.13	13.42	-0.88	-0.949	7.11	-0.75	-0.76	1.72
3	-0.12	-0.23	91.73	-0.10	-0.194	83.01	-0.09	-0.15	71.73
χ	-0.85	-1.32	61.96	-0.73	-1.15	59.51	-0.60	-0.94	57.19
SE	0.39	0.69	24.47	0.33	0.61	26.24	0.26	0.50	28.76
Σ	-2.57	-3.98	185.87	-2.21	-3.45	178.53	-1.80	-2.82	171.50
n	3	3	3	3	3	3	3	3	3

See Table 1.1 for captions

2. Effect of SFI on the time constants of inactivation

Table 2.1 - Effect of SFI on the time constants of inactivation at HP = -50 mV

Exp.	-25 mV						-20 mV					
	Control			SFI			Control			SFI		
	τ_1	A1	C	τ_1	A1	C	τ_1	A1	C	τ_1	A1	C
1	72.02	-0.69	-0.06	73.98	-1.25	-0.09	59.55	-1.26	-0.19	65.19	-2.54	-0.36
2	20.45	-0.32	-0.05	26.59	-1.60	0.01	16.61	-0.87	-0.06	44.85	-1.59	0.03
3	9.60	-0.29	-0.01	9.77	-0.34	-0.01	15.38	-0.31	-0.02	19.55	-0.36	-0.01
4	13.01	-0.09	-0.02	22.22	-0.18	-0.02	15.84	-0.15	-0.02	22.94	-0.23	-0.01
χ	28.77	-0.35	-0.03	33.14	-0.84	-0.03	26.85	-0.65	-0.08	38.13	-1.18	-0.09
SE	14.59	0.12	0.01	14.07	0.34	0.02	10.90	0.26	0.04	10.62	0.55	0.09
Σ	115.09	-1.40	-0.14	132.55	-3.37	-0.11	107.39	-2.59	-0.29	152.54	-4.71	-0.36
n	4	4	4	4	4	4	4	4	4	4	4	4

Table 2.1 - continue

Exp.	-15 mV						-10 mV					
	Control			SFI			Control			SFI		
	τ_1	A1	C	τ_1	A1	C	τ_1	A1	C	τ_1	A1	C
1	63.80	-1.83	-0.17	84.20	-2.81	-0.35	65.26	-1.93	-0.14	88.39	-2.53	-0.47
2	20.09	-1.06	-0.04	63.98	-1.50	0.09	24.04	-1.02	-0.04	75.89	-1.33	0.09
3	24.04	-0.28	-0.02	32.15	-0.31	-0.01	31.17	-0.25	-0.01	43.20	-0.26	-0.01
4	18.34	-0.18	-0.02	26.46	-0.24	-0.01	22.19	-0.18	-0.01	29.77	-0.22	-0.00
χ	31.57	-0.84	-0.06	51.70*	-1.21	-0.07	35.67	-0.84	-0.05	59.31*	-1.09	-0.10
SE	10.81	0.38	0.03	13.62	0.60	0.09	10.05	0.40	0.03	13.70	0.54	0.12
Σ	126.28	-3.35	-0.25	206.80	-4.85	-0.28	142.66	-3.37	-0.21	237.25	-4.34	-0.39
n	4	4	4	4	4	4	4	4	4	4	4	4

Table 2.1 - continue

Exp.	-5 mV						0 mV					
	Control			SFI			Control			SFI		
	τ_1	A1	C	τ_1	A1	C	τ_1	A1	C	τ_1	A1	C
1	68.33	-1.89	-0.11	89.44	-2.26	-0.49	70.25	-1.70	-0.07	82.49	-1.90	-0.49
2	27.75	-1.02	-0.01	77.52	-1.12	0.06	31.22	-0.90	0.00	76.14	-0.92	0.04
3	35.59	-0.23	-0.01	49.38	-0.24	-0.01	38.77	-0.20	-0.01	54.76	-0.21	-0.01
4	25.47	-0.16	-0.01	34.16	-0.21	-0.00	28.24	-0.16	-0.00	36.75	-0.19	0.00
χ	39.29	-0.83	-0.03	62.62*	-0.96	-0.11	42.12	-0.74	-0.02	62.53*	-0.81	-0.12
SE	9.92	0.40	0.02	12.67	0.48	0.12	9.63	0.36	0.01	10.45	0.40	0.12
Σ	157.15	-3.30	-0.14	250.50	-3.83	-0.44	168.49	-2.95	-0.08	250.12	-3.23	-0.46
n	4	4	4	4	4	4	4	4	4	4	4	4

Table 2.1 - continue

Exp.	5 mV					
	Control			SFI		
	τ_1	A1	C	τ_1	A1	C
1	69.87	-1.42	-0.07	76.60	-1.59	-0.47
2	35.52	-0.78	0.02	70.94	-0.73	0.01
3	41.79	-0.17	-0.00	56.90	-0.18	-0.01
4	31.15	-0.14	-0.00	38.70	-0.17	0.00
χ	44.58	-0.63	-0.01	60.78*	-0.67	-0.12
SE	8.70	0.30	0.02	8.44	0.33	0.11
Σ	178.33	-2.51	-0.05	243.13	-2.66	-0.46
n	4	4	4	4	4	4

τ_1 = time constant for inactivation
A_1 = maximum current through the channel (nA)
C = maximum current through channel that inactivates slowly or not at all
Exp. = Experiment number

χ = The statistical average
SE = The standard error of mean
Σ = The sum total of the column
n = The total number of experiments

Table 2.2 - Effect of SFI on the time constants of inactivation at HP = -90 mV.

Exp.	-25 mV						-20 mV					
	Control			SF1			Control			SF1		
	τ_1	A1	C	τ_1	A1	C	τ_1	A1	C	τ_1	A1	C
1	63.57	-0.81	0.26	60.58	-1.59	0.20	62.76	-1.398	0.26	86.62	3.34	0.33
2	9.78	-2.83	0.00	32.99	-1.99	0.08	14.21	-2.361	-0.01	48.32	-1.80	0.09
3	10.24	-0.48	0.01	22.29	-0.40	-0.02	13.58	-0.418	0.00	36.50	-0.36	-0.02
χ	27.86	-1.37	0.09	38.62	-1.33	0.09	30.18	-1.39	0.09	57.15*	0.39	0.13
SE	17.85	0.73	0.08	11.40	0.48	0.06	16.28	0.56	0.08	15.12	1.53	0.10
Σ	83.59	-4.12	0.27	115.86	-3.98	0.27	90.55	-4.18	0.25	171.44	1.18	0.40
n	3	3	3	3	3	3	3	3	3	3	3	3

Table 2.2 - continue

Exp.	-15 mV						-10 mV					
	Control			SF1			Control			SF1		
	τ_1	A1	C	τ_1	A1	C	τ_1	A1	C	τ_1	A1	C
1	56.32	-1.78	0.22	90.69	-3.14	-0.07	55.06	-1.87	0.24	90.34	-2.63	-0.30
2	19.12	-2.02	-0.01	64.63	-1.74	0.15	24.05	-1.77	-0.01	71.54	-1.51	0.14
3	17.08	-0.37	0.00	45.32	-0.33	-0.01	20.14	-0.33	0.01	54.54	-0.30	-0.00
χ	30.84	-1.39	0.07	66.88*	-1.74	0.02	33.08	-1.32	0.08	72.14*	-1.48	-0.05
SE	12.75	0.51	0.07	13.15	0.80	0.06	11.04	0.49	0.08	10.33	0.67	0.13
Σ	92.52	-4.17	0.21	200.64	-5.21	0.06	99.25	-3.97	0.23	216.42	-4.44	-0.16
n	3	3	3	3	3	3	3	3	3	3	3	3

Table 2.2 - continue

Exp.	-5 mV						0 mV					
	Control			SF1			Control			SF1		
	τ_1	A1	C	τ_1	A1	C	τ_1	A1	C	τ_1	A1	C
1	59.57	-1.81	0.32	86.65	-2.35	-0.32	61.54	-1.62	0.37	87.13	-2.05	-0.27
2	28.04	-1.56	0.02	74.89	-1.27	0.12	31.14	-1.36	0.03	73.78	-1.04	0.08
3	22.89	-0.29	0.02	57.68	-0.27	0.00	24.82	-0.25	0.02	59.23	-0.23	0.00
χ	36.83	-1.22	0.12	73.07*	-1.30	-0.07	39.17	-1.08	0.14	73.38*	-1.11	-0.06
SE	11.46	0.47	0.09	8.41	0.60	0.13	11.33	0.42	0.11	8.06	0.52	0.11
Σ	110.50	-3.66	0.35	219.21	-3.89	-0.21	117.50	-3.24	0.42	220.14	-3.32	-0.19
n	3	3	3	3	3	3	3	3	3	3	3	3

Table 2.2 - continue

Exp.	5 mV					
	Control			SFI		
	τ_1	A1	C	τ_1	A1	C
1	61.45	-1.37	0.38	81.37	-1.68	-0.22
2	33.99	-1.17	0.05	71.56	-0.84	0.06
3	27.56	-0.21	0.02	61.87	-0.19	0.01
χ	41.00	-0.92	0.15	71.59*	-0.90	-0.05
SE	10.39	0.35	0.11	5.62	0.43	0.08
Σ	123.00	-2.75	0.45	214.77	-2.71	-0.15
n	3	3	3	3	3	3

See Table 2.1 for captions, * significantly different from control ($p \leq 0.05$)

3. Effect of SFI on the voltage dependence of activation

Table 3.1 - Effect of SFI on the voltage dependence of activation at HP = -50 mV

Exp.	Control				SFI			
	g_{Ca}	E_{Ca}	V½	s	g_{Ca}	E_{Ca}	V½	s
1	0.04	39.43	-20.76	3.72	0.06	41.07	-23.23	2.60
2	0.02	53.17	-22.17	3.03	0.03	32.65	-26.90	1.08
3	0.04	50.2	-23.19	3.57	0.05	43.56	-25.01	2.24
χ	0.02	47.60	-22.04	3.44	0.04	39.09	-25.05	1.97*
SE	0.02	7.23	0.70	0.21	0.03	5.72	1.06	0.46
Σ	0.10	142.80	-66.12	10.32	0.14	117.28	-75.14	5.92
n	3	3	3	3	3	3	3	3

Exp. = Experiment number
g_{Ca} = Maximum conductance through the Ca^{2+} channel
E_{Ca} = The equilibrium potential of Ca^{2+}
V½ = membrane potential where 50 % of Ca^{2+} channels are activated.
S = slope of the voltage dependence

χ = The statistical average
SE = The standard error of mean
Σ = The sum total of the column
n = The total number of experiments

* significantly different from control ($p \leq 0.05$)

4. Effect of SFI on the time of the current to reach a peak

Table 4.1 - Effect of SFI on the time of the current to reach a peak at HP = -50 mV

Exp.	-30 mV		-20 mV		-10 mV		-5 mV		0 mV		5 mV	
	Contr. (ms)	SFI (ms)	Contr. (ms)	SFI (ms)	Contr. (ms)	SFI (ms)	Contr. (ms)	SFI (ms)	Contr. (ms)	SFI (ms)	Contr. (ms)	SFI (ms)
1	42.45	45.60	20.25	22.20	11.85	13.95	9.00	10.50	9.15	9.90	9.45	8.70
2	22.05	21.90	16.80	20.70	11.25	14.40	11.40	13.05	11.40	12.30	9.45	12.30
3	18.60	12.60	15.00	18.45	10.95	12.60	10.35	11.70	8.70	11.25	9.30	9.45
4	26.55	15.00	13.35	19.60	9.15	17.35	7.95	17.20	7.95	16.45	8.70	16.60
χ	27.41	23.78	16.35	20.24*	10.80	14.58*	9.68	13.11	9.30	12.48	9.23	11.76
SE	5.27	7.53	1.48	0.79	0.58	1.00	0.75	1.45	0.74	1.41	0.17	1.78
Σ	109.65	95.10	65.40	80.95	43.20	58.30	38.70	52.45	37.20	49.90	36.90	47.05
n	4	4	4	4	4	4	4	4	4	4	4	4

χ = The statistical average
SE = The standard error of mean
Σ = The sum total of the column
n = The total number of experiments
ms = time of the current to reach peak (in ms)

* significantly different from control ($p \leq 0.05$)

Table 4.2 - Effect of SFI on the time of the current to reach a peak at HP = -90 mV

Exp.	-30 mV		-20 mV		-10 mV		-5 mV		0 mV		5 mV	
	Contr. (ms)	SFI (ms)	Contr. (ms)	SFI (ms)	Contr. (ms)	SFI (ms)	Contr. (ms)	SFI (ms)	Contr. (ms)	SFI (ms)	Contr. (ms)	SFI (ms)
1	20.55	16.20	20.40	16.20	20.40	16.20	20.40	16.20	20.55	16.35	20.40	16.20
2	15.00	14.85	15.00	12.60	15.00	11.85	15.00	9.90	15.00	9.30	15.15	9.15
3	10.05	41.25	12.00	23.40	10.95	14.25	10.05	10.95	9.30	12.45	9.30	9.30
χ	15.20	24.10	15.80	17.40*	15.45	14.10*	15.15	12.35	14.95	12.70	14.95	11.55
SE	3.03	8.58	2.45	3.17	2.73	1.25	2.98	1.94	3.24	2.03	3.20	2.32
Σ	45.60	72.30	47.40	52.20	46.35	42.30	45.45	37.05	44.85	38.10	44.85	34.65
n	3	3	3	3	3	3	3	3	3	3	3	3

See Table 4.1 for captions;

* significantly different from control ($p \leq 0.05$)

ADDENDUM C

1. The antagonistic effect of SFII on Ca^{2+} channels at different test potentials

Table 1.1 - The antagonistic effect of SFII on Ca^{2+} channels at different test potentials (HP = -50 mV)

Exp.	-30 mV			-25 mV			-20 mV			-15 mV		
	Contr. (nA)	SFII (nA)	% Inhibit.	Contr. (nA)	SFII (nA)	% Inhibit.	Contr. (nA)	SFII (nA)	% Inhibit.	Contr. (nA)	SFII (nA)	% Inhibit.
1	-0.32	-0.16	48.60	-0.50	-0.29	42.57	-0.56	-0.35	36.69	-0.53	-0.36	31.90
2	-0.29	-0.05	81.97	-0.46	-0.12	72.65	-0.52	-0.18	64.82	-0.52	-0.24	83.08
3	-0.06	-0.06	13.03	-0.13	-0.06	51.52	-0.29	-0.09	67.47	-0.44	-0.14	68.18
χ	-0.22	-0.09	47.87	-0.36	-0.16	55.58	-0.46	-0.21*	56.33	-0.50	-0.25*	61.05
SE	0.02	0.01	0.01	0.01	0.04	0.01	0.08	0.08	9.85	0.03	0.06	15.20
Σ	-0.68	-0.28	143.60	-1.09	-0.47	166.73	-1.37	-0.63	168.98	-1.49	-0.75	183.15
n	3	3	3	3	3	3	3	3	3	3	3	3

Exp.	-10 mV			-5 mV			0 mV			5 mV		
	Contr. (nA)	SFII (nA)	% Inhibit.	Contr. (nA)	SFII (nA)	% Inhibit.	Contr. (nA)	SFII (nA)	% Inhibit.	Contr. (nA)	SFII (nA)	% Inhibit.
1	-0.48	-0.34	27.88	-0.40	-0.26	34.25	-0.30	-0.22	24.41	-0.22	-0.18	18.35
2	-0.50	-0.24	52.98	-0.42	-0.19	54.98	-0.36	-0.15	59.12	-0.26	-0.09	65.76
3	-0.53	-0.14	73.67	-0.51	-0.13	73.72	-0.43	-0.13	70.83	-0.31	-0.09	72.52
χ	-0.50	-0.24*	51.51	-0.44	-0.20*	54.32	-0.36	-0.17*	51.45	-0.26	-0.12	52.21
SE	0.02	0.06	13.24	0.03	0.03	11.40	0.04	0.03	13.94	0.03	0.03	17.04
Σ	-1.51	-0.72	154.53	-1.33	-0.59	162.95	-1.09	-0.50	154.36	-0.79	-0.35	156.63
n	3	3	3	3	3	3	3	3	3	3	3	3

Exp. = Experiment number
Contr. = Control
% Inhibit. = Percentage inhibition
nA = current in nano Ampere measured at the specific test potentials

mV = test potential measured in millivolts
χ = The statistical average
SE = The standard error of mean
Σ = The sum total of the column
n = The total number of experiments

* significantly different from control ($p \leq 0.05$)

2. Effect of SFII on the time constants of inactivation

Table 2.1 Effect of SFII on the time constants of inactivation at HP = -50 mV

Exp.	-25 mV						-20 mV					
	Control			SFII			Control			SFII		
	τ_1	A1	C	τ_1	A1	C	τ_1	A1	C	τ_1	A1	C
1	37.17	-0.45	-0.05	41.05	-0.25	-0.03	39.15	-0.54	-0.03	33.75	-0.32	-0.02
2	45.74	-0.39	-0.07	50.68	-0.12	-0.01	47.23	-0.44	-0.07	37.19	-0.18	0.02
3	147.20	-0.13	0.02	152.38	0.06	0.02	93.93	-0.25	-0.02	67.90	-0.09	0.01
χ	76.70	-0.32	-0.03	81.37*	-0.10	-0.02	60.10	-0.41	-0.04	46.28	-0.20	0.01
SE	35.33	0.10	0.03	35.61	0.09	0.01	17.07	0.08	0.01	10.85	0.06	0.01
Σ	230.11	-0.97	-0.10	244.11	-0.31	-0.02	180.30	-1.23	-0.12	138.84	-0.59	0.01
n	3	3	3	3	3	3	3	3	3	3	3	3

Table 2.1 - continue

Exp.	-15 mV						-10 mV					
	Control			SFII			Control			SFII		
	τ_1	A1	C	τ_1	A1	C	τ_1	A1	C	τ_1	A1	C
1	44.50	-0.54	-0.01	35.84	-0.36	-0.01	45.12	-0.48	-0.01	37.20	-0.33	0.00
2	50.09	-0.50	-0.04	35.81	-0.25	0.01	47.37	-0.46	-0.03	33.70	-0.25	0.03
3	61.10	-0.43	-0.01	57.08	-0.12	0.01	52.36	-0.50	-0.01	45.83	-0.14	0.01
χ	51.90	-0.49	-0.02	42.91	-0.24	0.01	48.28	-0.48	-0.02	38.91*	-0.24	0.01
SE	4.88	0.03	0.01	7.08	0.07	0.01	2.14	0.01	0.01	3.60	0.06	0.01
Σ	155.70	-1.47	-0.06	128.72	-0.73	0.01	144.85	-1.44	-0.05	116.74	-0.71	0.04
n	3	3	3	3	3	3	3	3	3	3	3	3

Table 2.1 - continue

Exp.	-5 mV						0 mV					
	Control			SFII			Control			SFII		
	τ_1	A1	C	τ_1	A1	C	τ_1	A1	C	τ_1	A1	C
1	46.96	-0.22	0.01	37.76	-0.28	0.03	43.09	-0.29	0.01	37.65	-0.23	0.01
2	46.03	-0.39	-0.03	31.39	-0.22	0.04	47.26	-0.31	-0.01	33.59	-0.17	0.06
3	48.53	-0.48	-0.34	47.88	-0.13	0.02	51.80	-0.39	0.00	46.78	-0.11	0.02
χ	47.17	-0.36	-0.12	39.01	-0.21	0.03	47.38	-0.33	0.00	39.34*	-0.17	0.03
SE	0.73	0.08	0.11	4.80	0.04	0.01	2.51	0.03	0.00	3.90	0.03	0.01
Σ	141.52	-1.08	-0.35	117.03	-0.62	0.09	142.15	-1.00	0.00	118.01	-0.52	0.09
n	3	3	3	3	3	3	3	3	3	3	3	3

Table 2.1 - continue

Exp.	5 mV					
	Control			SFII		
	τ_1	A1	C	τ_1	A1	C
1	46.96	-0.22	0.011	38.32	-0.17	0.01
2	44.13	-0.23	0.01	35.94	-0.14	0.08
3	53.66	-0.28	-0.01	45.33	-0.09	0.03
χ	48.25	-0.24	0.00	39.86*	-0.13	0.04
SE	2.82	0.02	0.01	2.82	0.02	0.02
Σ	144.75	-0.73	0.01	119.58	-0.40	0.12
n	3	3	3	3	3	3

τ_1 = time constant of inactivation
A_1 = maximum current through the channel (nA)
C = maximum current through channel that inactivates slowly or not at all
Exp. = Experiment number

χ = The statistical average
SE = The standard error of mean
Σ = The sum total of the column
n = The total number of experiments

* significantly different from control ($p \leq 0.05$)

3. Effect of SFII on the time of the current to reach a peak

Table 3.1 Effect of SFII on the time of the current to reach a peak at HP = -50 mV

Exp.	-30 mV		-20 mV		-10 mV		-5 mV		0 mV		5 mV	
	Contr. (ms)	SFII	Contr. (ms)	SFII	Contr. (ms)	SFII	Contr. (ms)	SFII	Contr. (ms)	SFII	Contr. (ms)	SFII
1	22.50	13.05	13.65	16.50	10.95	12.15	13.50	11.85	10.65	16.20	11.25	17.10
2	26.40	40.05	15.00	14.85	12.90	9.70	14.25	10.65	8.70	9.00	9.30	9.75
3	25.20	41.10	19.65	9.15	14.25	14.40	13.95	13.80	14.70	11.85	12.45	11.25
χ	24.70	31.40	16.10	13.50	12.70	12.08	13.90	12.10	11.35	12.35	11.00	12.70
SE	1.15	9.18	1.82	2.23	0.96	1.36	0.22	0.92	1.77	2.09	0.92	2.24
Σ	74.10	94.20	48.30	40.50	38.10	36.25	41.70	36.30	34.05	37.05	33.00	38.10
n	3	3	3	3	3	3	3	3	3	3	3	3

χ = The statistical average
SE = The standard error of mean
Σ = The sum total of the column
n = The total number of experiments
ms = time of the current to reach peak (in ms)

ADDENDUM D

1. The antagonistic effect of SFIII on Ca^{2+} channels at different test potentials

Table 1.1 - The antagonistic effect of SFIII on Ca^{2+} channels at different test potentials (HP = -50 mV)

Exp.	-30 mV			-25 mV			-20 mV			-15 mV		
	Contr. (nA)	SFIII (nA)	% Inhibit.	Contr. (nA)	SFIII (nA)	% Inhibit.	Contr. (nA)	SFIII (nA)	% Inhibit.	Contr. (nA)	SFIII (nA)	% Inhibit.
1	-1.08	-0.72	33.15	-1.07	-0.86	19.05	-1.03	-0.82	20.37	-0.93	-0.76	18.30
2	-0.10	-0.79	21.16	-1.39	-1.13	18.40	-1.87	-1.48	20.88	-2.13	-1.70	20.08
3	-0.13	-0.07	45.11	-0.48	-0.11	76.41	-0.76	-0.16	79.45	-0.87	-0.16	81.63
4	-0.27	-0.20	26.12	-0.60	-0.35	41.29	-0.74	-0.45	39.24	-0.77	-0.46	40.39
χ	-0.62	-0.44	31.39	-0.88	-0.62*	38.79	-1.10	-0.73*	39.98	-1.17	-0.77*	40.10
SE	0.24	0.18	5.19	0.21	0.23	13.62	0.26	0.28	13.86	0.32	0.33	14.72
Σ	-2.47	-3.54	125.54	-3.54	-2.46	155.15	-4.40	-2.90	159.94	-4.70	-3.08	160.40
n	4	4	4	4	4	4	4	4	4	4	4	4

Exp.	-10 mV			-5 mV			0 mV			5 mV		
	Contr. (nA)	SFIII (nA)	% Inhibit.	Contr. (nA)	SFIII (nA)	% Inhibit.	Contr. nA)	SFIII (nA)	% Inhibit.	Contr. (nA)	SFIII (nA)	% Inhibit.
1	-0.85	-0.68	17.21	-0.74	-0.59	20.35	-0.66	-0.54	18.43	-0.56	-0.47	16.52
2	-2.16	-1.66	23.22	-1.99	-1.53	22.99	-1.77	-1.35	23.82	-1.49	-1.10	26.06
3	-0.84	-0.15	81.84	-0.75	-0.14	80.86	-0.63	-0.10	83.68	-0.52	-0.07	86.99
4	-0.73	-0.43	41.05	-0.67	-0.38	44.06	-0.57	-0.31	45.87	-0.48	-0.24	49.79
χ	-1.14	-0.73*	40.83	-1.04	-0.66*	42.07	-0.91	-0.58*	42.95	-0.76	-0.47*	44.84
SE	0.34	0.33	14.57	0.31	0.30	13.98	0.28	0.27	14.82	0.24	0.22	15.69
Σ	-4.58	-2.92	163.32	-4.15	-2.64	168.26	-3.63	-2.30	171.79	-3.05	-1.88	179.36
n	4	4	4	4	4	4	4	4	4	4	4	4

Exp. = Experiment number
Contr. = Control
% Inhibit. = Percentage inhibition
nA = current in nano Ampere measured at the specific test potentials
mV = test potential measured in millivolts
χ = The statistical average
SE = The standard error of mean
Σ = The sum total of the column
n = The total number of experiments

* significantly different from control ($p \leq 0.05$)

2. Effect of SFIII on the time constants of inactivation

Table 2.1 - Effect of SFIII on the time constants of inactivation at HP = -50 mV.

Exp.	-30 mV						-25 mV					
	Control			SFIII			Control			SFIII		
	τ_1	A1	C	τ_1	A1	C	τ_1	A1	C	τ_1	A1	C
1	13.15	-1.27	-0.01	12.61	-0.82	-0.02	17.80	-1.17	-0.03	18.24	-0.89	-0.04
2	30.16	-0.96	-0.10	29.21	-0.71	-0.13	38.50	-1.17	-0.31	40.13	-0.88	-0.30
3	-	-	-	-	-	-	56.96	-0.40	-0.08	96.02	-0.09	0.01
4	17.96	-0.24	-0.04	37.20	-0.14	-0.04	14.93	-0.61	-0.05	31.45	-0.32	-0.04
χ	20.42	-0.82	-0.05	26.34	-0.56	-0.06	32.05	-0.84	-0.12	46.46	-0.54	-0.09
SE	5.06	0.30	0.02	7.24	0.21	0.03	9.82	0.19	0.07	17.12	0.20	0.07
Σ	61.28	-2.47	-0.16	79.02	-1.67	-0.19	128.19	-3.35	-0.46	185.83	-2.17	-0.37
n	3	3	3	3	3	3	4	4	4	4	4	4

Exp.	-20 mV						-15 mV					
	Control			SFIII			Control			SFIII		
	τ_1	A1	C	τ_1	A1	C	τ_1	A1	C	τ_1	A1	C
1	23.62	-1.07	-0.02	25.95	-0.81	-0.04	28.55	-0.93	-0.01	32.68	-0.73	-0.02
2	44.33	-1.40	-0.50	53.18	-1.15	-0.38	56.87	-1.61	-0.56	56.36	-1.22	-0.45
3	53.62	-0.70	-0.08	83.76	-0.12	0.01	53.27	-0.80	-0.08	71.17	-0.16	0.02
4	19.30	-0.76	-0.03	29.82	-0.43	-0.03	22.74	-0.74	-0.02	35.59	-0.43	-0.02
χ	35.22	-0.98	-0.16	48.18*	-0.63	-0.11	40.36	-1.02	-0.17	48.95	-0.64	-0.12
SE	8.21	0.16	0.11	13.30	0.22	0.09	8.61	0.20	0.13	9.09	0.23	0.11
Σ	140.87	-3.93	-0.64	192.70	-2.51	-0.43	161.43	-4.09	-0.67	195.79	-2.55	-0.47
n	4	4	4	4	4	4	4	4	4	4	4	4

Exp.	-10 mV						-5 mV					
	Control			SFIII			Control			SFIII		
	τ_1	A1	C	τ_1	A1	C	τ_1	A1	C	τ_1	A1	C
1	34.72	-0.82	-0.01	39.61	-0.66	-0.01	41.20	-0.72	0.02	43.94	-0.57	0.00
2	60.36	-1.53	-0.61	60.22	-1.21	-0.43	63.64	-1.39	-0.55	59.96	-1.09	-0.39
3	55.65	-0.75	-0.08	53.99	-0.17	0.03	54.68	-0.69	-0.06	50.27	-0.15	0.03
4	28.76	-0.72	-0.01	41.16	-0.41	-0.02	34.04	-0.68	0.00	42.56	-0.35	-0.01
χ	44.87	-0.96	-0.18	48.75	-0.61	-0.11	48.39	-0.87	-0.15	49.18	-0.54	-0.09
SE	7.74	0.19	0.14	5.00	0.22	0.11	6.64	0.17	0.14	3.96	0.20	0.10
Σ	179.49	-3.82	-0.71	194.98	-2.46	-0.43	193.56	-3.49	-0.59	196.73	-2.16	-0.37
n	4	4	4	4	4	4	4	4	4	4	4	4

Exp.	0 mV						5 mV					
	Control			SFIII			Control			SFIII		
	τ_1	A1	C	τ_1	A1	C	τ_1	A1	C	τ_1	A1	C
1	46.82	-0.62	0.01	49.95	-0.49	-0.00	52.28	-0.53	0.01	54.19	-0.45	0.00
2	61.85	-1.27	-0.50	58.29	-0.99	-0.33	61.64	-1.08	-0.40	55.93	-0.81	-0.28
3	52.53	-0.58	-0.050	52.05	-0.12	0.04	49.10	-0.46	-0.04	51.06	-0.10	0.06
4	37.66	-0.58	0.01	45.82	-0.29	-0.01	42.59	-0.48	0.00	46.40	-0.22	0.00
χ	49.72	-0.76	-0.13	51.53	-0.47	-0.08	51.40	-0.64	-0.10	51.90	-0.40	-0.06
SE	5.07	0.17	0.12	2.59	0.18	0.08	3.96	0.14	0.09	2.09	0.15	0.07
Σ	198.86	-3.05	-0.53	206.11	-1.90	-0.30	205.61	-2.56	-0.43	207.58	-1.58	-0.24
n	4	4	4	4	4	4	4	4	4	4	4	4

τ_1 = time constant of inactivation
A_1 = maximum current through the channel (nA)
C = maximum current through channel that inactivates slowly or not at all
Exp. = Experiment number

χ = The statistical average
SE = The standard error of mean
Σ = The sum total of the column
n = The total number of experiments

* significantly different from control ($p \leq 0.05$)

3. Effect of SFIII on the voltage dependence of activation

Table 3.1 - Effect of SFIII on the voltage dependence of activation at HP = -50 mV

Exp.	Control				SFIII			
	g_{Ca}	E_{Ca}	V½	s	g_{Ca}	E_{Ca}	V½	s
1	0.03	33.04	-10.42	4.34	0.007	55.46	-13.14	3.70
2	0.02	54.07	-15.00	4.04	0.006	16.50	-15.15	4.49
3	0.02	27.64	-17.51	4.29	0.007	11.88	-20.84	4.47
χ	0.02	38.25	-14.31	4.22	0.007*	27.95*	-16.38*	4.22
SE	0.007	13.96	3.59	0.09	0.001	9.34	3.77	0.26
Σ	0.12	114.75	-42.93	12.67	0.03	83.84	-49.13	12.66
n	4	4	4	4	4	4	4	4

Exp. = Experiment number
g_{Ca} = Maximum conductance through the Ca^{2+} channel
E_{Ca} = The equilibrium potential of Ca^{2+}
V½ = membrane potential where 50 % of Ca^{2+} channels are activated.
S = slope of the voltage dependence
* significantly different from control ($p \leq 0.05$)

χ = The statistical average
SE = The standard error of mean
Σ = The sum total of the column
n = The total number of experiments

4. Effect of SFIII on the time of the current to reach a peak

Table 4.1 Effect of SFIII on the time of the current to reach a peak at HP = -50 mV

Exp.	-30 mV		-20 mV		-10 mV		-5 mV		0 mV		5 mV	
	Control	SFIII	Control	SFIII	Control	SFIII	Control	SFIII	Control	SFIII	Control	SFIII
1	20.70	30.15	13.80	18.60	12.45	14.40	10.80	14.40	10.50	13.50	10.50	13.05
2	23.10	22.95	14.55	14.10	10.05	10.35	9.60	8.85	7.95	9.45	7.80	8.10
3	19.65	15.90	19.50	14.55	14.10	10.35	9.15	12.00	7.80	10.35	9.60	16.20
4	26.25	27.45	19.50	21.90	16.05	18.00	15.90	17.85	15.15	16.80	18.15	20.55
χ	22.42	24.11	16.84	17.29	13.16	13.28	11.36	13.28	10.35	12.52*	11.51	14.47*
SE	1.46	3.11	1.54	1.84	1.27	1.84	1.55	1.90	1.72	1.67	2.28	2.62
Σ	89.70	96.45	67.35	69.15	52.65	53.10	45.45	53.10	41.40	50.10	46.05	57.90
n	4	4	4	4	4	4	4	4	4	4	4	4

χ = The statistical average
SE = The standard error of mean
Σ = The sum total of the column
n = The total number of experiments
ms = time of the current to reach peak (in ms)
* significantly different from control ($p \leq 0.05$)

References

ADAMS, M.E. 2004. Agatoxins: ion channel specific toxins from the American funnel web spider, *Agelenopsis aperta. Toxicon,* 43:509-525.

AKAIKE, N. 1998. Heterogeneous distribution of LVA and HVA calcium channels in mammalian brain tissue. (*In* Tsien, R.W., Clozel, J-P. & Nargeot, J., *eds.* Low-Voltage-Activated T-type Calcium Channels: Proceedings from the International Electrophysiology Meeting, Montpellier, Oct. 21-22 1996. Tattenhall, Chester, England: Adis International. p. 53-62).

ALVAREZ, J.L. & VASSORT, G. 1992. Properties of the low threshold Ca current in single frog atrial cardiomyocytes - a comparison with the high threshold Ca current. *Journal of General Physiology,* 100: 519-545, Sept.

ANDERSON, P.A.V. & GREENBERG, R.M. 2001. Phylogeny of ion channels: clues to structure and function. *Comparative Biochemistry and Physiology part B,* 129:17-28.

ARIKKATH, J. & CAMPBELL, K.P. 2003. Auxiliary subunits: essential components of the voltage-gated calcium channel complex. *Current opinion in Neurobiology,* 13:298-307.

ARMSTRONG, C.M. 1998. Calcium channel properties in endocrine cells of pituitary origin. (*In* Tsien, R.W., Clozel, J-P. & Nargeot, J., *eds.* Low-Voltage-Activated T-type Calcium Channels: Proceedings from the International Electrophysiology Meeting, Montpellier, Oct. 21-22 1996. Tattenhall, Chester, England: Adis International. p. 5-15).

ASHCROFT, F.M. 2000. Ion channels and disease. San Diego, California. 481p.

BALKE, C.W. & GOLD, M.R. 1992. Calcium channels in the heart: an overview. *Heart disease and stroke,* 398-403, Nov./Dec.

BALKE, C.W., ROSE, W.C., MARBAN, E. & WIER, W.G. 1992. Macroscopic and unitary properties of physiological ion flux through T-type Ca^{2+} channels in guinea-pig heart cells. *Journal of Physiology,* 456:247-265.

BALSER, J.R. 1999. Structure and function of the cardiac sodium channels. *Cardiovascular Research,* 42:327-338.

BEAN, B.P. 1985. Two kinds of calcium channels in canine atrial cells, differences in kinetics, selectivity and pharmacology. *Journal of general Physiology,* 86:1-30.

BEAN, B.P. 1989. Multiple types of calcium channels in heart muscle and neurons: modulation by drugs and neurotransmitters. *Annals of the New York Academy of Science,* 560:334-345.

BELLES, B., MALECOT, C.O., HESCHELELR, J. & TRAUTWEIN, W. 1988. "Run-down" of the Ca current during whole-cell recordings in guinea pig heart cells: role of phosphorylation and intracellular calcium. *Pflügers Archives,* 411:353-360.

BERGMAN, N.J. 1997. Clinical description of *Parabuthus transvaalicus* scorpionism in Zimbabwe. *Toxicon,* 35(5): 759-771.

BERS, D.M. & PEREZ-REYES, E. 1999. Ca channels in cardiac myocytes: structure and function in Ca influx and intracellular Ca release. *Cardiovascular research,* 42: 339-360.

BIRNBAUMER, L., QIN, N., OLCESSE, R., TAREILUS, E. STEFANI, E. 1998. Studies on the regulation of the human neuronal α1E calcium channel by ß and $\alpha_2\delta$ subunits. (*In* Tsien, R.W., Clozel, J-P. & Nargeot, J., *eds.* Low-Voltage-Activated T-type Calcium Channels: Proceedings from the International Electrophysiology Meeting, Montpellier, Oct. 21-22 1996. Tattenhall, Chester, England: Adis International. p. 258-268).

BLUMENTHAL, K. 1995. Ion channels as targets for toxins. (*In* Sperelakis, N., *ed.* Cell Physiology Source Book. Academic Press. P.389-400).

BOTHA, E.M. 2002. Die effek van *Parabuthus granulatus* venom op kalsiumkanale in ventrikulêre miosite geêre miosite geïsoleer uit marmothart. Potchefstroom : PU vir CHO. (Verhandeling – M. Sc.) 75p.

BROWN, R.H. 1993. Ion channel mutations in Periodic paralysis and related myotonic diseases. *Annals of the New York Academy of Science,* 707:305-315.

CARBONE, E. & LUX, H.D. 1989. Modulation of Ca channels in peripheral neurons. *Annals of the New York Academy of Science,* 560:346-357.

CARBONE, E., ZUCKER, H., LUX, H.D., CARABELLI, V., MAGNELLI, V., BALDELLI, P. & AICARDI, G. 1998. Mg^{2+} block of LVA and HVA channels: a probe for studying calcium channel structure. (*In* Tsien, R.W., Clozel, J-P. & Nargeot, J., *eds.* Low-Voltage-Activated T-type Calcium Channels: Proceedings from the International Electrophysiology Meeting, Montpellier, Oct. 21-22 1996. Tattenhall, Chester, England: Adis International. p. 81-91).

CARMELIET, E. 1986. Calcium channel-antagonists and the cardiovascular system. *Acta Cardiologica,* XLI (2): 133-146.

CATTERALL, W.A. 1991. Functional subunit structure of Voltage-gated calcium channels. *Science,* 253:1499-1500.

CATTERALL, W.A. 1993. Structure and modulation of Na^{+} and Ca^{2+} channels. *Annals of the New York Academy of Science,* 707:1-19.

CATTERALL, W.A. 2000. Structure and regulation of voltage-gated Ca^{2+} channels. *Annual reviews of Biology,* 16:521-555.

CATTERALL, W.A., STRIESSING, J., SNUTCH, T.P. & PEREZ-REYES, E. 2003. International union of pharmacology. XL. Compendium of voltage-gated ion channels: Calcium channels. *Pharmacological Reviews,* 55(4):579-581.

CHUANG, R.S-I., JAFFE, H., CRIBBS, L., PEREZ-REYES, E. & SWARTZ, K.J. 1998. Inhibition of T-type voltage-gated calcium channels by a new scorpion toxin. *Nature neuroscience,* 1(8): 668-674.

CHUNG, S-H. & KUYUCAK, S. 2002. Recent advances in ion channel research. *Biochimica et Biophysica Acta,* 1565:267-286.

CONDE, R., ZAMUDIO, F.Z., RODRIGUEZ, M.H. & POSSANI, L.D. 2000. Scorpine, an anti-malaria and anti-bacterial agent purified from scorpion venom. *Federation of European Biochemical Societies letters*, 471:165-168.

CORRY, B., ALLEN, T.W., KUYUCAK, S. & CHUNG, S-H. 2000. A model of calcium channels. *Biochimica et Biophysica Acta,* 1590:1-6.

CORZO, G., ADACHI-AKAHANE, S., NAGAO, T., KUSUI, Y. & NAKAJIMA, T. 2001. Novel peptides from assassin bugs (Hemitrope: Reduviidae): isolation, chemical and biological characterization. *Federation of European Biochemical Societies letters,* 499:256-261.

CORZO, G. ESCOUBAS, P., VILLEGAS, E., BARNHAM, K.J., HE, W., NORTON, R.S. & NAKAJIMA, T. 2001. Characterization of unique amphipathic antimicrobial peptides from venom of the scorpion *Pandinus imperator. Biochemical Journal,* 359:35-45.

CUMMINGS, D.M., AMIADIO, P., NELSON, L. & FITZGERALD, J.M. 1991. The role of Ca^{2+} channel blockers in the treatment of essential hypertension. *Archives of internal medicine,* 151:250-259, Feb.

DARBON, H., BLANC, E. & SABATIER, J.M. 1999. Three-dimensional structure of scorpion toxins: towards a new model of interaction with potassium channels. *Perspectives in Drug Discovery and Design,* 15/16: 41-60.

DEBONT, T., SWERTS, A., VAN DER WALT, J.J., MÜLLER, G.J., VERDONCK, F., DAENENS, P. & TYTGAT, J. 1998. Comparison and characterization of three *Parabuthus* scorpion species occurring in southern Africa. *Toxicon,* 36(2): 341-352.

DYASON, K., BRANDT, W., PRENDINI, L., VERDONCK, F., TYTGAT, J., DU PLESSIS, J., MÜLLER, G. & VAN DER WALT, J. 2002. Determination of species-specific components in the venom of *Parabuthus* scorpions from southern Africa using matrix-assisted laser desorption time-of-flight mass spectrometry. *Rapid communications in mass spectrometry,* 16:768-773.

FOZZARD, H.A. 1992. Mechanisms of pharmacologic intervention at the level of the calcium channel. *The American Journal of Cardiology,* 69:4D-10D.

GORDON, D., SAVARIN, P., GUREVITZ, M. & ZINN-JUSTIN, S. 1998. Functional anatomy of scorpion toxins affecting sodium channels. *Journal of toxicology-toxin reviews,* 17(2): 131-159.

GRACE, A.A. & CAMM, A.J. 2000. Voltage-gated calcium-channels and antiarrhythmic drug action. *Cardiovascular research,* 45:43-51.

GWEE, M.C.E., NIRTHANAN, S., KHOO, H-E., GOPALAKRIHNAKONE, P., KINI, R.M. & CHEAH, L-S. 2002. Autonomic effects of some scorpion venoms and toxins. *Clinical and Experimental Pharmacology and Physiology,* 29:795-801.

HADLEY, R.W. & LEDERER, W.J. 1991. Ca^{2+} and voltage inactivate Ca^{2+} channels in guinea-pig ventricular myocytes through independent mechanisms. *Journal of Physiology,* 444:257-268.

HAGIWARA, N., IRISAWA, H. & KAMEYAMA, M. 1988. Contribution of two types of calcium currents to the pacemaker potentials of rabbit sino-atrial node cells. *Journal of Physiology,* 395:233-253.

HARPOLD, M.M., WILLIAMS, M.E., BRUST, P.F., STAUDERMAN, K., URRUTIA, A., JOHNSON, E.C. & HANS, M. 1998. Human neuronal voltage-gated

calcium channels: splice variants, subunit interactions and subtypes. (*In* Tsien, R.W., Clozel, J-P. & Nargeot, J., *eds.* Low-Voltage-Activated T-type Calcium Channels: Proceedings from the International Electrophysiology Meeting, Montpellier, Oct. 21-22 1996. Tattenhall, Chester, England: Adis International. p. 218-229).

HERLITZE, S., HOCKERMAN, G.H., SCHEUER, T. & CATTERALL, W.A. 1997. Molecular determinants of inactivation and G protein modulation in the intracellular loop connecting domains I and II of the calcium channel α_1A subunit. *Proceedings of the National Academy of Sciences of the United states of America*, 94:1512-1516, Febr.

HESS, P., LANSMAN, J.B., TSIEN, R.W. 1984. Different modes of Ca^{2+} channel gating behavior favored by dihydropyridine Ca^{2+} agonists and antagonists. *Nature,* 311:538-544, Oct.

HESS, P., LANSMAN, J.B., NILIUS, B. & TSIEN, R.W. 1986. Ca^{2+} channel types in cardiac myocytes: modulation by Dihydropyridines and β-adrenergic stimulation. *Journal of Cardiovascular pharmacology,* 8(Sppl. 9): S11-S21.

HESS, P., PROD'HOM, B. & PIETROBON, D. 1989. Mechanisms of interaction of permeant ions and protons with dihydropyridine-sensitive calcium channels. *Annals of the New York Academy of Science,* 560:80-92.

HILLE, B. 2001. Ion channels of excitable membranes. 3rd ed. Sunderland Mass: Sinauer. 607p.

HOSEY, M.M., CHIEN, A.J. & PURI, T.S. 1996. Structure and regulation of L-type calcium channels, A current assessment of the properties and roles of channel subunits. *Trends in Cardiovascular medicine,* 6(8): 265-273.

HUYS, I., DYASON, K., WAELKENS, E., VERDONCK, F., VAN ZYL, J., DU PLESSIS, J., MÜLLER, G.J., VAN DER WALT, J., CLYNEN, E., SSCHOOFS, L. & TYTGAT, J. 2002. Purification, characterization and biosynthesis of parabutoxin

3, a component of *Parabuthus transvaalicus* venom. *European Journal of Biochemistry*, 269:1854-1865.

ISMAIL, M. 1995. The scorpion envenoming syndrome. *Toxicon*, 33(7): 825-858.

JIMéNEZ, C., BOURINET, E., LEURANGUER, V., RICHARD, S., SNUTCH, T.P. & NARGEOT, J. 2000. Determinants of voltage-dependent inactivation affect Mibefradil block of calcium channels. *Neuropharmacology*, 39:1-10.

JORDAAN, E.E. 2002. Die elektrofisiologiese effekte van KLII en Sephadex Fraksies I-IV, geïsoleer uit die venom van Parabuthus granulatus, op Ca^{2+} -kanale in dorsale wortel ganglia van die rot. Potchefstroom : PU vir CHO. (Skripsie – Honns.) 42p.

KAMEYAMA, A., KAMEYAMA, A., NAKAYAMA, T. & KAIBARA, M. 1988. Tissue extract recovers cardiac Ca^{2+} channels from "run-down". *Pflügers Archives*, 412:328-330.

KAMP, T.J., SANGUINETTI, M.C. & MILLER, R.J. 1989. Voltage- and use-dependent modulation of cardiac calcium channels by the dihydropyridine (+)-202-791. *Circulation Research*, 64:338-351).

KATZ, A.M. 1993. Cardiac ion channels. *The New England Journal of medicine*, 328(17): 1244-1251.

KATZ, A.M. 1997. Molecular biology of calcium channels in the cardiovascular system. *The American Journal of Cardiology*, 80(9A): 171-221, Nov.

KEPPLINGER, K.J.F., FÖRSTNER, G., KAHR, H., LEITNER, K., PAMMER, P., GROSCHNER, K., SOLDATOV, N.M. & ROMANIN, C. 2000. Molecular determinant for run-down of L-type Ca^{2+} channels localized in the carboxyl terminus of the α_{1C} subunit. *Journal of Physiology*, 529:119-130.

KOCHEGAROV, A.A. 2003. Pharmacological modulators of voltage-gated calcium channels and their therapeutical application. *Cell calcium*, 33:145-162.

KOZLOV, S., LIPKIN, A., NOSYREVA, E., BLAKE, A., WINDASS, J.D. & GRISHIN, E. 2000. Purification an cDNA cloning of an insecticidal protein from the venom of the scorpion *Orthochirus scrobiculosus. Toxicon,* 38:361-371.

KUSHMERICK, C., MESQUITA DE CARVALHO, F., DE MARIA, M., MASSENSINI, A.R., ROMANA-SILVA, M.A., GOMEZ, M.V., KALAPOTHAKIS, E. & PRADO, M.A.M. 2001. Effects of a *Lasiodora* spider venom on Ca^{2+} and Na^{+} channels. *Toxicon,* 39:991-1002.

LACINOVA, L., KLUGBAUER, N. & HOFMANN, F. 2000. Regulation of the calcium channel α_{1G} subunit by divalent cations and organic blockers. *Neuropharmacology,* 39:1254-1266.

LAN, Z-D., DAI, L., ZHUO, X-L., FENG, J-C., XU, K. & CHI, C-W. 1999. Gene cloning and sequencing of BmK AS and BmK AS-1, two novel neurotoxins from the scorpion *Buthus martensi* Karsch. *Toxicon,* 37:815-823.

LAWRENCE, J.H., GORDON, F., TOMASELLI, M.D. & EDUARDO, M. 1993. Ion channels: Structure and Function. *Heart disease and Stroke,* 2:75-80.

LECOMTE, C., SABATIER, J.M. VAN RIETSCHOTES, J. & ROCHAT, H. 1998. Synthetic peptides as tools to investigate the structure and pharmacology of potassium channel-acting short-chain scorpion toxins. *Biochimie,* 80:151-154.

LEEMING, J. 2003. Scorpions of southern Africa. Cape Town: Struik Publishers. 88p.

LE GRAND, B., DEROUBAIX, E., COULOMBE, A. & CORABOEUF, E. 1990. Stimulatory effect of ouabain on T- and L-type calcium currents in guinea pig cardiac myocytes. *American Journal of Physiology, Heart and circulation Physiology,* 258:H1620-H1623.

LEGROS, C., CéARD, B., BOUGIS & MARTIN-EAUCLAIRE, M-F. 1998. Evidence for a new class of scorpion toxins active against K^+ channels. *Federation of European Biochemical Societies letters,* 431:375-380.

LEHMANN-HORN, F. & JURKAT-ROTT, K. 1999. Voltage-gated ion channels and hereditary disease. *Physiological reviews,* 79(4): 1317-1372.

LIPKIN, A., KOZLOV, S., NOSYREVA, E., BLAKE, A., WINDASS, J.D. & GRISHIN, E. 2002. Novel insecticide toxins from the venom of the spider *Segestria florentina. Toxicon,* 40:125-130.

LIU, H. & CAMPBELL, K.P. 1998. Structural determinants of calcium channel ß subunit function. (*In* Tsien, R.W., Clozel, J-P. & Nargeot, J., *eds.* Low-Voltage-Activated T-type Calcium Channels: Proceedings from the International Electrophysiology Meeting, Montpellier, Oct. 21-22 1996. Tattenhall, Chester, England: Adis International. p. 229-243).

LÓPEZ-GONZÁLEZ, I., OLAMENDI-PORTUGAL, T., DE LA VEGA-BELTRÁN, J.L., VAN DER WALT, J., DYASON, K., POSSANI, L.D., FELIX, R. & DARZON, A. 2003. Scorpion toxins that block T-type Ca^{2+} channels in spermatogenic cells inhibit the sperm acrosome reaction. *Biochemical and Biophysical research communications,* 300:408-414.

LORET, E. & HAMMOCK, B. 2001. Structure and Neurotoxicity of venoms (*In* Brownell, P. & Polis, G. Scorpion biology and research, Oxford University Press, New York, 204p.)

MAZZANTI, M., DeFELICE, L.J. & LIU, Y-M. 1991. Gating of L-type Ca^{2+} channels in embryonic chick ventricle cells: dependence on voltage, current and channel density. *Journal of Physiology,* 443:307-334.

MAZZEI DE DAVILA, C.A., DAVILA, D.F. DONIS, J.H., ARATA DE BELLABARBA, G., VILLARREAL, V. & BARBOZA, J.S. 2002. Sympathetic

nervous system activation, antivenin administration and cardiovascular manifestations of scorpion envenomation. *Toxicon,* 1339-1346.

MCDONALD, T., PELZER, D. & TRAUTWEIN, W. 1989. Dual action (stimulation, inhibition) of D600 on contractility and calcium channels in guinea pig and cat heart cells. *Journal of Physiology,* 414:569-586.

MCINTOSH, J.M. & JONES, R.M. 2001. Cone venom – from accidental stings to deliberate injection. *Toxicon,* 39:1447-1451.

MÉNEZ, A., BONTEMS, F., ROUMESTAND, C., GILQUIN, B. & TOMA, F. 1992. Structural basis for functional diversity of animal toxins. *Proceedings of the Royal society of Edinburgh,* 99B(1/2): 83-103.

MEHRKE,G., ZONG, X.G., FLOCKERZI, V. & HOFMANN, F. 1994. The Ca++-channel blocker Ro 40-5967 blocks differently T-type and L-type Ca++ channels. *The Journal of Pharmacology and experimental therapeutics,* 271:1483-1488.

MEIR, A., GINSBURG, S., BUTKEVICH, A., KACHALSKY, S.G., KAISERMAN, I., AHDUT, R., DEMIRGOREN, S. & RAHAMIMOFF, R. 1999. Ion channel in Presynaptic nerve terminals and Control of Transmitter release. *Physiological Reviews,* 79(3): 1019-1063.

MIKOSHIBA, K., FURUICHI, T., MIYAWAKI, A., YOSHIKAWA, S., NAKADE, S., MICHIKAWA, T., NAKAGAWA, T., OKANO, H., KUME, S., MUTO, A., ARUGA, J., YAMADA, N., HAMANAKA, Y., FUJINO, I. & KOBAYASHI, M. 1993. Structure and function of Inositol 1,4,5-Triphosphate receptor. *Annals of the New York Academy of Science,* 707:178-197.

MILJANICH, G.P. 1997. Venom peptides as human pharmaceuticals. *Science and medicine,* 6-15, Sep/Oct.

MITTERDORFER, J., HERING, S., ACZEL, S., BERJUKOW, S., DEGTIAR, V., DöRING, F., GRABNER, M.M KRAUS, R., SINNEGGER, M.J. STRIESSNIG, J., WANG, Z. & GLOSSMANN, H. 1998. Molecular basis of drug interactions with calcium channels: a constructive approach. (*In* Tsien, R.W., Clozel, J-P. & Nargeot, J., *eds.* Low-Voltage-Activated T-type Calcium Channels: Proceedings from the International Electrophysiology Meeting, Montpellier, Oct. 21-22 1996. Tattenhall, Chester, England: Adis International. p. 351-377).

MORI, Y., NIIDOME, T., FUJITA, Y., MYNLIEFF, M., DIRKSEN, R.T., BEAM, K.G., IWABE, N., MIYATA, T., FURUTAMA, D., FURUICHI, T. & MIKOSHIBA, K. 1993. Molecular diversity of Voltage dependent calcium channels. *Annals of the New York Academy of Science,* 707:87-108.

MüLLER, G.J. 1993. Scorpionism in South Africa – A report of 42 serious scorpion envenomations. *South African Medical Journal,* 83:405-411.

NARGEOT, J., LORY, P. & RICHARD, S. 1997. Molecular basis of the diversity of calcium channels in cardiovascular tissues. *European Heart Journal,* 18:A15-A26.

NOLL, G. & LüSCHER, T.F. 1998. Comparative pharmacological properties among calcium channel blockers: T-channel versus L-channel blockade. *Cardiology,* 89:10-15.

OLAMENDI-PORTUGAL, T., INÉS GARCÍA, B., LÓPEZ-GONZÁLEZ, I., VAN DER WALT, J., DYASON, K., ULENS, C., TYTGAT, J., FELIX, R., DARZON, A. & POSSANI, L.D. 2002. Two new scorpion toxins that target voltage-gated Ca^{2+} and Na^{+} channels. *Biochemical and Biophysical research communications,* 299:562-568.

OLIVERA, B.M. & CRUZ, L.J. 2001. Conotoxins, in retrospect. *Toxicon,* 39:7-14.

OPIE, L.H. 1998. The heart: Physiology, from cell to circulation. 3rd ed. United States of America. 637p.

PARENT, L. & GOPALAKRISHNAN, M. 1995. Glutamate substitution in repeat IV alters divalent and monovalent cation permeation in the heart Ca^{2+} channel. *Biophysical journal,* 69:1801-1813.

PENG, S., HAJELA, R.K. & ATCHISON, W.D. 2002. Characteristics of block by Pb^{2+} of function of human neuronal L-, N-, and R-type Ca^{2+} channels transiently expressed in human embryonic kidney 293 cells. *Molecular pharmacology, 62*(6): 1418-1430.

PEREZ-REYES, E. 2003. Molecular Physiology of low-voltage activated T-type calcium channels. *Physiology reviews,* 83:117-161.

POSSANI, L.D., MERINO, E., CORONA, M., BOLIVAR, F. & BECERRIL, B. 2000. Peptides and genes coding for scorpion toxins that affect ion-channels. *Biochimie,* 82:861-868.

PRENDINI, L. 2001. Phylogeny of *Parabuthus* (Scorpiones, Buthidae). *Zoologica Scripta,* 30:13-35, Jan.

RAMPE, D., ANDERSON, B., RAPIEN-PRYOR, W., LI, T. & DAGE, R.C. 1993. Comparison of the in Vivo and in Vitro cardiovascular effects of two structurally distinct Ca^{2+} channel activators, Bay K8644 and FPL 64176. *The Journal of Pharmacology and Experimental therapeutics,* 265(3): 1125-1130.

RANDALL, A. & TSIEN, R.W. 1996. Distinctive biophysical and pharmacological features of T-type calcium channels. (*In* Tsien, R.W., Clozel, J-P. & Nargeot, J., *eds.* Low-Voltage-Activated T-type Calcium Channels: Proceedings from the International Electrophysiology Meeting, Montpellier, Oct. 21-22 1996. Tattenhall, Chester, England: Adis International. p. 29-43).

REES, B. & BILWES, A. 1993. Three dimensional structures of neurotoxins and cardiotoxins. *Chemical research in Toxicology,* 6(4): 385-404.

RICHARD, S., NEVEU, D., CARNAC, G., BODIN, P., TRAVO, P. & NARGEOT, J. 1992. Differential expression of voltage-gated Ca^{2+} currents in cultivated aortic myocytes. *Biochimica et Biophysica Acta,* 1160:95-104.

RICHARD, S., LECLERCQ, F., LEMAIRE, S., PIOT, C. & NARGEOT, J. 1998. Ca^{2+} currents in compensated hypertrophy and heart failure. *Cardiovascular research,* 37:300-311.

ROSE, W.C., BALKE, C.W., WIER, W.G. & MARBAN, E. 1992. Macroscopic and unitary properties of physiological ion flux through L-type Ca^{2+} channels in guinea-pig heart cells. *Journal of Physiology,* 456:267-284.

ROSSIER, M.F., BURNAY, M.M. & CAPPONI, A.M. 1998. Distinct functions of T- and L-type calcium channels during activation of aldosterone production in adrenal glomerulosa cells. (*In* Tsien, R.W., Clozel, J-P. & Nargeot, J., *eds.* Low-Voltage-Activated T-type Calcium Channels: Proceedings from the International Electrophysiology Meeting, Montpellier, Oct. 21-22 1996. Tattenhall, Chester, England: Adis International. p. 176-185).

SANGUINETTI, M.C., KRAFTE, D.S. & KASS, R.S. 1986. Voltage-dependent modulation by Ca channel current in heart cells by Bay K 8644. *Journal of general Physiology,* 88:369-392.

SATHER, W.A. & McCLESKEY. 2003. Permeation and selectivity in calcium channels. *Annual reviews of Physiology*, 65:133-159, March.

SCHNEIDER, T., IGELMUND, P. & HESCHELER, J. 1997. G protein interaction with K^+ and Ca^{2+} channels. *Trends in Pharmacological Sciences,* 18:8-11.

SEINO, S., CHEN, L., SEINO, M., BLONDEL, O., TAKEDA, J., JOHNSON, J.H. & BELL, G.I. 1992. Cloning of the α1 subunit of a voltage-dependent Ca^{2+} channel expressed in pancreatic β cells. *Proc. Natl. acad. Sci. USA,* 89:584-588, Jan.

SHEKTER, L.R., PHILIPSON, L.H., RHIM, H., TOTH, P.T. & MILLER, R.J. 1998. Regulation of human neuronal calcium channels by receptors and G proteins. (*In* Tsien, R.W., Clozel, J-P. & Nargeot, J., *eds.* Low-Voltage-Activated T-type Calcium Channels: Proceedings from the International Electrophysiology Meeting, Montpellier, Oct. 21-22 1996. Tattenhall, Chester, England: Adis International. p. 332-342).

SHER, E., BIANCARDI, E., POLLO, A., CARBONE, E., LI, G., WOLHEIM, C.B. & CLEMENTI, F. 1992. ω-Conotoxin-sensitive, voltage-operated Ca^{2+} channels in insulin-secreting cells. *European journal of pharmacology,* 216:407-414.

SHEN, G.S., LAYER, R.T. & MCCABE, R.T. 2000. Conopeptides: from deadly venoms to novel therapeutics. *DDT,* 5(3): 98-106, March.

SHOROFKSY, S.R. & BALKE, C.W. 2001. Calcium currents and Arrythmias: Insights from molecular biology. *The American journal of Medicine,* 110:127-140.

SIDACH, S.S. & MINTZ, I.M. 2002. Kurtoxin, a gating modifier of neuronal high- and low-threshold Ca channels. *Journal of Neuroscience,* 22(6): 2023-2034, March.

SIMARD, M.J. & WATT, D.D. 1990. Venoms and toxins. (*In* Polis, G.A., *ed.* The biology of scorpions. Stanford University press. P. 414-444).

SNUTCH, T.P., SUTTON, K.G. & ZAMPONI, G.W. 2001. Voltage-dependent calcium channels – beyond dihydropyridine antagonists. *Current opinion in Pharmacology,* 1:11-16.

SUTTON, K.G., SIOK, C., STEA, A., ZAMPONI, G.W., HECK, S.D., VOLKMANN, R.A., AHLIJANIAN, M.K. & SNUTCH, T.P. 1998. Inhibition of neuronal calcium channels by a novel peptide spider toxin, DW 13.3. *Molecular pharmacology,* 54:407-418.

TERLAU, H. & STÜHMER, W. 1998. Structure and function of Voltage-gated ion channels. *Naturwissenschaften,* 85:437-444.

TERLAU, H. & OLIVERA, B.M. 2004. *Conus* venoms: A rich source of novel ion channels-targeted peptides. *Physiological reviews,* 84:41-68.

TAKESHIMA, H. 1993. Primary Structure and expression from cDNAs of the Ryanodine receptor. *Annals of the New York Academy of Science,* 707:165-177.

TIAHO, F., RICHARD, S., LORY, P., NERBONNE, J.M. & NARGEOT, J. 1990. Cyclic-AMP-dependent phosphorylation modulates the stereospecific activation of cardiac Ca channels by Bay K 8644. *Pflügers Archives,* 417:58-66.

TIAHO, F., NARGEOT, J. & RICHARD, S. 1991. Voltage-dependent regulation of L-type cardiac Ca channels by isoproterenol. *Pflügers Archives,* 419:596-602.

TOTTENE, A., FORTI, L., MORETTI, A. & PIETROBON, D. 1998. G2 and G3: two different R-type (toxin-resistant) calcium channels coexpressed in rat cerebellar granule cells. (*In* Tsien, R.W., Clozel, J-P. & Nargeot, J., *eds.* Low-Voltage-Activated T-type Calcium Channels: Proceedings from the International Electrophysiology Meeting, Montpellier, Oct. 21-22 1996. Tattenhall, Chester, England: Adis International. p. 73-79).

TRIGGLE, D.J. 1999. The pharmacology of ion channels: with particular reference to voltage-gated Ca^{2+} channels. *European journal of Pharmacology,* 375:311-325.

TSIEN, R.W. 1983. Ca^{2+} channels in excitable cell membranes. *Annual Reviews of Physiology,* 45:341-358.

TUANA, B.S. & MURPHY, B.J. 1990. Biochemical analysis of L-type calcium channels from skeletal and cardiac muscle. *Canadian Journal of Physiology and Pharmacology,* 68:1428-1488.

TYTGAT, J., VEREECKE, J. & CARMELIET, E. 1988. Differential effects of verapamil and flunarizine on cardiac L-type and T-type Ca channels. *Naunyn-Schmiedeberg's Archives of Pharmacology*, 337(590-692).

TYTGAT, J., DEBONT, T., ROSTOLL, K., MÜLLER, G.J., VERDONCK, F., DAENENS, P., VAN DER WALT, J. & POSSANI, L.D. 1998. Purification and partial characterization of a 'short' insectotoxin-like peptide from the venom of the scorpion *Parabuthus schlechteri. Federation of European Biochemical Societies letters,* 441:387-391.

TYTGAT, J., CHANDY, K.G., GARCIA, M.L., GUTMAN, G.A., MARTIN-EAUCLAIRE, M-F., VAN DER WALT, J.J. & POSSANI, L.D. 1999. A unified nomenclature for short-chain peptides isolated from scorpion venoms: α-KTx molecular subfamilies. *Trends in Pharmacological Sciences,* 20:444-447.

UCHITEL, O.D. & KATZ, E. 1997. Calcium channel diversity at the vertebrate neuromuscular junction. (*In* Sotelo, J.R. & Benech, J.C. *eds.* Calcium and cellular metabolism, transport and regulation: Proceedings of an International Workshop on Calcium and cellular metabolism: Transport and regulation held September 25-October 6, 1995, Montevideo, Uruguay. New York: Plenum Press. p. 37-46.)

VALDIVIA, H.H. & POSSANI, L.D. 1998. Peptide toxins as probes of ryanodine receptor structure and function. *Trends in Cardiovascular Medicine,* 8(3): 111-118.

WALKER, D. & DE WAARD, M. 1998. Subunit interaction sites in voltage dependent Ca^{2+} channels: role in channel function. *Trends in Neuroscience,* 21:148-154.

WELLING,A., LACINOVA, L., DONATIN, K., LUDWIG, A., BOSSE, E., FLOCKERZI, V. & HOFMANN, F. 1995. Expression of the L-type calcium channel with two different β subunits and its modulation by R40-5967. *Pflügers Archives – European Journal of Physiology,* 429:400-411.

ZAMPONI, G.W., BOURINET, E. & SNUTCH, T.P. 1998. Limitations of Ni^{2+} as a tool for discrimination between high- and low-threshold calcium channels. (*In* Tsien, R.W., Clozel, J-P. & Nargeot, J., *eds.* Low-Voltage-Activated T-type Calcium Channels: Proceedings from the International Electrophysiology Meeting, Montpellier, Oct. 21-22 1996. Tattenhall, Chester, England: Adis International. p. 92-98).

ZHANG, J-F., RANDALL, A.D., ELLINOR, P.T., HORNE, W.A., SATHER, W.A., TANABE, T., SCHWARTZ, T.L. & TSIEN, R.W. 1993. Distinctive pharmacology and kinetics of cloned neuronal Ca^{2+} channels and their possible counterparts in mammalian CNS neurons. *Neuropharmacology,* 32(11): 1075-1088.